



1

2

3

4

5

6

7

8

9

10

11

Global Sea Level Budget 1993-Present

12

13

14

WCRP Global Sea Level Budget Group*

15

16

*A full list of authors and their affiliations appears at the end of the paper

17

18

19

20

21

22

23

24

25

26

Corresponding author: Anny Cazenave, LEGOS, 18 Avenue Edouard Belin, 31401 Toulouse,

27

Cedex 9, France; anny.cazenave@legos.obs-mip.fr

28

29



30 **Abstract**

31 Global mean sea level is an integral of changes occurring in the climate system in response to
32 unforced climate variability as well as natural and anthropogenic forcing factors. Its temporal
33 evolution allows detecting changes (e.g., acceleration) in one or more components. Study of
34 the sea level budget provides constraints on missing or poorly known contributions, such as
35 the unsurveyed deep ocean or the still uncertain land water component. In the context of the
36 World Climate Research Programme Grand Challenge entitled “Regional Sea Level and
37 Coastal Impacts”, an international effort involving the sea level community worldwide has
38 been recently initiated with the objective of assessing the various data sets used to estimate
39 components of the sea level budget during the altimetry era (1993 to present). These data sets
40 are based on the combination of a broad range of space-based and in situ observations, model
41 estimates and algorithms. Evaluating their quality, quantifying uncertainties and identifying
42 sources of discrepancies between component estimates is extremely useful for various
43 applications in climate research. This effort involves several tens of scientists from about fifty
44 research teams/institutions worldwide ([www.wcrp-climate.org/grand-challenges/gc-sea-](http://www.wcrp-climate.org/grand-challenges/gc-sea-level)
45 [level](http://www.wcrp-climate.org/grand-challenges/gc-sea-level)). The results presented in this paper are a synthesis of the first assessment performed
46 during 2017-2018. We present estimates of the altimetry-based global mean sea level (average
47 rate of 3.1 +/- 0.3 mm/yr and acceleration of 0.1 mm/yr² over 1993-present), as well as of the
48 different components of the sea level budget (<http://doi.org/10.17882/54854>). We further
49 examine closure of the sea level budget, comparing the observed global mean sea level with
50 the sum of components. Ocean thermal expansion, glaciers, Greenland and Antarctica
51 contribute by 42%, 21%, 15% and 8% to the global mean sea level over the 1993-present. We
52 also study the sea level budget over 2005-present, using GRACE-based ocean mass estimates
53 instead of sum of individual mass components. Results show closure of the sea level budget
54 within 0.3 mm/yr. Substantial uncertainty remains for the land water storage component, as
55 shown in examining individual mass contributions to sea level.

56



57 **1. Introduction**

58

59 Global warming has already several visible consequences, in particular increase of the Earth's
60 mean surface temperature and ocean heat content (Rhein et al., 2013, Stocker et al., 2013),
61 melting of sea ice, loss of mass of glaciers (Gardner et al., 2013), and ice mass loss from the
62 Greenland and Antarctica ice sheets (Rignot et al., 2011, Shepherd et al., 2012). On average
63 over the last 50 years, about 93% of heat excess accumulated in the climate system because of
64 greenhouse gas emissions has been stored in the ocean, and the remaining 7% has been
65 warming the atmosphere and continents, and melting sea and land ice (von Schuckmann et al.,
66 2016). Because of ocean warming and land ice mass loss, sea level rises. After about 3000
67 years of nearly constant evolution since the end of the last deglaciation (e.g., Lambeck et al.,
68 2010, Kemp et al., 2011, Kopp et al. 2014), direct observations from in situ tide gauges
69 available since the mid-to-late 19th century show that the 20th century global mean sea level
70 has been rising at a rate of 1.2 mm/yr to 1.9 mm/yr (Church and White, 2011, Jevrejeva et al.,
71 2014a, Hay et al., 2015, Dangendorf et al., 2017). Since the early 1990s, this rate, now
72 measured by high-precision altimeter satellites, has increased to ~3 mm/yr on average
73 (Legeais et al., 2018, Nerem et al., 2018).

74 Accurate assessment of present-day global mean sea level variations and its components
75 (ocean thermal expansion, ice sheet mass loss, glaciers mass change, changes in land water
76 storage, etc.) is important for many reasons. The global mean sea level is an integral of
77 changes occurring in the Earth's climate system in response to unforced climate variability as
78 well as natural and anthropogenic forcing factors e.g., net contribution of ocean warming,
79 land ice mass loss, and changes in water storage in continental river basins. Temporal changes
80 of the components are directly reflected in the global mean sea level curve. If accurate
81 enough, study of the sea level budget provides constraints on missing or poorly known
82 contributions, e.g., the deep ocean, marginal seas and shelf areas, and polar regions
83 undersampled by current observing systems, or still uncertain changes in water storage on
84 land due to human activities (e.g. ground water depletion in aquifers). Global mean sea level
85 corrected for ocean mass change in principle allows one to independently estimate temporal
86 changes in total ocean heat content, from which the Earth's energy imbalance can be deduced
87 (von Schuckmann et al., 2016). The sea level and/or ocean mass budget approach can also be
88 used to constrain models of Glacial Isostatic Adjustment (GIA). The GIA phenomenon has
89 significant impact on the interpretation of GRACE-based space gravimetry data over the
90 oceans (for ocean mass change) and over Antarctica (for ice sheet mass balance). However,



91 there is still incomplete consensus on best estimates, a result of uncertainties in deglaciation
92 models and mantle viscosity structure. Finally, observed changes of the global mean sea level
93 and its components are fundamental for validating climate models used for projections.

94 In the context of the Grand Challenge entitled “Regional Sea Level and Coastal Impacts” of
95 the World Climate Research Programme (WCRP), an international effort involving the sea
96 level community worldwide has been recently initiated with the objective of assessing the sea
97 level budget during the altimetry era (1993 to present). To estimate the different components
98 of the sea level budget, different data sets are used. These are based on the combination of a
99 broad range of space-based and in situ observations. Evaluating their quality, quantifying their
100 uncertainties, and identifying the sources of discrepancies between component estimates,
101 including the altimetry-based sea level time series, are extremely useful for various
102 applications in climate research.

103 Several previous studies have addressed the sea level budget over different time spans and
104 using different data sets (e.g., Cazenave et al., 2009, Leuliette and Willis, 2010, Church and
105 White, 2011, Chambers et al., 2017, Dieng et al., 2017, Chen et al., 2017, Nerem et al., 2018).
106 Assessments of the published literature have also been performed in past IPCC
107 (Intergovernmental Panel on Climate Change) reports (e.g., Church et al., 2013). Building on
108 these previous works, here we intend to provide a collective update of the global mean sea
109 level budget, involving the many groups worldwide interested in present-day sea level rise and
110 its components. We focus on observations rather than model-based estimates and consider the
111 high-precision altimetry era starting in 1993 that includes the period since the mid-2000s
112 where new observing systems, like the Argo float project (Roemmich et al., 2012) and the
113 GRACE space gravimetry mission (Tapley et al., 2004) that provide improved data sets of
114 high value for such a study. Only the global mean budget is considered here. Regional budget
115 will be the focus of a future assessment.

116 Section 2 describes for each component of the sea level budget equation the different data sets
117 used to estimate the corresponding contribution to sea level, discusses associated errors and
118 provides trend estimates for the two periods. Section 3 addresses the mass and sea level
119 budgets over the study periods. A discussion is provided in Section 4, followed by a
120 conclusion.

121

122 **2. Methods and Data**



123 In this section, we briefly present the global mean sea level budget (sub section 2.1), then
 124 provide, for each term of the budget equation, an assessment of the most up-to-date published
 125 results. Multiple organisations and research groups routinely generate the basic measurements
 126 as well as the derived data sets and products used to study the sea level budget. Sub sections
 127 2.2 to 2.7 summarize the measurements and methodologies used to derive observed sea level,
 128 as well as steric and mass components. In most cases, we focus on observations but in some
 129 instances (e.g., for GIA corrections applied to the data), model-based estimates are the only
 130 available information.

131

132 2.1 Sea level budget equation

133 Global mean sea level (GMSL) change as a function of time t is usually expressed by the sea
 134 level budget equation:

$$135 \quad \text{GMSL}(t) = \text{GMSL}(t)_{\text{steric}} + \text{GMSL}(t)_{\text{ocean mass}} \quad (1)$$

136 where $\text{GMSL}(t)_{\text{steric}}$ refers to the contributions of ocean thermal expansion and salinity to sea
 137 level change, and $\text{GMSL}(t)_{\text{ocean mass}}$ refers to the change in mass of the oceans. Due to water
 138 conservation in the climate system, the ocean mass term (also noted as $M(t)_{\text{ocean}}$) can further
 139 be expressed as:

140

$$141 \quad M(t)_{\text{ocean}} + M(t)_{\text{glaciers}} + M(t)_{\text{Greenland}} + M(t)_{\text{Antarctica}} + M(t)_{\text{TWS}} + M(t)_{\text{WV}} + M(t)_{\text{Snow}} \\ 142 \quad + \text{uncertainty} = 0 \quad (2)$$

143

144 where $M(t)_{\text{glaciers}}$, $M(t)_{\text{Greenland}}$, $M(t)_{\text{Antarctica}}$, $M(t)_{\text{TWS}}$, $M(t)_{\text{WV}}$, $M(t)_{\text{Snow}}$ represent temporal
 145 changes in mass of glaciers, Greenland and Antarctica ice sheets, terrestrial water storage
 146 (TWS), atmospheric water vapor (WV), and snow mass changes. The uncertainty is a result of
 147 uncertainties in all of the estimates and potentially missing mass terms, for example,
 148 permafrost melting.

149

150 From equation (2), we deduce:

151

$$152 \quad \text{GMSL}(t)_{\text{ocean mass}} = - [M(t)_{\text{glaciers}} + M(t)_{\text{Greenland}} + M(t)_{\text{Antarctica}} + M(t)_{\text{TWS}} + M(t)_{\text{WV}} + M(t)_{\text{Snow}} \\ 153 \quad + \text{missing mass terms}] \quad (3)$$

154



155 In the next subsections, we successively discuss the different terms of the budget (equations 1
156 and 2) and how they are estimated from observations. We do not consider the atmospheric
157 water vapor and snow components, assumed to be small. Two periods are considered: (1)
158 1993-present (i.e. the entire altimetry era), and (2) 2005-present (i.e. the period covered by
159 both Argo and GRACE).

160

161 **2.2 Altimetry-based global mean sea level over 1993-present**

162 The launch of the TOPEX/Poseidon (T/P) altimeter satellite in 1992 led to a new paradigm for
163 measuring sea level from space, providing for the first time precise and globally distributed
164 sea level measurements at 10-day intervals. At the time of the launch of T/P, the
165 measurements were not expected to have sufficient accuracy for measuring GMSL changes.
166 However, as the radial orbit error decreased from ~10 cm at launch to ~1 cm presently, and
167 other instrumental and geophysical corrections applied to altimetry system improved (e.g.,
168 Stammer and Cazenave, 2017), several groups regularly provided an altimetry-based GMSL
169 time series (e.g., Nerem et al. 2010, Church et al. 2011, Ablain et al., 2015, Legeais et al.,
170 2018). The initial T/P GMSL time series was extended with the launch of Jason-1 (2001),
171 Jason-2 (2008) and Jason-3 (2016). By design, each of these missions has an overlap period
172 with the previous one in order to inter-compare the sea level measurements and estimate
173 instrument biases (e.g., Nerem et al., 2010; Ablain et al., 2015). This has allowed the
174 construction of an uninterrupted GMSL time series that is currently 25-year long.

175

176 **2.2.1 Global mean sea level datasets**

177 Six groups (AVISO/CNES, SL_cci/ESA, University of Colorado, CSIRO, NASA/GSFC,
178 NOAA) provide altimetry-based GMSL time series. All of them use 1-Hz altimetry
179 measurements derived from T/P, Jason-1, Jason-2 and Jason-3 as reference missions. These
180 missions provide the most accurate long-term stability at global and regional scales (Ablain et
181 al. 2009, 2017a), and are all on the same historical T/P ground track. This allows computation
182 of a long-term record of the GMSL from 1993 to present. In addition, complementary
183 missions (ERS-1, ERS-2, Envisat, Geosat Follow-on, CryoSat-2, SARAL/AltiKa and
184 Sentinel-3A) provide increased spatial resolution and coverage of high latitude ocean areas, >
185 66°N/S latitude (e.g. the European Space Agency/ESA Climate Change Initiative/CCI sea
186 level data set; Legeais et al. 2018).



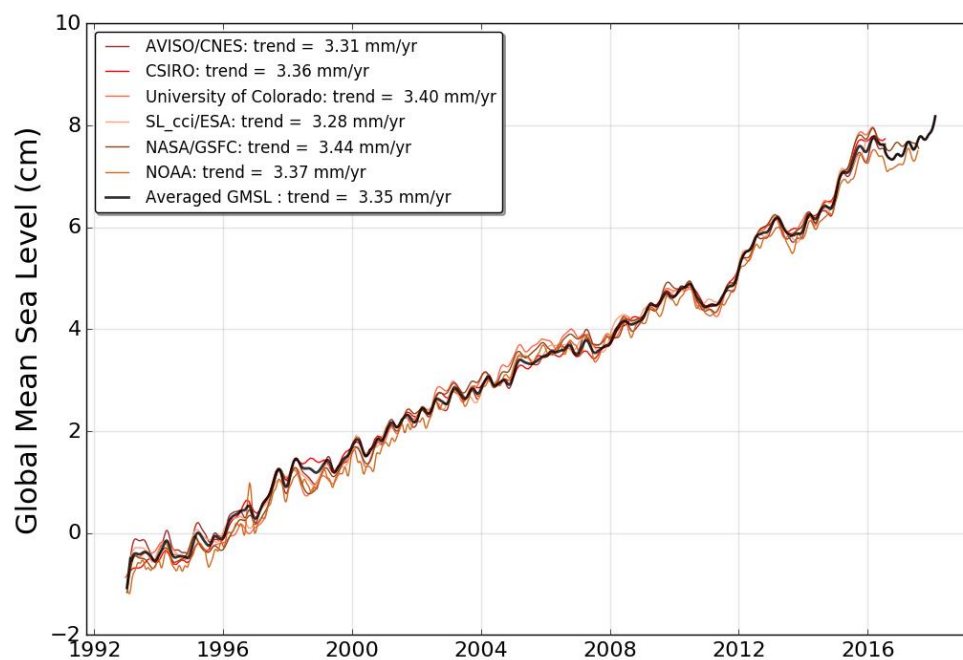
7

187 The above groups adopt different approaches when processing satellite altimetry data. The
188 most important differences concern the geophysical corrections needed to account for various
189 physical phenomena such as atmospheric propagation delays, sea state bias, ocean tides, and
190 the ocean response to atmospheric dynamics. Other differences come from data editing,
191 methods to spatially average individual measurements during orbital cycles and link between
192 successive missions (Masters et al. 2012; Henry et al. 2014).

193 Overall, the quality of the different GMSL time series is similar. Long-term trends agree well
194 to within 6% of the signal, approximately 0.2 mm/yr (see Figure 1) within the GMSL trend
195 uncertainty range (~ 0.3 mm/yr; see next section). The largest differences are observed at
196 interannual time scales and during the first years (before 1999; see below). Here we use an
197 ensemble mean GMSL based on averaging all individual GMSL time series.

198

199



200

201

202 *Figure 1: Evolution of GMSL time series from 6 different groups (AVISO/CNES, SL_cci/ESA,*
203 *University of Colorado, CSIRO, NASA/GSFC, NOAA) products. Annual signals are removed*
204 *and 6-month smoothing applied. All GMSL time series are centered in 1993 with zero mean.*
205 *A GIA correction of -0.3 mm/yr has been subtracted to each data set.*



206 **2.2.2 Global mean sea level uncertainties and TOPEX-A drift**

207 Based on an assessment of all sources or uncertainties affecting the altimetric system (Ablain
208 et al. 2017), the GMSL trend uncertainty (90% confidence interval) is estimated as ~ 0.4
209 mm/yr over the whole altimetry era (1993-2017). The main contribution to the uncertainty is
210 the wet tropospheric correction with a drift uncertainty in the range of 0.2-0.3 mm/yr (Legeais
211 et al. 2018) over a 10-year period. To a lesser extent, the orbit error (Couhert et al. 2015;
212 Escudier et al., 2017) and the altimeter parameters' (range, sigma-0 and significant wave
213 height/SWH) instability (Ablain et al., 2012) also contribute to the GMSL trend uncertainty,
214 at the level of 0.1 mm/yr. Furthermore, imperfect links between successive altimetry missions
215 lead to another trend uncertainty of about 0.15 mm/yr over the 1993-2017 period (Zawadzki
216 and Ablain, 2016).

217 Uncertainties are higher during the first decade (1993-2002) where T/P measurements display
218 larger errors at climatic scales. For instance, the orbit solutions are much more uncertain due
219 to gravity field solutions calculated without GRACE data. Furthermore, the switch from
220 TOPEX-A to TOPEX-B in February 1999 (with no overlap between the two instrumental
221 observations) leads to an error of ~ 3 mm in the GMSL time series (Escudier et al., 2017).

222 However, the most significant error that affects the first 6 years (January-1993 to February
223 1999) of the T/P GMSL measurements is due to an instrumental drift of the TOPEX-A
224 altimeter, not included in the formal uncertainty estimates discussed above. This effect on the
225 GMSL time series was recently highlighted via comparisons with tide gauges (Valladeau et
226 al. 2012; Watson et al. 2015; Chen et al. 2017; Ablain et al. 2017), via a sea level budget
227 approach (i.e., comparison with the sum of mass and steric components; Dieng et al., 2017)
228 and by comparing with Poseidon-1 measurements (Zawadzki, personal communication). In a
229 recent study, Beckley et al. (2017) asserted that the corresponding error on the 1993-1998
230 GMSL resulted from incorrect onboard calibration parameters.

231 All three approaches conclude that during the period January 1993 to February 1999, the
232 altimetry-based GMSL was overestimated. TOPEX-A drift correction was estimated close to
233 1.5 mm/yr (in terms of sea level trend) with an uncertainty of ± 0.5 to ± 1.0 mm/yr (Watson et
234 al. 2015; Chen et al. 2017; Dieng et al. 2017). Beckley et al. (2017) proposed to not apply the
235 suspect onboard calibration correction on TOPEX-A measurements. The impact of this
236 approach is similar to the TOPEX-A drift correction estimated by Dieng et al. (2017) and
237 Ablain et al. (2017b). In the latter study, accurate comparison between TOPEX A-based
238 GMSL and tide gauge measurements leads to a drift correction to about -1.0 mm/yr between



239 January 1993 and July 1995, and +3.0 mm/yr between August 1995 and February 1999, with
240 an uncertainty of 1.0 mm/yr (with a 68% confidence level, see Table 1).

241

TOPEX-A drift correction	to be subtracted from the first 6-years (Jan. 1993 to Feb. 1999) of the uncorrected GMSL record
Watson et al. (2015)	1.5 +/- 0.5 mm/yr over Jan.1993/ Feb.1999
Chen et al. (2017); Dieng et al. (2017)	1.5 +/- 0.5 mm/yr over Jan.1993/ Feb.1999
Beckley et al. (2017)	No onboard calibration applied
Ablain et al. (2017b)	-1.0 +/- 1.0 mm/yr over Jan.1993/ Jul.1995 +3.0 +/-1.0 mm/yr over Aug.1995- Feb.1999

242 *Table 1. TOPEX-A GMSL drift corrections proposed by different studies*

243

244 **2.2.3 Global Mean Sea Level variations**

245

246 The ensemble mean GMSL rate after correcting for the TOPEX-A drift (for all of the
247 proposed corrections) amounts to 3.1 mm/yr over 1993-2017 (Figure 2). This corresponds to a
248 mean sea level rise of about 7.5 cm over the whole altimetry period. More importantly, the
249 GMSL curve shows a net acceleration, estimated at 0.08 mm/yr² (Chen et al. 2017; Dieng et
250 al. 2017) and 0.084 +/- 0.025 mm/yr² (Nerem et al., 2018) (Note Watson et al. found a smaller
251 acceleration after correcting for the instrumental bias over a shorter period up to the end of
252 2014.). GMSL trends calculated over 10-year moving windows illustrate this acceleration
253 (Figure 3). GMSL trends are close to 2.5 mm/yr over 1993-2002 and 3.0 mm/yr over 1996-
254 2005. After a slightly smaller trend over 2002-2011, the 2008-2017 trend reaches 4.2 mm/yr.
255 Uncertainties (90% confidence interval) associated to these 10-year trends regularly decrease
256 through time from 1.3 mm/yr over 1993-2002 (corresponding to T/P data) to 0.65 mm/yr for
257 2008-2017 (corresponding to Jason-2 and Jason-3 data).

258 Removing the trend from the GMSL time series highlights inter-annual variations. Their
259 magnitudes depend on the period (+3 mm in 1998-1999, -5 mm in 2011-2012, and +10 mm in
260 2015-2016) and are well correlated in time with El Niño and La Niña events (Nerem et al.
261 2010; Cazenave et al. 2014, Nerem et al., 2018). However, substantial differences (of 1-3

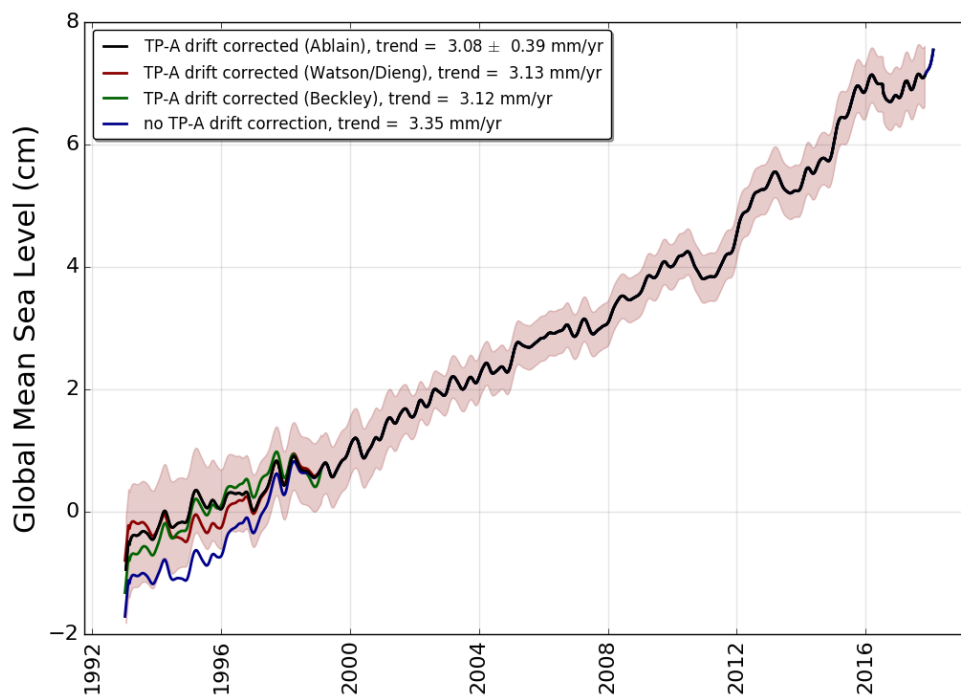


10

262 mm) exist between the six detrended GMSL time series. This issue needs further
 263 investigation.

264

265



266

267

268 *Figure 2: Evolution of ensemble mean GMSL time series (average of the 6 GMSL products*
 269 *from AVISO/CNES, SL_cci/ESA, University of Colorado, CSIRO, NASA/GSFC, and NOAA).*

270 *On the black, red and green curves, the TOPEX-A drift correction is applied respectively*
 271 *based on (Ablain et al, 2017b), (Watson et al. 2015; Dieng et al. 2017) and Beckley et al.,*
 272 *2017). Annual signal removed and 6-month smoothing applied; GIA correction also applied.*

273 *Uncertainties (90% confidence interval) of correlated errors over a 1-year period are*
 274 *superimposed for each individual measurement (shaded area).*

275

276

277

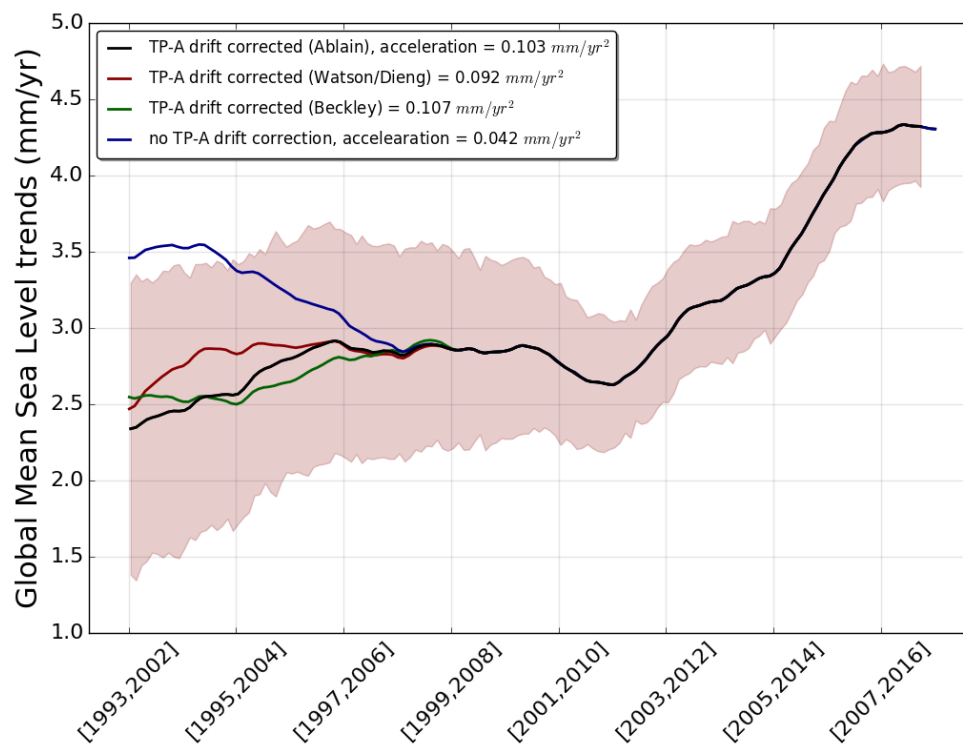
278

279

280



11



281

282

283 *Figure 3: Ensemble mean GMSL trends calculated over 10-year moving windows. On the*
284 *black, red and green curves, the TOPEX-A drift correction is applied respectively based on*
285 *(Ablain et al., 2017b), and Beckley et al., 2017). Uncorrected GMSL trends are shown by the*
286 *blue curve. The shaded area represents trend uncertainty over 10-year periods (90%*
287 *confidence interval).*

288

289 For the sea level budget assessment (section 3), we will use the ensemble mean GMSL time
290 series corrected for the TOPEX A drift using the Ablain et al. (2017b) correction.

291

292 **2.2.4. Comparison with tide gauges**

293

294 Prior to 1992 global sea level rise estimates rely on the tide gauge measurements, and it is
295 worth mentioning past attempts to produce global sea level reconstructions utilizing these
296 measurements (e.g. Gornitz et al. 1982; Barnett 1984; Douglas 1991, 1997, 2001). Here we
297 focus on global sea level reconstructions that overlap with satellite altimetry data over a
298 substantial common time span. Some of these reconstructions rely on tide gauge data only



299 (Jevrejeva et al. 2006, 2014; Merrifield et al. 2009; Wenzel and Schroter 2010; Ray and
300 Douglas 2011; Hamlington et al. 2011, Spada and Galassi 2012; Thompson and Merrifield
301 2014; Dangendorf et al. 2017; Frederikse et al. 2017). In addition, there are reconstructions
302 that jointly use satellite altimetry and tide gauge records (Church and White 2006, 2011) and
303 reconstructions which combines tide gauge records with ocean models (Meysignac et al.
304 2011) or physics-based and model-derived geometries of the contributing processes (Hay et
305 al. 2015).

306 For the period since 1993, with most of the world coastlines densely sampled, the rates of sea
307 level rise from all tide gauge based reconstructions and estimates from satellite altimetry
308 agree within their specific uncertainties, e.g., rates of $3.0 \pm 0.7 \text{ mm} \cdot \text{yr}^{-1}$ (Hay et al. 2015); 2.8
309 $\pm 0.5 \text{ mm} \cdot \text{yr}^{-1}$ (Church and White 2011; Rhein et al. 2013); $3.1 \pm 0.6 \text{ mm} \cdot \text{yr}^{-1}$ (Jevrejeva et
310 al, 2014); $3.1 \pm 1.4 \text{ mm} \cdot \text{yr}^{-1}$ (Dangendorf et al. 2017) and the estimate from satellite altimetry
311 $3.2 \pm 0.4 \text{ mm} \cdot \text{yr}^{-1}$ (Nerem et al. 2010; Rhein et al. 2013). However, classical tide gauge-
312 based reconstructions still tend to overestimate the inter-annual to decadal variability of
313 global mean sea level (e.g. Calafat et al., 2012; Dangendorf et al. 2015; Natarov et al. 2017)
314 compared to global mean sea level from satellite altimetry, due to limited and uneven spatial
315 sampling of the global ocean afforded by the tide gauge network. Sea level rise being non
316 uniform, spatial variability of sea-level measured at tide gauges is evidenced by 2D
317 reconstruction methods. The most widely used approach is the use of empirical orthogonal
318 functions (EOF) calibrated with the satellite altimetry data (e.g. Church and White, 2004).
319 Alternatively, Choblet et al. (2014) implemented a Bayesian inference method based on a
320 Voronoi tessellation of the Earth's surface to reconstruct sea level during the twentieth
321 century. Considerable uncertainties remain however in long term assessments due to poorly
322 sampled ocean basins such as the South Atlantic, or regions which are significantly influenced
323 by open-ocean circulation (e.g. Subtropical North Atlantic) (Frederikse et al. 2017).
324 Uncertainties involved in specifying vertical land motion corrections at tide gauges also
325 impact tide gauge reconstructions (Jevrejeva et al. 2014; Woppelmann and Marcos 2016;
326 Hamlington et al. 2016). Frederikse et al. (2017) recently also demonstrated that both global
327 mean sea level reconstructed from tide gauges and the sum of steric and mass contributors
328 show a good agreement with altimetry estimates for the overlapping period 1993-2014.

329

330 **2.3 Steric sea level**



331 Steric sea level variations result from temperature (T) and salinity (S) related density changes
332 of sea water associated to volume expansion and contraction. These are referred as
333 thermosteric and halosteric components. Despite clear detection of regional salinity changes
334 and the dominance of the salinity effect on density changes at high latitudes (Rhein et al.,
335 2013), the halosteric contribution to present-day global mean steric sea level rise is negligible,
336 as the ocean's total salt content is essentially constant over multidecadal timescales (Gregory
337 and Lowe, 2000). Hence in this study, we essentially consider the thermosteric sea level
338 component.

339 Averaged over the 20th century, ocean thermal expansion associated with ocean warming has
340 been the largest contribution to global mean sea level rise (Church et al., 2013). This remains
341 true for the altimetry period starting in the year 1993 (e.g., Chen et al. 2017; Dieng et al.,
342 2017, Nerem et al., 2018). But sum of all land ice components (glaciers, Greenland and
343 Antarctica) during this period, total land ice mass loss now dominates the sea level budget
344 (see section 3).

345 Until the mid-2000s, the majority of ocean temperature data have been retrieved from
346 shipboard measurements. These include vertical temperature profiles along research cruise
347 tracks from the surface sometimes all the way down to the bottom layer (e.g. Purkey and
348 Johnson, 2010) and upper-ocean broadscale measurements from ships of opportunity
349 (Abraham et al., 2013). These upper-ocean in situ temperature measurements however are
350 limited to the upper 700 m depth due to common use of expandable bathy thermographs
351 (XBTs). Although the coverage has been improved through time, large regions characterized
352 by difficult meteorological conditions remained undersampled, in particular the southern
353 hemisphere oceans and the Arctic area.

354

355 ***2.3.1 Thermosteric data sets***

356 Over the altimetry era, several research groups have produced gridded time series of
357 temperature data for different depth levels, based on XBTs (with additional data from
358 mechanical bathythermographs -MBTs- and conductivity-temperature-depth (CTD) devices
359 and moorings) and Argo float measurements. The temperature data have further been used to
360 provide thermosteric sea level products. These differ because of different strategies adopted
361 for data editing, temporal and spatial data gaps filling, mapping methods, baseline
362 climatology and instrument bias corrections (in particular the time-to-depth correction for
363 XBT data, Boyer et al., 2016).

364 The global ocean in situ observing system has been dramatically improved through the



365 implementation of the international Argo program of autonomous floats, delivering a unique
 366 inside of the interior ocean from the surface down to 2000 m depth of the ice-free global
 367 ocean (Roemmich et al., 2012, Riser et al., 2016). More than 80% of initially planned full
 368 deployment of Argo float program was achieved during the year 2005, with virtually global
 369 coverage of the ice-free ocean by the start of 2006. At present, more than 3800 floats provide
 370 systematic T/S data, with quasi (60°S-60°N latitude) global coverage down to 2000 m depth.
 371 A full overview on in situ ocean temperature measurements is given for example in Abraham
 372 et al. (2013).

373 In this section, we consider a set of 11 direct (in situ) estimates, publically available over the
 374 entire altimetry era, to review global mean thermosteric sea level rise and, ultimately, to
 375 construct an ensemble mean timeseries. These data sets are:

- 376 1. CORA = Coriolis Ocean database for ReAnalysis, Copernicus Service, France
 377 marine.copernicus.eu/, product name :
 378 INSITU_GLO_TS_OA_REP_OBSERVATIONS_013_002_b
- 379 2. CSIRO (RSOI) = Commonwealth Scientific and Industrial Research
 380 Organisation/Reduced-Space Optimal Interpolation, Australia
- 381 3. ACECRC/IMAS-UTAS = Antarctic Climate and Ecosystem Cooperative Research
 382 Centre/Institute for Marine and Antarctic Studies-University of Tasmania, Australia
 383 http://www.cmar.csiro.au/sealevel/thermal_expansion_ocean_heat_timeseries.html
- 384 4. ICCES = International Center for Climate and Environment Sciences, Institute of
 385 Atmospheric Physics, China
 386 <http://ddl.escience.cn/f/PKFR>
- 387 5. ICDC = Integrated Climate Data Center, University of Hamburg, Germany
- 388 6. IPRC = International Pacific Research Center, University of Hawaii, USA
 389 http://apdrc.soest.hawaii.edu/projects/Argo/data/gridded/On_standard_levels/index-1.html
- 390 7. JAMSTEC = Japan Agency for Marine-Earth Science and Technology, Japan
 391 ftp://ftp2.jamstec.go.jp/pub/argo/MOAA_GPV/Glb_PRS/OI/
- 392 8. MRI/JMA = Meteorological Research Institute/Japan Meteorological Agency, Japan
 393 <https://climate.mri-jma.go.jp/~ishii/wcrp/>
- 394 9. NCEI/NOAA = National Centers for Environmental Information/National Oceanic
 395 and Atmospheric Administration, USA
- 396 10. SIO = Scripps Institution of Oceanography, USA
 397 Deep/abyssal: <https://cchdo.ucsd.edu/>
- 398 11. SIO = Scripps Institution of Oceanography, USA
 399 Deep/abyssal: <https://cchdo.ucsd.edu/> (for the abyssal ocean)

400

401
402 Their characteristics are presented in Table 2.

403

404



Product/Institution	Period	Depth-integration (m)				Temporal resolution / Latitudinal range	Reference
		0-700	700-2000	0-2000	≥2000		
1 CORA	1993-2016*	Y	Y	Y	---	Monthly 60°S-60°N	http://marine.cornell.edu/services-portfolio/access-to-products/
2 CSIRO (RSOI)	2004-2017	Y/E (0-300)	Y/E	Y/E	---	Monthly 65°S-65°N	Roemmich et al. (2015); Wijffels et al. (2016)
3 CSIRO/ACE CRC/IMAS-UTAS	1970-2017	Y/E (0-300)	---	---	---	Yearly (3-yr run. mean) 65°S-65°N	Domingues et al. (2008); Church et al. (2011)
4 ICCES	1970-2016	Y/E (0-300)	Y/E	Y/E	---	Yearly 89°S-89°N	Cheng and Zhu (2016); Cheng et al. (2017)
5 ICDC	1993-2016*	Y (1993)	---	Y (2005)	---	Monthly	Gouretzki and Koltermann (2007)
6 IPRC	2005-2016*	---	---	Y	---	Monthly	http://apdrc.soest.hawaii.edu/projects/argo
7 JAMSTEC	2005-2016*	---	---	Y	---	Monthly	Hosoda et al. (2008)
8 MRI/JMA	1970-2016 (rel. to 1961-1990 averages)	Y/E (0-300)	Y/E	Y/E	---	Yearly 89°S-89°N	Ishii et al. (2017)
9 NCEI/NOAA	1970-2016	Y/E	Y/E	Y/E	---	Yearly 89°S-89°N	Antonov et al. (2005)
10 SIO	2005-2016*	---	---	Y	---	Monthly	Roemmich and Gilson (2009)
11 SIO (Deep/abysal)	1990-2010 (as of 01/2018)	---	---	---	Y/E	Linear trend 89°S-89°N, as an aggregation of 32	Purkey and Johnson (2010)



							deep ocean basins	
--	--	--	--	--	--	--	-------------------------	--

405 *Table 2: In situ datasets and relevant information from originators and/or contributors.*

406

407

408 **2.3.2 Individual estimates**

409

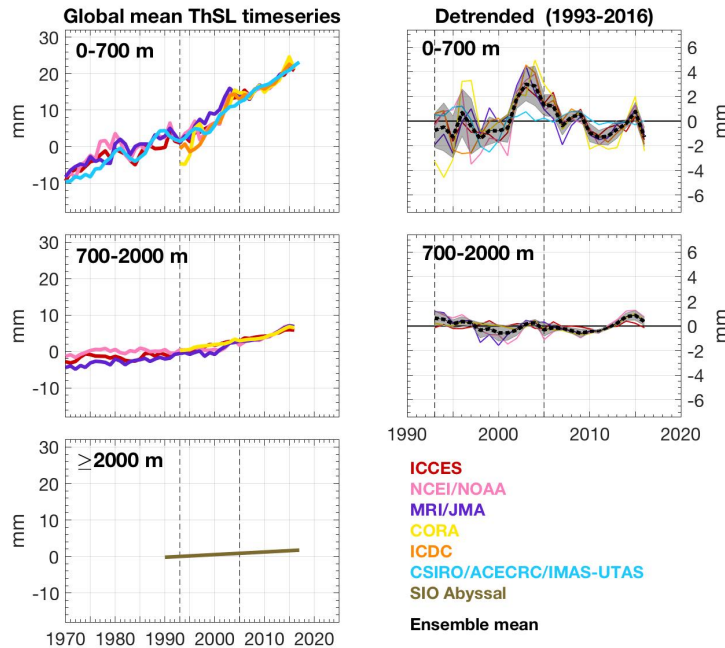
410 All in situ estimates compiled in this study show a steady rise in global mean thermosteric sea
 411 level, independent of depth-integration and decadal/multidecadal periods (Figure 4 and 5, left
 412 panels). As the deep/abyssal ocean estimate only illustrates the updated version of the linear
 413 trend from Purkey and Johnson (2010) for 1990-2010 extrapolated to 2016, it does not have
 414 any variability superimposed.

415 Interannual to decadal variability during the Altimeter era (since 1993) is similar for both 0-
 416 700 m and 700-2000 m, with larger amplitude in the upper ocean (Figure 4 and 5, right
 417 panels). For the 0-700 m, there is an apparent change in amplitude before/after the Argo era
 418 (since 2005), mostly due to a maximum (2-4 mm) around 2001-2004, except for one estimate.
 419 Higher amplitude and larger spread in variability between estimates before the Argo era is a
 420 symptom of the much sparser in situ coverage of the global ocean. Interannual variability over
 421 the Argo era (Figures 4 and 5, right panels) is mainly modulated by El Niño Southern
 422 Oscillation (ENSO) phases in the upper 500 m ocean, particularly for the Pacific, the largest
 423 ocean basin (Roemmich et al., 2011; Johnson and Birnbaum, 2017).

424 In terms of depth contribution, on average, the upper 300 m explains the same percentage
 425 (almost 70%) of the 0-700 m linear rate over both altimetry and Argo eras, but the
 426 contribution from the 0-700 m to 0-2000 m varies: about 75% for 1993-2016 and 65% for
 427 2005-2016. Thus, the 700-2000 m contribution increases by 10% during the Argo decade,
 428 when the number of observations within 700-2000 m has significantly increased.

429

430

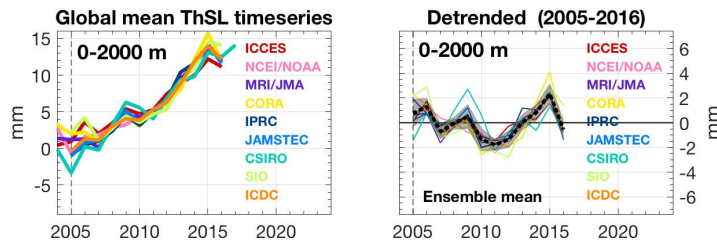


431

432 Figure 4. *Left- panels. Annual mean global mean thermosteric anomaly timeseries since 1970,*
 433 *from various research groups (colour) and for three depth-integrations: 0-700 m (top), 700-*
 434 *2000 m (middle), and below 2000 m (bottom). Vertical dashed lines are plotted along 1993*
 435 *and 2005. For comparison, all timeseries were offset arbitrarily. Right panels. Respective*
 436 *linearly detrended timeseries for 1993-2016. Black bold dashed line is the ensemble mean*
 437 *and gray shadow bar the ensemble spread (1-standard deviation). Units are mm.*

438

439



440

441 Figure 5. *Left- panel. Annual mean global mean thermosteric anomaly timeseries since 2004,*
 442 *from various research groups (colour) in the upper 2000 m. A vertical dashed line is plotted*
 443 *along 2005. For comparison, all timeseries were offset arbitrarily. Right panel. Respective*
 444 *linearly detrended timeseries for 2005-2016. Black bold dashed line is the ensemble mean*
 445 *and gray shadow bar the ensemble spread (1-standard deviation). Units are mm.*

446

447



448 **2.3.3. Ensemble mean thermosteric sea level**

449 Given that the global mean thermosteric sea level anomaly estimates compiled for this study
450 are not necessarily referenced to the same baseline climatology, they cannot be directly
451 averaged together to create an ensemble mean. To circumvent this limitation, we created an
452 ensemble mean in three steps, as explained below.

453 Firstly, we detrended the individual timeseries by removing a linear trend for 1993-2016 and
454 averaged together to obtain an “ensemble mean variability timeseries”. Secondly, we
455 averaged together the corresponding linear trends of the individual estimates to obtain an
456 “ensemble mean linear rate”. Thirdly, we combined this “ensemble mean linear rate” with the
457 “ensemble mean variability timeseries” to obtain the final ensemble mean timeseries. We
458 applied the same steps for the Argo era (2005-2016).

459 To maximise the number of individual estimates used in the final full-depth ensemble mean
460 timeseries, the three steps above were actually divided into depth-integrations and then
461 summed. For the Argo era, we summed 0-2000 m (9 estimates) and ≥ 2000 m (1 estimate). For
462 the altimetry era, we summed 0-700 m (6 estimates), 700-2000 (4 estimates) and ≥ 2000 m (1
463 estimate), although there is no statistical difference if the calculation was only based on the
464 sum of 0-2000 m (4 estimates) and ≥ 2000 m (1 estimate). There is also no statistical
465 difference between the full-depth ensemble mean timeseries created for the Altimeter and
466 Argo eras during their overlapping years (since 2005).

467 Figure 6 shows the full-depth ensemble mean timeseries over 1993-2016 and 2005-2016. It
468 reveals a global mean thermosteric sea level rise of about 30 mm over 1993-2016 (24 years)
469 or about 18 mm over 2005-2016 (12 years) , with a record high in 2015. These thermosteric
470 changes are equivalent to a linear rate of 1.32 ± 0.4 mm/yr and 1.31 ± 0.4 mm/yr
471 respectively.

472
473
474
475
476
477
478
479
480
481
482
483
484



485
486
487
488
489
490
491
492
493
494
495
496
497
498
499
500
501
502
503
504
505
506
507
508
509
510
511

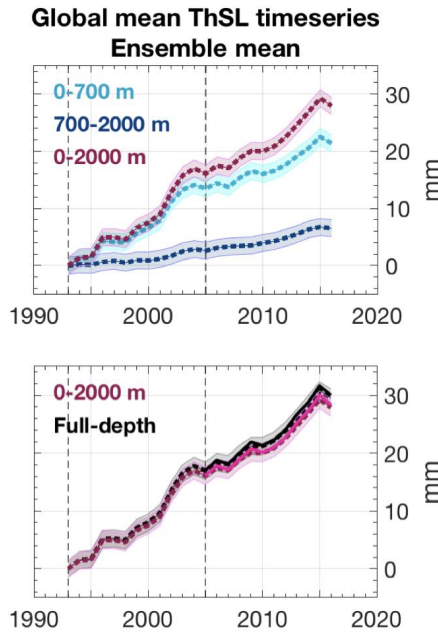
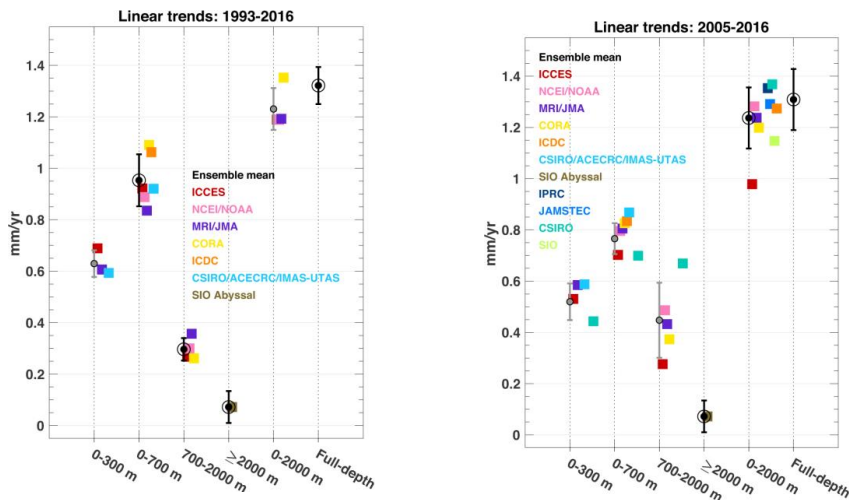


Figure 6: Ensemble mean timeseries for global mean thermosteric anomaly, for three-depth integrations (top) and for 0-2000 m and full-depth (bottom). In the bottom panel, dashed lines are relative to 1993-2016 whereas solid lines are relative to 2005-2016. Errorbars represent the ensemble spread (standard deviation). Units are mm.

512
513
514
515
516
517
518

Figure 7 shows thermosteric sea level trends for each of the data sets used over the 1996-2016 (left panel) and 2005-2016 (right panel) time spans and different depth ranges (including full depth), as well as associated ensemble mean trends. The full depth ensemble mean trend amounts to 1.3 ± 0.4 mm/yr over 2005-2016. It is similar to the 1993-2016 ensemble mean trend, suggesting negligible acceleration of the thermosteric component over the altimetry era.

519
520
521
522
523
524
525
526
527
528
529





530 *Figure 7: Linear rates of global mean thermosteric sea level for depth-integrations (x-axis), for*
531 *individual estimates and ensemble means, over 1993-2016 (left) and 2005-2016 (right). Ensemble*
532 *mean rates with a black circle were used in the estimation of the timeseries described in Section 2.3.4.*
533 *Errorbars are standard deviation due to spread of the estimates except for ≥ 2000 m. Units are mm/yr.*

534

535

536 2.4 Glaciers

537 Glaciers have strongly contributed to sea-level rise during the 20th century – around 40% -
538 and will continue to be an important part of the projected sea-level change during the 21st
539 century – around 30% (Kaser et al., 2006, Church et al., 2013, Gardner et al., 2013, Marzeion
540 et al., 2014, Zemp et al., 2015; Huss and Hock, 2015). Because glaciers are time-integrated
541 dynamic systems, a response lag of at least 10 years to a few hundred years is observed
542 between changes in climate forcing and glacier shape, mainly depending on glacier length and
543 slope (Johannesson et al., 1989, Bahr et al., 1998). Today, glaciers are globally (a notable
544 exception is the Karakoram/Kunlun Shan region, e.g. Brun et al., 2017) in a strong
545 disequilibrium with the current climate and are losing mass, due essentially to the global
546 warming in the second half of the 20th century (Marzeion et al., 2018).

547 Global glacier mass changes are derived from in situ measurements of glacier mass changes
548 or glacier length changes. Remote sensing methods measure elevation changes over entire
549 glaciers based on differencing digital elevation models (DEMs) from satellite imagery
550 between two epochs (or at points from repeat altimetry), surface flow velocities for
551 determination of mass fluxes, and glacier mass changes from space-based gravimetry. Mass
552 balance modeling driven by climate observations is also used (Marzeion et al., 2017 reviews
553 of these different methods).

554 Glacier contribution to sea level is primarily the result of their surface mass balance and
555 dynamic adjustment, plus iceberg discharge and frontal ablation (below sea level) in the case
556 of marine-terminating glaciers. The sum of worldwide glacier mass balances (MBs) does not
557 correspond to the total glacier contribution to sea-level change for the following reasons:

558 - Glacier ice below sea level does not contribute to sea-level change, apart from a
559 small lowering when replacing ice with seawater of a higher density. Total volume of glacier
560 ice below sea level is estimated to be 10 – 60 mm sea-level equivalent (SLE, Huss and
561 Farinotti, 2012, Haeberli and Linsbauer, 2013, Huss and Hock, 2015).

562 - Incomplete transfer of melting ice from glaciers to the ocean: meltwater stored in
563 lakes or wetlands, meltwater intercepted by natural processes and human activities (e.g.



564 drainage to lakes and aquifers in endorheic basins, impoundment in reservoirs, agriculture use
565 of freshwater, Loriaux and Casassa, 2013, Käab et al., 2015).

566 Despite considerable progress in observing methods and spatial coverage (Marzeion et al.,
567 2017), estimating glacier contribution to sea-level change remains challenging due to the
568 following reasons:

569 - Number of regularly observed glaciers (in the field) remains very low (0.25% of the
570 200 000 glaciers of the world have at least one observation and only 37 glaciers have long-
571 term observations, Zemp et al. 2015).

572 - Uncertainty of the total glacier ice mass remains high (Figure 8, Grinsted et al., 2013,
573 Pfeffer et al., 2014, Farinotti et al., 2017, Frey et al. 2014).

574 - Uncertainties in glacier inventories and DEMs are not negligible. Sources of
575 uncertainties include debris-covered glaciers, disappearance of small glaciers, positional
576 uncertainties, wrongly mapped seasonal snow, rock glaciers, voids and artifacts in DEMs
577 (Paul et al., 2004, Bahr and Radić, 2012).

578 - Uncertainties of satellite retrieval algorithms from space-based gravimetry and
579 regional DEM differencing are still high, especially for global estimates (Gardner et al. 2013,
580 Marzeion et al., 2017, Chambers et al., 2017).

581 - Uncertainties of global glacier modeling (e.g. initial conditions, model assumptions
582 and simplifications, local climate conditions, Marzeion et al., 2012).

583 - Knowledge about some processes governing mass balance (e.g. wind redistribution
584 and metamorphism, sublimation, refreezing, basal melting) and dynamic processes (e.g. basal
585 hydrology, fracturing, surging) remains limited (Farinotti et al., 2017).

586 An annual assessment of glacier contribution to sea-level change is difficult to perform (from
587 ground-based or space-based observations except space-based gravimetry), due to the sparse
588 and irregular observation of glaciers, and the difficulty of assessing accurately the annual
589 mass balance variability. Global annual averages are highly uncertain because of the sparse
590 coverage, but successive annual balances are uncorrelated and therefore averages over several
591 years are known with greater confidence.

592

593 ***2.4.1 Glacier datasets***

594 The following datasets are considered, with a focus on the trends of annual mass changes:

595 1. Update of Gardner et al., 2013 (Reager et al., 2016), from satellite gravimetry and
596 altimetry, and glaciological records, called G16.



597 2. Update of Marzeion et al, 2012 (Marzeion et al., 2017), from global glacier
598 modeling and mass balance observations, called M17.

599 3. Update of Cogley (2009) (Marzeion et al., 2017), from geodetic and direct mass-
600 balance measurements, called C17.

601 4. Update of Leclercq et al., 2011 (Marzeion et al., 2017), from glacier length changes,
602 called L17.

603 5. Average of GRACE-based estimates of Marzeion et al. (2017), from spatial
604 gravimetry measurements, called M17-G.

605 In general it is not possible to align measurements of glacier mass balance with the calendar.
606 Most in-situ measurements are for glaciological years that extend between successive annual
607 minima of the glacier mass at the end of the summer melt season. Geodetic measurements
608 have start and end dates several years apart and distributed irregularly through the calendar
609 year; some are corrected to align with annual mass minima but most are not. Consequently
610 measurements discussed here for 1993-2016 (the altimetry era) and 2005-2016 (the GRACE
611 and Argo era) are offset by up to a few months from the nominal calendar years.

612 Peripheral glaciers around the Greenland and Antarctic ice sheets are not treated in detail in
613 this section (see sections 2.5 and 2.6 for mass-change estimates that combine the peripheral
614 glaciers with the Greenland Ice Sheet and Antarctic Ice Sheet respectively). This is primarily
615 because of the lack of observations (especially ground-based measurements) and also because
616 of the high spatial variability of mass balance in those regions, and the slightly different
617 climate (e.g. precipitation regime) and processes (e.g. refreezing). In the past, these regions
618 have often been neglected. However Radić and Hock (2010) estimated the total ice mass of
619 peripheral glaciers around Greenland and Antarctica as 191 ± 70 mm SLE, with an actual
620 contribution to sea-level rise of around 0.23 ± 0.04 mm/yr (Radić and Hock, 2011). Gardner
621 et al. (2013) found a contribution from Greenland and Antarctic peripheral glaciers equal to
622 0.12 ± 0.05 mm/yr.

623 Note that some new or updated datasets for peripheral glaciers surrounding polar ice sheets
624 are under development and would hopefully be available in coming years in order to
625 incorporate Greenland and Antarctic peripheral glaciers in the estimates of global glacier
626 mass changes.

627

628 **2.4.2 Methods**

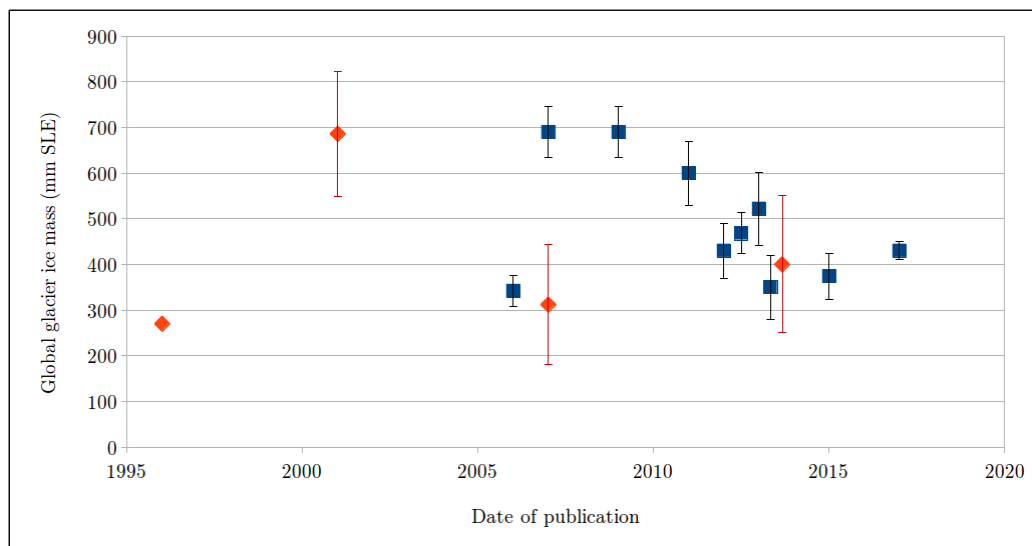
629 No globally complete observational dataset exists for glacier mass changes (except GRACE
630 estimates, see below). Any calculation of the global glacier contribution to sea-level change



631 has to rely on spatial interpolation or extrapolation or both, or to consider limited knowledge
632 of responses to climate change (due to the heterogeneous spatial distribution of glaciers
633 around the world). Consequently, most observational methods to derive glacier sea-level
634 contribution must extend local observations (in situ or satellite) to a larger region. Thanks to
635 the recent global glacier outline inventory (Randolph Glacier Inventory – RGI – first release
636 in 2012) as well as global climate observations, glacier modeling can now also be used to
637 estimate the contribution of glaciers to sea level (Marzeion et al., 2012, Huss and Hock, 2015,
638 Maussion et al., 2018, *subm.*). Still, those global modeling methods need to globalize local
639 observations and glacier processes which require fundamental assumptions and
640 simplifications. Only GRACE-based gravimetric estimates are global but they suffer from
641 large uncertainties in retrieval algorithms (signal leakage from hydrology, GIA correction)
642 and coarse spatial resolution, not resolving smaller glacierized mountain ranges or those
643 peripheral to the Greenland ice sheet.

644 DEM differencing method is not yet global, but regional, and can hopefully in the near future
645 be applied globally. This method needs also to convert elevation changes to mass changes
646 (using assumptions on snow and ice densities). In contrast, very detailed glacier surface mass
647 balance and glacier dynamic models are today far from being applicable globally, mainly due
648 to the lack of crucial observations (e.g., meteorological data, glacier surface velocity and
649 thickness) and of computational power for the more demanding theoretical models. However,
650 somewhat simplified approaches are currently developed to make best use of the steadily
651 increasing datasets. Modeling-based estimates suffer also from the large spread in estimates of
652 the actual global glacier ice mass (Figure 8). The mean value is 469 +/- 146 mm SLE, with
653 recent studies converging towards a range of values between 400 and 500 mm SLE global
654 glacier ice mass. But as mentioned above, a part of this ice mass will not contribute to sea
655 level.

656



657 Fig 8. Evolution of global glacier ice mass estimates (red marks are IPCC reports). Note that
658 Antarctica and Greenland peripheral glaciers are taken into account in this figure.

659

660 **2.4.3 Results (trends)**

661 Table 3 presents most recent estimates of trends in global glacier mass balances.

662

	1993 – 2016 mm/yr SLE	2005 – 2016 mm/yr SLE
G16		0.70 +/- 0.070 ^a
M17	0.68 +/- 0.032	0.80 +/- 0.048
C17	0.63 +/- 0.070	0.75 +/- 0.070 ^b
L17		0.84 +/- 0.640 ^c
M17-G		0.61 +/- 0.070 ^d

663

664 Table 3: All data are in mm/yr SLE. ^a The time period of G16 is 2002 – 2014. ^b The time
665 period of C17 is 2003 – 2009. ^c The time period of L17 is 2003 – 2009. ^d The time period of
666 M17-G is 2002/2005 – 2013/2015 because this value is an average of different estimates.

667

668 The ensemble mean contribution of glaciers to sea-level rise for the time period 1993 – 2016
669 is 0.65 +/- 0.051 mm/yr SLE and 0.74 +/- 0.18 mm/yr for the time period 2005 – 2016



670 (uncertainties are averaged). Different studies refer to different time periods. However,
671 because of the probable low variability of global annual glacier changes, compared to other
672 components of the sea-level budget, averaging trends for slightly different time periods is
673 appropriate.

674 The main source of uncertainty is that the vast majority of glaciers are unmeasured, which
675 makes interpolation or extrapolation necessary, whether for in situ or satellite measurements,
676 and for glacier modeling. Other main contributions to uncertainty in the ensemble mean stem
677 from methodological differences, such as the downscaling of atmospheric forcing required for
678 glacier modeling, the separation of glacier mass change to other mass change in the spatial
679 gravimetry signal and the derivation of observational estimates of mass change from different
680 raw measurements (e.g. length and volume changes, mass balance measurements and geodetic
681 methods) all with their specific uncertainties.

682

683 **2.5 Greenland**

684 Ice sheets are the largest potential source of future sea level rise (SLR) and represent the
685 largest uncertainty in projections of future sea level. Almost all land ice (~99.5%) is locked in
686 the ice sheets, with a volume in sea level equivalent/SLE terms of 7.4 m for Greenland, and
687 58.3 m for Antarctica. It has been estimated that approximately 25% to 30% of total land ice
688 contribution to sea level rise over the last decade has been from the Greenland ice sheet (e.g.
689 Dieng et al., 2017, Box and Colgan, 2017).

690 There are three main methods that can be used to estimate the mass balance of the Greenland
691 ice sheet: (1) measurement of changes in elevation of the ice surface over time (dh/dt) either
692 from imagery or altimetry; (2) the mass budget or Input-Output Method (IOM) which
693 involves estimating the difference between the surface mass balance and ice discharge; and
694 (3) consideration of the redistribution of mass via gravity anomaly measurements which only
695 became viable with the launch of GRACE in 2002. Uncertainties due to, for example, the GIA
696 correction are small in Greenland compared to Antarctica: on the order of ± 20 Gt/yr mass
697 equivalent (Khan et al., 2016). Prior to 2003, mass trends are reliant on IOM and altimetry.
698 Both techniques have limited sampling in time and/or space for parts of the satellite era
699 (1992-2002) and errors for this earlier period are, therefore, higher (van den Broeke et al.,
700 2016, Hurkmans et al., 2014).

701 The consistency between the three methods mentioned above was demonstrated for Greenland
702 by (Sasgen et al., 2012) for the period 2003-2009. Ice sheet wide estimates showed excellent



703 agreement although there was less consistency at a basin scale. We have, therefore, high
704 confidence and relatively low uncertainties in the rates for the Greenland ice sheet in the
705 satellite era.

706

707 **2.5.1 Datasets considered for the assessment**

708 This assessment of sea level budget contribution from the Greenland ice sheet considers the
709 following datasets:

Reference	Time period	Method
Update from Barletta et al. (2013)	2003-2016	GRACE
Groh and Horwath (2016)	2003-2015	GRACE
Update from Luthcke et al. (2013)	2003-2015	GRACE
Update from Sasgen et al. (2012)	2003-2016	GRACE
Update from Schrama et al. (2014)	2003-2016	GRACE
Update from (van den Broeke et al., 2016)	1993-2016	Input/output Method (IOM)
Wiese et al. (2016)	2003-2016	GRACE
Update from Wouters et al. (2008)	2003-2016	GRACE

710 *Table 4. The datasets received for consideration in this assessment*

711

712 **2.5.2. Methods and analyses**

713 All but one of these datasets are based on GRACE data and therefore provide annual time
714 series from ~2002 onwards. The one exception uses IOM (van den Broeke et al., 2016) to
715 give an annual mass time series for a longer time period (1993 onwards).

716 Notwithstanding this, each group has chosen their own approach to estimate mass balance
717 from GRACE observations. As the aim of this Global Sea Level Budget assessment is to
718 compile existing results (rather than undertake new analyses), we have not imposed a specific
719 methodology. Instead, we asked for the contributed datasets to reflect each group's 'best
720 estimate' of annual trends for Greenland using the method(s) they have published.

721 Greenland contains glaciers and ice caps around the margins of the main ice sheet, often
722 referred to as peripheral GIC (PGIC), which are a significant proportion of the total mass
723 imbalance (circa 15-20%) (Bolch et al., 2013). Some studies consider the mass balance of the
724 ice sheets and the PGIC separately but there has been, in general, no consistency in the



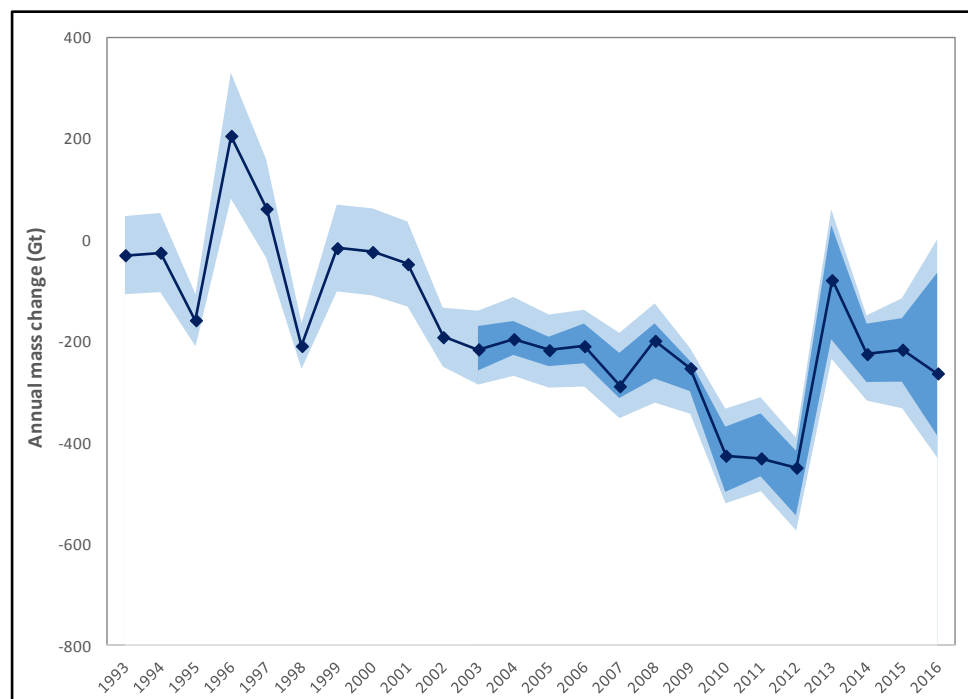
725 treatment of PGIC and many studies do not specify if they are included or excluded from the
 726 total. The GRACE satellites have an approximate spatial resolution of 300 km and the large
 727 number of studies that use GRACE, by default, include all land ice within the domain of
 728 interest. For this reason, the results below for Greenland mass trends all include PGIC.

729 From these datasets, for each year from 1993 to 2015 (and 2016 where available), we have
 730 calculated an average change in mass (calculated as the weighted mean based on the stated
 731 error value for each year) and an error term. Prior to 2003, the results are based on just one
 732 dataset (van den Broeke et al., 2016).

733

734 **2.5.3 Results**

735



736

737 *Figure 9. Greenland annual mass change 1993 to 2016. The medium blue region shows the*
 738 *range of estimates from the datasets listed in Table 1. The lighter blue region shows the range*
 739 *of estimates when stated errors are included, to provide upper and lower bounds. The dark*
 740 *blue line shows the weighted mean mass trend.*

741

742

743



744

Year	Δ mass (Gt/yr)	Error (Gt.yr)	σ (Gt)
1993	-30	76	
1994	-25	77	
1995	-159	51	
1996	205	123	
1997	61	97	
1998	-209	45	
1999	-16	85	
2000	-24	85	
2001	-48	83	
2002	-192	58	
2003	-216	13	28
2004	-196	12	24
2005	-218	13	21
2006	-210	12	29
2007	-289	10	31
2008	-199	11	39
2009	-253	11	21
2010	-426	9	42
2011	-431	9	47
2012	-450	10	41
2013	-80	13	76
2014	-225	13	38
2015	-217	13	48
2016	-263	23	123
Average estimate 1993-2015	-167	54	
Average estimate 1993-2016	-171	53	
Average estimate 2005-2015	-272	11	
Average estimate 2005-2016	-272	13	

745



746 *Table 5. Annual time series of Greenland mass change (GT/yr, negative values mean*
747 *decreasing mass). Δ mass is calculated as the weighted mean based on the stated error value*
748 *for each year. The error for each year is calculated as the mean of all stated 1-sigma errors*
749 *divided by \sqrt{N} where N is the number of datasets available for that year, assuming that*
750 *the errors are uncorrelated. The standard deviation (σ) is also given to illustrate the level of*
751 *agreement between datasets for each year when multiple datasets are available (2003*
752 *onwards).*

753

754 There is generally a good level of agreement between the datasets (Figure 9), and taken
755 together they provide an average estimate of 171 Gt/yr of ice mass loss (or sea level budget
756 contribution) from Greenland for the period 1993 to 2016, increasing to 272 Gt/yr for the
757 period 2005 to 2016 (Table 5).

758 All the datasets illustrate the previously documented accelerating mass loss up to 2012
759 ((Rignot et al., 2011); (Velicogna, 2009)). In 2012, the ice sheet experienced exceptional
760 surface melting reaching as far as the summit (Nghiem et al., 2012) and a record mass loss
761 since, at least 1958, of over 400 Gt (van den Broeke et al., 2016) . The following years,
762 however, show a reduced loss (not more than 270 Gt in any year). Inclusion of the years since
763 2012 in the 2005-2016 trend estimate reduces the overall rate of mass loss acceleration and its
764 statistical significance. There is greater divergence in the GRACE time series for 2016. We
765 associate this with the degradation of the satellites as they came towards the end of their
766 mission. For 2005-2012, it might be inferred that there is a secular trend towards greater mass
767 loss and from 2010-2012 the value is relatively constant. Inter-annual variability in mass
768 balance of the ice sheet is driven, primarily, by the surface mass balance (i.e. atmospheric
769 weather) and it is apparent that the magnitude of this year to year variability can be large:
770 exceeding 360 Gt (or 1 mm sea level equivalent) between 2012 and 2013. Caution is required,
771 therefore, in extrapolating trends from a short record such as this.

772

773 **2.6 Antarctica**

774 The annual turn over of mass of Antarctica is about 2,200 Gt/yr (over 6 mm/yr of SLE), 5
775 times larger than in Greenland (Wessem et al. 2017). In contrast with Greenland, ice and
776 snow melt have a negligible influence on Antarctica's mass balance which is therefore
777 completely controlled by the balance between snowfall accumulation in the drainage basins
778 and ice discharge along the periphery. The continent is also 7 times larger than Greenland,



779 which makes satellite techniques absolutely essential to survey the continent. Interannual
780 variations in accumulation are large in Antarctica, showing decadal to multi-decadal
781 variability, so that many years of data are required to extract trends, and missions limited to
782 only a few years may produce misleading results (e.g. Rignot et al., 2011).

783 As in Greenland, the estimation of the mass balance has employed a variety of techniques,
784 including 1) the gravity method with GRACE since April 2002 until the end of the mission in
785 late 2016; 2) the input and output method (IOM) using a series of Landsat and Synthetic-
786 Aperture Radar (SAR) satellites for measuring ice motion along the periphery (Rignot et al.,
787 2011), ice thickness from airborne depth radar sounders such as Operation IceBridge
788 (Leuschen et al., 2014), and reconstructions of surface mass balance using regional
789 atmospheric climate models constrained by re-analysis data (RACMO, MAR and others); and
790 3) radar/laser altimetry method which mix various satellite altimeters and correct ice elevation
791 changes with density changes from firm models. The largest uncertainty in the GRACE
792 estimate in Antarctica is the GIA which is larger than in Greenland and a large fraction of the
793 observed signal. The IOM method compares two large numbers with large uncertainties to
794 estimate the mass balance as the difference. In order to detect an imbalance at the 10% level,
795 surface mass balance and ice discharge need to be estimated with a precision typically of 5 to
796 7%. The altimetry method is limited to areas of shallow slope, hence is difficult to use in the
797 Antarctic Peninsula and in the deep interior of the Antarctic continent due to unknown
798 variations of the penetration depth of the signal in snow/firn. The only method that expresses
799 the partitioning of the mass balance between surface processes and dynamic processes is the
800 IOM method (e.g. Rignot et al., 2011). The gravity method is an integrand method which does
801 not suffer from the limitations of SMB models but is limited in spatial resolution (e.g.
802 Velicogna et al., 2014). The altimetry method provides independent evidence of changes in
803 ice dynamics, e.g. by revealing rapid ice thinning along the ice streams and glaciers revealed
804 by ice motion maps, as opposed to large scale variations reflecting a variability in surface
805 mass balance (McMillan et al., 2014).

806 All these techniques have improved in quality over time and have accumulated a decade to
807 several decades of observations, so that we are now able to assess the mass balance of the
808 Antarctic continent using methods with reasonably low uncertainties, and multiple lines of
809 evidence as the methods are largely independent, which increases confidence in the results.
810 There is broad agreement in the mass loss from the Antarctic Peninsula and West Antarctica;
811 most residual uncertainties are associated with East Antarctica as the signal is relatively small



812 compared to the uncertainties, although most estimates tend to indicate a low contribution to
813 sea level (e.g. Shepherd et al., 2012).

814

815 **2.6.1 Datasets considered for the assessment**

816 This assessment consider the following datasets:

817

Reference	Method	2005-2015 SLE Trend (mm/yr)	1993-2015 SLE Trend (mm/yr)
Update from Martín-Español et al. (2016)	Joint inversion GRACE/altimetry /GPS	0.43±0.07	-
Update from Fosberg et al. (2017)	Joint inversion GRACE/CryoSat	0.31±0.02	-
Update from Groh and Horwath (2016)	GRACE	0.32±0.11	-
Update from Luthcke et al. (2013)	GRACE	0.36±0.06	-
Update from Sasgen et al. (2013)	GRACE	0.47±0.07	-
Update from Velicogna et al. (2014)	GRACE	0.33±0.08	-
Update from Wiese et al. (2016)	GRACE	0.39±0.02	-
Update from Wouters et al. (2013)	GRACE	0.41±0.05	-
Update from Rignot et al. 2011	Input/output method (IOM)	0.46±0.05	0.25±0.1
Update from Schrama et al. (2014); version 1	GRACE ICE6G GIA model	0.47±0.03	
Update from Schrama et al. (2014); version 2	GRACE Updated GIA models	0.33±0.03	

818 Table 6. The datasets received for consideration in this assessment including trend for the
819 2005-2015 and 1993-2015 expressed in mm/yr SLE. Positive values mean positive
820 contribution to sea level (i.e. sea level rise)

821

822



823 2.6.2 Methods and analyses

824 The datasets used in this assessment are Antarctica mass balance time series generated using
825 different approaches. Two estimates are a joint inversion of GRACE/altimetry/GPS data
826 Martín-Español et al. (2016), and GRACE and CryoSat data Fosberg et al. (2017). Two
827 methods are mascon solutions obtained from the GRACE intersatellite range-rate
828 measurements (Luthcke et al., 2013; Wiese et al., 2016), three estimates use the GRACE
829 spherical harmonics solutions (Velicogna et al., 2014; Wiese et al., 2016; Wouters et al.,
830 2013) and one gridded GRACE products (Sasgen et al., 2013).

831 All GRACE time series were provided as monthly time series except for the one using the
832 Martín-Español et al. (2016) method that were provided as annual estimates. In addition,
833 different groups use different GIA corrections, therefore the spread of the trend solutions
834 represents also the error associated to the GIA correction which, in Antarctica, is the largest
835 source of uncertainty. Sasgen et al. (2013) used their own GIA solution (Sasgen et al., 2017),
836 Martín-Español et al. (2016) as well, Luthcke et al., (2013), Velicogna et al. (2014) and
837 Groh and Horwath (2016) used IJ05-R2 (Ivins et al., 2013), Wouter et al. (2013) used
838 Whitehouse et al. (2012), and Wise et al. (2016) used A et al. (2013). In addition, Groh and
839 Horwath (2016) did not include the peripheral glaciers and ice caps, while all other estimates
840 do.

841 Table 6 shows the Antarctic sea level contribution to sea level during 2005-2015 from the
842 different GRACE solutions, for the input and output method (IOM), and from the altimetry
843 method. We a single dataset, OIB (Rignot et al. 2011) that provides trends for the period
844 1993-2015. For the period 2005-2015, we calculated the annual sea level contribution from
845 Antarctica using GRACE, IOM and altimetry estimates (Table 7).

846 As we are interested in evaluating the long term trend and inter-annual variability of the
847 Antarctic contribution to sea level, for each GRACE datasets available in monthly time series,
848 we first removed the annual and sub-annual components of the signal by applying a 13-month
849 averaging filter and we then used the smoothed time series to calculate to annual mass
850 change. Figure 10 shows the annual sea level contribution from Antarctica calculated from
851 the GRACE derived estimates and for the Input and Output Method (IOM). The GRACE
852 mean annual estimates are calculated as the mean of the annual contributions from the
853 different groups, and the associated error calculated as the sum of the spread of the annual
854 estimates and the mean annual error.

855

856



857

858

859 **2.6.3 Results**

860

861

862

863

864

865

866

867

868

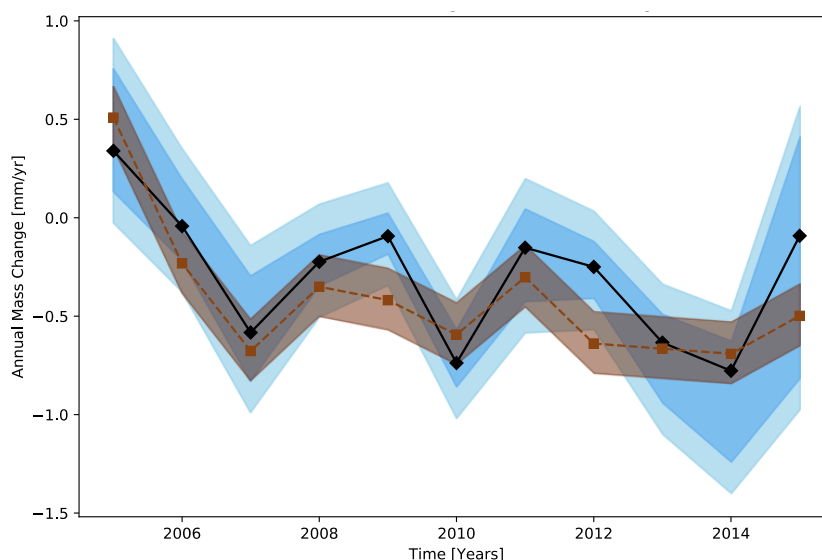
869

870

871

872

873



874

875

876

877

878

879

880

Figure 10. Antarctic annual sea level contribution during 2005 to 2015. The black squares are the mean annual sea level calculated using the GRACE datasets listed in Table 2.6a. The darker blue band shows the range of estimates from the datasets. The light blue band account for the error in the different GRACE estimates. The brown squares are the annual sea level contribution calculated using the input output method (updated from Rignot et al. 2011), the light brown band is the associated error.

Year	GRACE mm/yr SLE	IOM mm/yr SLE	Mean mm/yr SLE
2005	-0.34±0.47	-0.51±0.16	-0.42±0.31
2006	0.04±0.36	0.23±0.16	0.14±0.26
2007	0.58±0.42	0.68±0.16	0.63±0.29
2008	0.22±0.29	0.35±0.16	0.29±0.22
2009	0.09±0.26	0.42±0.16	0.26±0.21
2010	0.74±0.30	0.59±0.16	0.67±0.23



2011	0.15±0.39	0.30±0.16	0.23±0.27
2012	0.25±0.30	0.64±0.16	0.44±0.23
2013	0.63±0.38	0.67±0.16	0.65±0.27
2014	0.78±0.46	0.69±0.16	0.73±0.31
2015	0.09±0.77	0.50±0.16	0.29±0.46
Average estimate 2005-2015	0.38±0.06	0.46±0.05	0.42±0.06

881 *Table 7. Annual sea level contribution from Antarctica during 2005-2015 from GRACE and*
 882 *input and Output Method (IOM) calculated as described above and expressed in mm/yr SLE.*
 883 *Also shown is the mean of the estimate from the two methods, associated errors are the mean*
 884 *of the two estimate errors. Positive values mean positive contribution to sea level (i.e. sea*
 885 *level rise)*

886

887 There is generally broad agreement between the GRACE datasets (Figure 10), as most of the
 888 differences between GRACE estimates are caused by differences in GIA correction. We find
 889 a reasonable agreement between GRACE and the IOM estimates although the IOM estimates
 890 indicate higher losses. Taken together, these estimates yield an average of 0.42 mm/yr sea
 891 level budget contribution from Antarctica for the period 2005 to 2015 (Table 7) and 0.25
 892 mm/yr sea level for the time period 1993-2005, where the latter value is based on IOM only.

893 All the datasets illustrate the previously documented accelerating mass loss of Antarctica
 894 ((Rignot et al., 2011) ; (Velicogna, 2009)). In 2005-2010, the ice sheet experienced ice mass
 895 loss driven by an increase in mass loss in the Amundsen Sea sector of West Antarctica
 896 (Mouginot et al., 2014). The following years showed a reduced increase in mass loss, as
 897 colder ocean conditions prevailed in the Amundsen Sea Embayment (ASE) sector of West
 898 Antarctica in 2012-2013 which reduced the melting of the ice shelves in front of the glaciers
 899 (Dutrieux et al., 2014). Divergence in the GRACE time series is observed after 2015 due to
 900 the degradation of the satellites towards the end of the mission.

901 The large inter-annual variability in mass balance in 2005-2015, characteristic of Antarctica,
 902 nearly masks out the trend in mass loss, which is more apparent in the longer time series than
 903 in short time series. The longer record highlights the pronounced decadal variability in ice
 904 sheet mass balance in Antarctica, demonstrating the need for multi decadal time series in
 905 Antarctica, which have been obtained only by IOM and Altimetry. The inter-annual
 906 variability in mass balance is driven almost entirely by surface mass balance processes. The



907 mass loss of Antarctica, about 200 Gt/yr in recent years, is only about 10% of its annual turn
908 over of mass (2,200 Gt/yr), in contrast with Greenland where the mass loss has been growing
909 rapidly to nearly 100% of the annual turn over of mass. This comparison illustrates the
910 challenge of detecting mass balance changes in Antarctica, but at the same time that satellite
911 techniques and their interpretation have made tremendous progress over the last 10 years,
912 producing realistic and consistent estimates of the mass using a number of independent
913 methods.

914

915 **2.7 Terrestrial Water Storage**

916 Human transformations of the Earth's surface have impacted the terrestrial water balance,
917 including continental patterns of river flow and water exchange between land, atmosphere and
918 ocean, ultimately affecting global sea level. For instance, massive impoundment of water in
919 man-made reservoirs has reduced the direct outflow of water to the sea through rivers, while
920 groundwater abstractions, wetland and lake storage losses, deforestation and other land use
921 changes have caused changes to the terrestrial water balance, including changing
922 evapotranspiration over land, leading to net changes in land-ocean exchanges (Chao et al.,
923 2008; Wada et al., 2012a,b; Konikow 2011; Church et al., 2013; Doll et al. ???). Overall, the
924 combined effects of direct anthropogenic processes have reduced land water storage,
925 increasing the rate of sea level rise (SLR) by 0.3-0.5 mm yr⁻¹ during recent decades (Church
926 et al., 2013; Gregory et al., 2013; Wada et al., 2016). Additionally, recent work has shown
927 that climate driven changes in water stores can perturb the rate of sea level change over
928 interannual to decadal time scales, making global land mass budget closure sensitive to
929 varying observational periods (Cazenave et al., 2014; Dieng et al., 2015; Reager et al., 2016;
930 Rietbroek et al., 2016). Here we discuss each of the major component contributions from
931 land, with a summary in Table 8, and estimate the net terrestrial water storage (TWS)
932 contribution to sea level.

933

934 ***2.7.1 Direct anthropogenic changes in terrestrial water storage***

935

936 *Water impoundment behind dams*

937 Wada et al. (2016) built on work by Chao et al. (2008) to combine multiple global reservoir
938 storage data sets in pursuit of a quality-controlled global reservoir database. The result is a list
939 of 48064 reservoirs that have a combined total capacity of 7968 km³. The time history of



940 growth of the total global reservoir capacity reflects the history of the human activity in dam
941 building. Applying assumptions from Chao et al. (2008), Wada et al. (2016) estimated that
942 humans have impounded a total of 10,416 km³ of water behind dams, accounting for a
943 cumulative 29 mm drop in global mean sea level. From 1950 to 2000 when global dam-
944 building activity was at its highest, impoundment contributed to the average rate of sea level
945 change at -0.51 mm/year. This was an important process in comparison to other natural and
946 anthropogenic sources of sea level change over the past century, but has now largely slowed
947 due to a global decrease in dam building activity.

948

949 *Global groundwater depletion*

950 Groundwater currently represents the largest secular trend component to the land water
951 storage budget. The rate of groundwater depletion (GWD) and its contribution to sea level has
952 been subject to debate (Gregory et al., 2013; Taylor et al., 2013). In the IPCC AR4 (Solomon
953 et al., 2007), the contribution of non-frozen terrestrial waters (including GWD) to sea-level
954 variation was not considered due to its perceived uncertainty (Wada, 2016). Observations
955 from GRACE opened a path to monitor total water storage changes including groundwater in
956 data scarce regions (Strassberg et al., 2007; Rodell et al. 2009; Tiwari et al. 2009; Jacob et al.,
957 2012; Shamsudduha et al., 2012; Voss et al., 2013). Some studies have also applied global
958 hydrological models in combination with the GRACE data (see Wada et al., 2016 for a
959 review).

960 Earlier estimates of GWD contribution to sea level range from 0.075 mm yr⁻¹ to 0.30 mm yr⁻¹
961 (Sahagian et al., 1994; Gornitz, 1995, 2001; Foster and Loucks, 2006). More recently, Wada
962 et al. (2012b), using hydrological modelling, estimated that the contribution of GWD to
963 global sea level increased from 0.035 (±0.009) to 0.57 (±0.09) mm yr⁻¹ during the 20th century
964 and projected that it would further increase to 0.82 (±0.13) mm yr⁻¹ by 2050. Döll et al. (2014)
965 used hydrological modeling, well observations, and GRACE satellite gravity anomalies to
966 estimate a 2000–2009 global GWD of 113 km³ yr⁻¹ (0.314 mm yr⁻¹). This value represents the
967 impact of human groundwater withdrawals only and does not consider the effect of climate
968 variability on groundwater storage. A study by Konikow (2011) estimated global GWD to be
969 145 (±39) km³ yr⁻¹ (0.41 ±0.1 mm yr⁻¹) during 1991–2008 based on measurements of changes
970 in groundwater storage from in situ observations, calibrated groundwater modelling, GRACE
971 satellite data and extrapolation to unobserved aquifers.

972 An assumption of most existing global estimates of GWD impacts on sea level change is that
973 nearly 100% of the GWD ends up in the ocean. However, groundwater pumping can also



974 perturb regional climate due to land-atmosphere interactions (Lo and Famiglietti, 2013). A
975 recent study by Wada et al. (2016) used a coupled land-atmosphere model simulation to track
976 the fate of water pumped from underground and found it more likely that ~80% of the GWD
977 ends up in the ocean over the long-term, while 20% re-infiltrates and remains in land storage.
978 They estimated an updated contribution of GWD to global SLR ranging from 0.02 (± 0.004)
979 mm yr^{-1} in 1900 to 0.27 (± 0.04) mm yr^{-1} in 2000 (Figure 11). This indicates that previous
980 studies had likely overestimated the cumulative contribution of GWD to global SLR during
981 the 20th century and early 21st century by 5-10 mm.

982

983 Land cover and land-use change

984 Humans have altered a large part of the land surface, replacing 33% (Vitousek et al., 1997) or
985 even 41 % (Sterling et al., 2013) of natural vegetation by anthropogenic land cover such as
986 crop fields or pasture. Such land cover change can affect terrestrial hydrology by changing the
987 infiltration-to-runoff ratio, and can impact subsurface water dynamics by modifying recharge
988 and increasing groundwater storage (Scanlon et al., 2007). The combined effects of
989 anthropogenic land cover changes on land water storage can be quite complex. Bosmans et
990 al. (2016), in a modelling study with PCR-GLOBWB, estimated that land cover change has
991 contributed to a discharge increase of $1058 \text{ km}^3 \text{ yr}^{-1}$, on the same order of magnitude as the
992 effect of human water use. These recent model results suggest that land-use change is an
993 important topic for further investigation in the future. So far, this contribution remains highly
994 uncertain.

995

996 Deforestation/afforestation

997 At present, large losses in tropical forests and moderate gains in temperate-boreal forests
998 result in a net reduction of global forest cover (FAO, 2015; Keenan et al., 2015; MacDicken,
999 2015; Sloan and Sayer, 2015). Net deforestation releases carbon and water stored in both
1000 biotic tissues and soil, which leads to sea level rise through three primary processes:
1001 deforestation-induced runoff increases (Gornitz et al., 1997), carbon loss-related decay and
1002 plant storage loss, and complex climate feedbacks (Butt et al., 2011; Chagnon and Bras, 2005;
1003 Nobre et al., 2009; Shukla et al., 1990; Spracklen et al., 2012). Due to these three causes, and
1004 if uncertainties from the land-atmospheric coupling are excluded, a summary by Wada et al.
1005 (2016) suggests that the current net global deforestation leads to an upper-bound contribution
1006 of $\sim 0.035 \text{ mm/yr SLE}$.

1007

1008 Wetland degradation

1009 Wetland degradation contributes to sea level primarily through (i) direct water drainage or
1010 removal from standing inundation, soil moisture, and plant storage, and (ii) water release from
1011 vegetation decay and peat combustion. Wada et al. (2016) consider a recent wetland loss rate
1012 of 0.565% yr⁻¹ since 1990 (Davidson, 2014) and a present global wetland area of 371 mha
1013 averaged from three databases: Matthews natural wetlands (Matthews and Fung, 1987),
1014 ISLSCP (Darras, 1999), and DISCover (Belward et al., 1999; Loveland and Belward, 1997).
1015 They assume a uniform 1-meter depth of water in wetlands (Milly et al., 2010), to estimate a
1016 contribution of recent global wetland drainage to sea level of 0.067 mm/yr. Wada et al. (2016)
1017 apply a wetland area and loss rate as used for assessing wetland water drainage, to determine
1018 the annual reduction of wetland carbon stock since 1990, if completely emitted, releases water
1019 equivalent to 0.003–0.007 mm yr⁻¹ SLE. Integrating the impacts of wetland drainage,
1020 oxidation and peat combustion, Wada et al. (2016) suggest that the recent global wetland
1021 degradation results in an upper bound of 0.074 mm/yr SLE.

1022

1023 Lake storage changes

1024 Lakes store the greatest mass of liquid water on the terrestrial surface (Oki and Kanae, 2006),
1025 yet, because of their “dynamic” nature (Sheng et al., 2016; Wang et al., 2012), their overall
1026 contribution to sea level remains uncertain. In the past century, perhaps the greatest
1027 contributor in global lake storage was the Caspian Sea (Milly et al., 2010), where the water
1028 level exhibits substantial oscillations attributed to meteorological, geological, and
1029 anthropogenic factors (Ozyavav et al., 2010, Chen et al., 2017). Assuming the lake level
1030 variation kept pace with groundwater changes (Sahagian et al., 1994), the overall contribution
1031 of the Caspian Sea, including both surface and groundwater storage variations through 2014,
1032 has been about 0.03 mm yr⁻¹ SLE since 1900, 0.075 (±0.002) mm yr⁻¹ since 1995, or 0.109
1033 (±0.004) mm yr⁻¹ since 2002. Additionally, between 1960 and 1990, the water storage in the
1034 Aral Sea Basin declined at a striking rate of 64 km³ yr⁻¹, equivalent to 0.18 mm yr⁻¹ SLE
1035 (Sahagian, 2000; Sahagian et al., 1994; Vörösmarty and Sahagian, 2000) due mostly to
1036 upstream water diversion for irrigation (Perera, 1993), which was modeled by Pokhrel et al.
1037 (2012) to be ~500 km³ during 1951–2000, equivalent to 0.03 mm yr⁻¹ SLE. Dramatic decline
1038 in the Aral Sea continued in the recent decade, with an annual rate of 6.043 (±0.082) km³ yr⁻¹
1039 measured from 2002 to 2014 (Schwatke et al., 2015). Assuming that groundwater drainage
1040 has kept pace with lake level reduction (Sahagian et al., 1994), the Aral Sea has contributed
1041 0.0358 (±0.0003) mm yr⁻¹ to the recent sea level rise.



1042

1043

1044

1045 Water cycle variability

1046 Natural changes in the interannual to decadal cycling of water can have a large effect on the
1047 apparent rate of sea level change over decadal and shorter time periods (Milly et al., 2003;
1048 Lettenmaier and Milly, 2009; Llovel et al., 2010). For instance, ENSO-driven modulations of
1049 the global water cycle can be important in decadal-scale sea level budgets and can mask
1050 underlying secular trends in sea level (Cazenave et al., 2014, Nerem et al., 2018).

1051 Sea level variability due to climate-driven hydrology represents a super-imposed variability
1052 on the secular rates of SLR and not a long-term offset to the GMSL. While this term can be
1053 large and is important in the interpretation of the sea level record, it is arguably the most
1054 difficult term in the land water budget to quantify.

1055

1056

1057

1058

1059

1060

1061

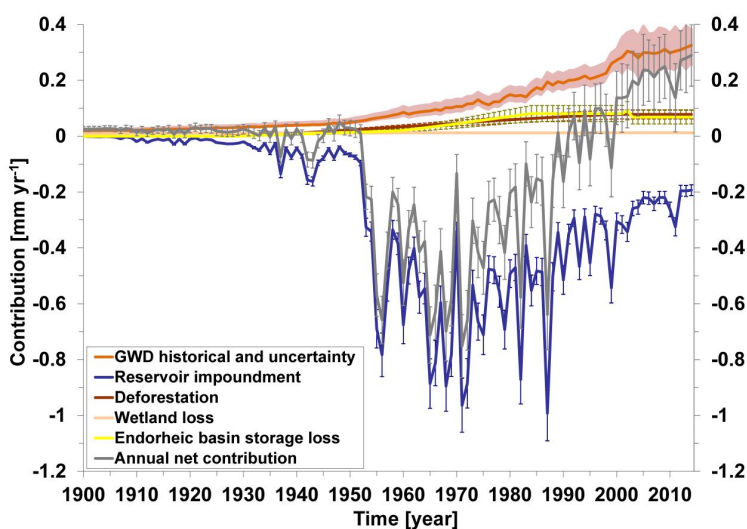
1062

1063

1064

1065

1066



1067

1068

1069 *Figure 11: Time series of the estimated annual contribution of terrestrial water storage*
1070 *change to global sea-level over the period 1900-2014 (rates in mm yr⁻¹ SLE) (modified from*
1071 *Wada et al., 2016).*

1072

1073 **2.7.2. Net terrestrial water storage**

1074

1075 GRACE-based estimates



40

1076 Measurements of non-ice-sheet continental land mass from GRACE satellite gravity have
1077 been presented in several recent studies (Jensen et al., 2013, Rietbroek et al., 2016; Reager et
1078 al., 2016, Scanlon et al., 2018), and can be used to constrain a global land mass budget. Note
1079 that these ‘top-down’ estimates contain both climate-driven and direct anthropogenic driven
1080 effects, which makes them most useful in assessing the total impact of land water storage
1081 changes and closing the budget of all contributing terms. GRACE observations, when
1082 averaged over the whole land domain following Reager et al. (2016), indicate a total TWS
1083 change (including glaciers) over the 2002-2014 study period of approximately $+0.32 \pm 0.13$
1084 mm year^{-1} sea level equivalent (i.e., ocean gaining mass). Global mountain glaciers have been
1085 estimated to lose mass at a rate of $0.65 \pm 0.09 \text{ mm yr}^{-1}$ (e.g. Gardner et al., 2013; Reager et
1086 al., 2016) during that period, such that a mass balance indicates that global glacier-free land
1087 gained water at a rate of $-0.33 \pm 0.16 \text{ mm yr}^{-1}$ SLE (i.e., ocean losing mass; Figure 12). A
1088 roughly similar estimate was found from GRACE using glacier free river basins globally ($-$
1089 $0.21 \pm 0.09 \text{ mm/yr}$) (Scanlon et al., 2018). Thus, the GRACE-based net TWS estimates
1090 suggest a negative sea level contribution from land over the GRACE period (Table 8).
1091 However, mass change estimate from GRACE incorporates uncertainty from all potential
1092 error sources that arise in processing and post-processing of the data, including from the GIA
1093 model, and from the geocenter and mean pole corrections.

1094

1095

1096

1097

1098

1099

1100

1101

1102

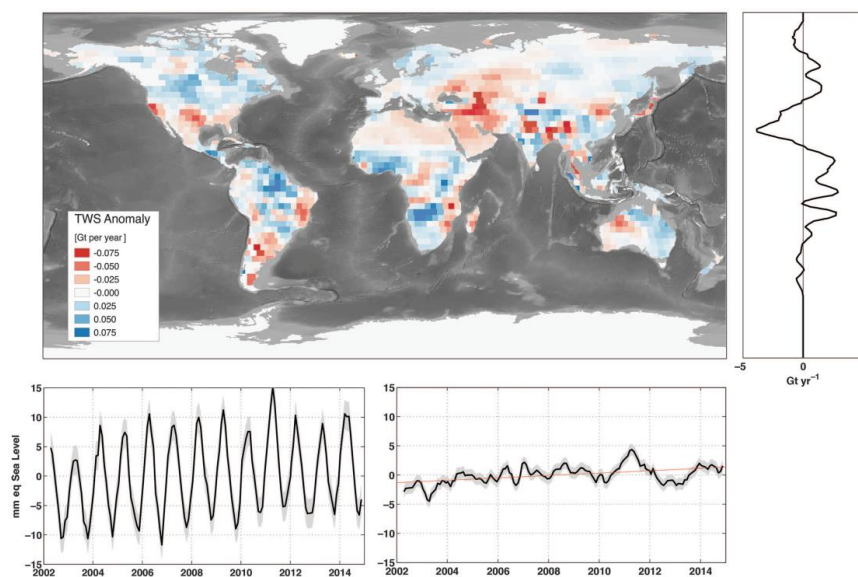
1103

1104

1105

1106

1107



1108 *Figure 12: An example of trends in land water storage from GRACE observations, April*
1109 *2002 to November 2014. Glaciers and ice sheets are excluded. Shown are the global map*

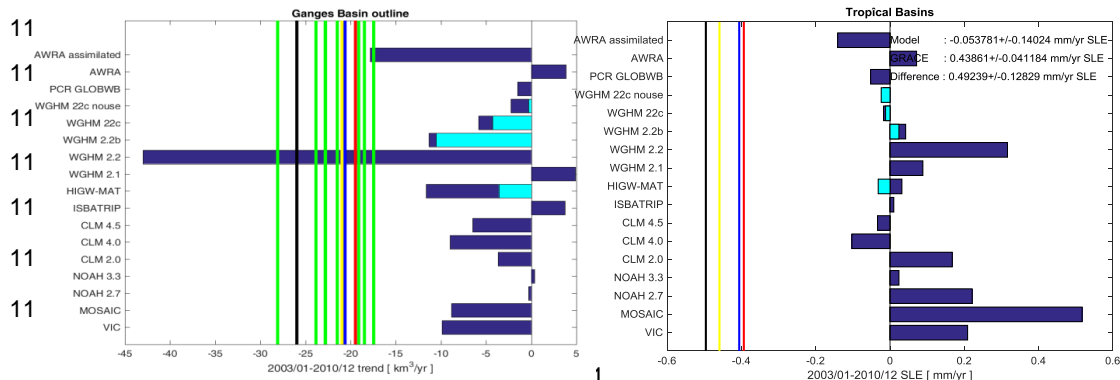
1110 (gigatons per year), zonal trends, and full time series of land water storage (in mm yr^{-1} SLE).
 1111 Following methods details in Reager et al., (2016), GRACE shows a total gain in land water
 1112 storage during the 2002-2014 period, corresponding to a sea level trend of $-0.33 \pm 0.16 \text{ mm}$
 1113 yr^{-1} SLE (modified from Reager et al., 2016). These trends include all human-driven and
 1114 climate-driven processes in Table 1, and can be used to close the land water budget over the
 1115 study period.

1116

1117 Estimates based on global hydrological models

1118 Global land water storage can also be estimated from global hydrological models (GHMs)
 1119 and global land surface models (LSMs). These compute water, or water and energy
 1120 balances, at the Earth surface, yielding time variations of water storage in response to
 1121 prescribed atmospheric data (temperature, humidity and wind) and the incident water and
 1122 energy fluxes from the atmosphere (precipitation and radiation). Meteorological forcing is
 1123 usually based on atmospheric model reanalyses. Model uncertainties result from several
 1124 factors. Recent work has underlined the large differences among different state-of-the-art
 1125 precipitation datasets (Beck et al., 2017) with large impacts on model results at seasonal
 1126 (Schellekens et al., 2017) and longer time scales (Felfelani et al., 2017). Another source of
 1127 uncertainty is the treatment of subsurface storage in soils and aquifers, as well as dynamic
 1128 changes in storage capacity due to representation of frozen soils and permafrost, the
 1129 complex effects of dynamic vegetation, atmospheric vapor pressure deficit estimation and
 1130 an insufficiently deep soil column. A recent study comparing water storage trends from 5
 1131 LSMs and 2 GHMs to GRACE storage trends found that models estimated the opposite
 1132 trend in net land water storage to GRACE for the 2002 – 2014 period, attributed to soil
 1133 depth limitations in models (Scanlon et al., 2018). These combined error sources are
 1134 responsible for a range of storage trends across models of approximately $0.5 \pm 0.2 \text{ mm/yr}$
 1135 SLE. Figure 13 shows model discrepancies at global and regional scales. In terms of global
 1136 land average, model differences can cause up to $\sim 0.4 \text{ mm/yr}$ SLE uncertainty.

1137





1145

1146 *Figure 13: Regional contribution to sea level rise (2003 – 2010) for the Ganges basin (left*
 1147 *panel) and tropical basins (right panel), as estimated from 17 different models (vertical axes)*
 1148 *and 4 GRACE products (JPL, CSR and GSFC mascons – black, red, blue – and GRGS*
 1149 *products - yellow) over the GRACE time period. Tropical regions are the main discrepancies*
 1150 *between model and GRACE estimates, possibly due to inconsistent model soil storage*
 1151 *capacity. The variability among GRACE products (up to 25%) is much smaller than*
 1152 *variability among models (up to 300%).*

1153

1154

Estimate Terrestrial Water Storage contribution to sea level	2002-2014/15 mm/yr SLE <i>(Positive values mean sea level rise)</i>
Human contributions by component	
Ground water depletion <i>Wada et al. (2016)</i>	0.30 (\pm 0.1)
Reservoir impoundment <i>Wada et al. (2017)</i>	-0.24 (\pm 0.02)
Deforestation (after 2010) <i>Wada et al. (2017)</i>	0.035
Wetland loss (after 1990) <i>Wada et al. (2017)</i>	0.074
Endorheic basin storage loss	
Caspian Sea <i>Wada et al. (2017)</i>	0.109 (\pm 0.004)
Aral Sea <i>Wada et al. (2017)</i>	0.036 (\pm 0.0003)
Aggregated human intervention (sum of above) <i>Scanlon et al. (2018)</i>	0.15 to 0.24
Hydrological model-based estimates	
WGHM model <i>(natural variability plus human intervention; P. Döll, personal communication)</i>	0.15 +/- 0.14
ISBA-TRIP model <i>(natural variability only ; Decharme et al., 2016) + human intervention from Wada et al. (2016) (from Dieng et al., 2017)</i>	0.23 +/- 0.10
GRACE-based estimates of total land water storage (not including glaciers) <i>(Reager et al., 2016; Rietbroek et al., 2016; Scanlon et al., 2018)</i>	
	-0.20 to -0.33 (\pm 0.09 - 0.16)

1155

1156 *Table 8. Estimates of TWS components due to human intervention and net TWS based on*
 1157 *hydrological models and GRACE*

1158

1159

1160 **2.7.3 Synthesis**

1161 Based on the different approaches to estimate the net land water storage contribution, we
 1162 estimate that corresponding sea level rate ranges from -0.33 to 0.23 mm/yr during the period



1163 of 2002-2014/15 due to water storage changes (Table 8). According to GRACE, the net TWS
1164 change (i.e. not including glaciers) over the period 2002-2014 shows a negative contribution
1165 to sea level of -0.33 mm/yr and -0.21 mm/yr, Reager et al. (2016) and Scanlon et al. (2018)
1166 respectively. Such a negative signal is not currently reproduced by hydrological models which
1167 estimate slightly positive trends over the same period (see Table 8). It is to be noted however
1168 that looking at trends only over periods of the order of a decade may not be appropriate due
1169 the strong interannual variability of TWS at basin and global scales. For example, Figure 5
1170 from Scanlon et al. (2018) (see also Figure S9 from their Supplementary Material), that
1171 compares GRACE TWS and model estimates over large river basins over 2002-2014, clearly
1172 show that the discrepancies between GRACE and models occur at the end of the record for
1173 the majority of basins. This is particularly striking for the Amazon basin (the largest
1174 contributor to TWS), for which GRACE and models agree reasonably well until 2011, and
1175 then depart significantly, with GRACE TWS showing strongly positive trend since then,
1176 unlike models. Such a divergence at the end of the record is also noticed for several other
1177 large basins (see Scanlon et al., Figure S9 SM). No clear explanation can be provided yet,
1178 even though one may question the quality of the meteorological forcing used by hydrological
1179 models for the recent years. But this calls for some caution when comparing GRACE and
1180 models on the basis of trends only. Much more work is needed to understand differences
1181 among models, and between models and GRACE. Of all components entering in the sea level
1182 budget, the TWS contribution currently appears as the most uncertain one.

1183

1184 **2.8 Glacial Isostatic Adjustment**

1185 The Earth's dynamic response to the waxing and waning of the late-Pleistocene ice sheets is
1186 still causing isostatic disequilibrium in various regions of the world. The accompanying slow
1187 process of GIA is responsible for regional and global fluctuations in relative and absolute sea
1188 level, 3D crustal deformations and changes of the Earth's gravity field (for a review, see
1189 Spada, 2017). To isolate the contribution of current climate change, geodetic observations
1190 must be corrected for the effects of GIA (King *et al.* 2010). These are obtained by solving the
1191 "Sea Level Equation" (Farrell and Clark 1976, Mitrovica and Milne 2003). The sea level can
1192 be expressed as $S=N-U$, where S is the rate of change of sea-level relative to the solid Earth, N
1193 is the geocentric rate of sea-level change, and U is the vertical rate of displacement of the
1194 solid Earth. The sea level equation accounts for solid Earth deformational, gravitational and
1195 rotational effects on sea level, which are sensitive to the Earth's mechanical properties and to



1196 the melting chronology of continental ice. Forward GIA modelling, based on the solution of
1197 the sea level equation, provides predictions of unique spatial patterns (or *fingerprints*, see Plag
1198 and Juettner, 2001) of relative and geocentric sea-level change (*e.g.*, Milne *et al.* 2009, Kopp
1199 *et al.* 2015). During the last decades, the two fundamental components of GIA modelling
1200 have been progressively constrained from the observed history of relative sea level during the
1201 Holocene (see *e.g.*, Lambeck and Chappell 2001, Peltier 2004). In the context of climate
1202 change, the importance of GIA has been recognised in the mid 1980s, when the awareness of
1203 global sea-level rise stimulated the evaluation of the isostatic contribution to tide gauge
1204 observations (see Table 1 in Spada and Galassi 2012). Subsequently, GIA models have been
1205 applied to the study of the pattern of sea level change from satellite altimetry (Tamisiea
1206 2011), and since 2002 to the study of the gravity field variations from GRACE. Our primary
1207 goal here is to analyse GIA model outputs that have been used to infer global mean sea level
1208 change and ice sheet volume change from geodetic datasets during the altimetry era. These
1209 outputs are the sea-level variations detected by satellite altimetry across oceanic regions (n),
1210 the ocean mass change (w) and the ice sheets mass balance from GRACE. We also discuss the
1211 GIA correction that needs to be applied to GRACE-based land water storage changes. The
1212 GIA correction applied to tide gauge-based sea level observations at the coastlines is not
1213 discussed here. Since GIA evolves on time scales of millennia (*e.g.*, Turcotte and Schubert,
1214 2014), the rate of change of all the isostatic signals in can be considered constant on the time
1215 scale of interest.

1216

1217 **2.8.1 GIA correction to altimetry-based sea level**

1218 Unlike tide gauges, altimeters directly sample the sea surface in a geocentric reference frame.
1219 Nevertheless, GIA contributes significantly to the rates of absolute sea-level change observed
1220 over the “altimetry era”, which require a correction N_{gia} that is obtained by solving the SLE
1221 (*e.g.*, Spada 2017). As discussed in detail by Tamisiea (2011), N_{gia} is sensitive to the assumed
1222 rheological profile of the Earth and to the history of continental ice sheets. The variance of
1223 N_{gia} over the surface of the oceans is much reduced, being primarily determined by the change
1224 of the Earth’s gravity potential, apart from a spatially uniform shift. As discussed by Spada
1225 and Galassi (2016), the GIA contribution N_{gia} is strongly affected by variations in the
1226 centrifugal potential associated with Earth rotation, whose fingerprint is dominated by a
1227 spherical harmonic contribution of degree $l=2$ and order $m=\pm 1$. Since N_{gia} has a smooth
1228 spatial pattern. The global the GIA correction to altimetry data can be obtained by simply
1229 subtracting its average $n = \langle N_{gia} \rangle$ over the ocean sampled by the altimetry missions. The



1230 computation of the GIA contribution N_{gia} has been the subject of various investigations, based
1231 on different GIA models. The estimate by Peltier (2001) of $n = -0.30$ mm/yr, based on GIA
1232 model ICE-4G (VM2), has been adopted in the majority of studies estimating GMSL rise
1233 from altimetry. Since n appears to be small compared to the global mean sea-level rise from
1234 altimetry (~ 3 mm/yr) and to its uncertainty (~ 0.3 mm/yr, see sub section 2.2), a more precise
1235 evaluation has not been of concern until recently. In Table 9, we summarize the values of n
1236 according to works in the literature where various GIA model models and averaging methods
1237 have been employed. Based on values in Table 9 for which a standard deviation is available,
1238 the weighted average of n , assumed to represent the best estimate, is $n = (-0.29 \pm 0.02)$ mm/yr
1239 where the uncertainty corresponds to 2σ .

1240

1241 **2.8.2 GIA correction to GRACE-based ocean mass**

1242 GRACE observations of present-day gravity variations are sensitive to GIA, due to the sheer
1243 amount of rock material that is transported by GIA throughout the mantle and the resulting
1244 changes in surface topography, especially over the formerly glaciated areas. The continuous
1245 change in the gravity field results in a nearly linear signal in GRACE observations. Since the
1246 gravity field is determined by global mass redistribution, GIA models used to correct GRACE
1247 data need to be global as well, especially when the region of interest is represented by all
1248 ocean areas. To date, the only global ice reconstruction publicly available is provided by the
1249 University of Toronto. Their latest product, named ICE-6G, has been published and
1250 distributed in 2015 (Peltier *et al.* 2015); note that the ice history has been simultaneously
1251 constrained with a specific Earth model, named VM5a. During the early period of the
1252 GRACE mission, the available Toronto model was ICE-5G (VM2) (Peltier, 2004). However,
1253 different groups have independently computed GIA model solutions based on the Toronto ice
1254 history reconstruction, by using different implementations of GIA codes and somehow
1255 different Earth models. The most widely used model is the one by Paulson *et al.* (2007), later
1256 updated by A *et al.* (2013). Both use a deglaciation history based on ICE-5G, but differ for the
1257 viscosity profile of the mantle: A *et al.* use a 3D compressible Earth with VM2 viscosity
1258 profile and a PREM-based elastic structure used by Peltier (2004), whereas Paulson *et al.*
1259 (2007) use an incompressible Earth with self-gravitation, and a Maxwell 1-D multi-layer
1260 mantle. Over most of the oceans, the GIA signature is much smaller than over the continents.
1261 However, once integrated over the global ocean, the signal w due to GIA is about -1 mm/yr of
1262 equivalent sea level change (Chambers *et al.* 2010), which is of the same order of magnitude
1263 as the total ocean mass change induced by increased ice melt (Leuliette and Willis 2011). The



1264 main uncertainty in the GIA contribution to ocean mass change estimates, apart from the
1265 general uncertainty in ice history and earth mechanical properties, originates from the
1266 importance of changes in the orientation of the Earth's rotation axis (Chambers *et al.* 2010,
1267 Tamisiea 2011). Different choices in implementing the so-called “rotational feedback” lead to
1268 significant changes in the resulting GIA contribution to GRACE estimates. The issue of
1269 properly accounting from rotational effects has not been settled yet (Mitrovica *et al.* 2005,
1270 Peltier and Luthcke 2009, Mitrovica and Wahr 2011, Martinec and Hagedoorn 2014). Table
1271 1(c) summarises the values of the mass-rate GIA contribution w according to the literature,
1272 where various models and averaging methods are employed. The weighed average of the
1273 values in Table 9 for which an assessment of the standard deviation is available, is $w = (-1.44$
1274 $\pm 0.36)$ mm/yr (the uncertainty is 2σ), which we assume to represent the preferred estimate.

1275

1276 **2.8.3 GIA correction to GRACE-based terrestrial water storage**

1277 As discussed in the previous section, the GIA correction to apply to GRACE over land is
1278 significant, especially in regions formerly covered by the ice caps (Canada and Scandinavia).
1279 Over Canada, GIA models significantly differ. Figure 14 that shows difference between two
1280 models of GIA correction to GRACE over land, the A *et al.* (2013) and Peltier *et al.* (2009)
1281 models.

1282

1283

1284

1285

1286

1287

1288

1289

1290

1291

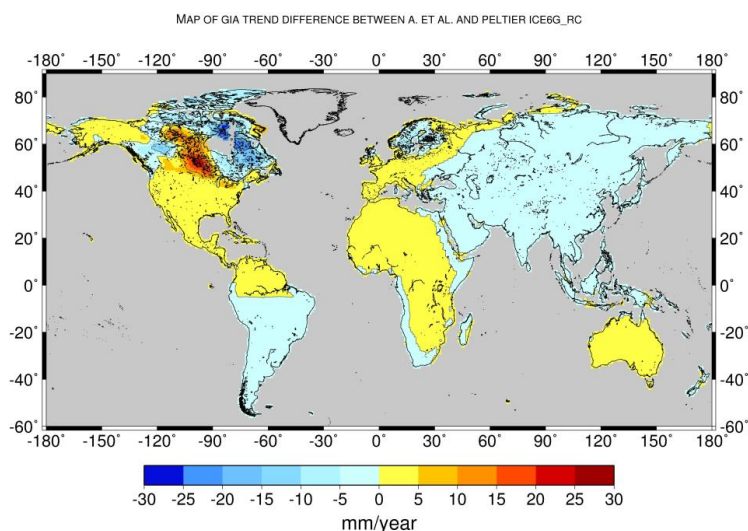
1292

1293

1294

1295

1296 *Figure 14: Difference map between two models of GIA correction to GRACE over land: A*
1297 *et al. (2013) minus Peltier et al. (2015) models. Unit in mm/yr SLE.*



1296



1298

1299 When averaged over the whole land surface as done in some studies to estimate the combined
1300 effect of land water storage and glacier melting from GRACE (e.g., Reager et al., 2015; see
1301 section 2.7), the GIA correction ranges from ~ 0.5 to 0.7 mm/yr (in mm/yr SLE). Values for
1302 different GIA models are given in Table 9.

1303

1304 **2.8.4 GIA correction to GRACE-based ice sheet mass balance**

1305 The GRACE gravity field observations allow the determination of mass balances of ice sheets
1306 and large glacier systems with an accuracy similar or superior to the input-output-method or
1307 satellite laser and radar altimetry (Shepherd *et al.* 2012). However, GRACE ice-mass balances
1308 rely on successfully separating and removing the apparent mass change related to GIA. While
1309 the GIA correction is small compared to the mass balance for Greenland ice sheet (ca. <
1310 10%), its magnitude and uncertainty in Antarctica is of the order of the ice-mass balance itself
1311 (e.g. Martín-Español *et al.* 2016). Particularly for today's glaciated areas, GIA remains poorly
1312 resolved due to the sparsity of data constraints, leading to large uncertainties in the climate
1313 history, the geometry and retreat chronology of the ice sheet, as well as the Earth structure.
1314 The consequences are ambiguous GIA predictions, despite fitting the same observational data.
1315 There are two principal approaches towards resolving GIA underneath the ice sheets.
1316 Empirical estimates can be derived making use of the different sensitivities of satellite
1317 observations to ice-mass changes and GIA (e.g. Riva *et al.* 2009, Wu *et al.* 2010).
1318 Alternatively, GIA can be modelled numerically by forcing an Earth model with a fixed ice
1319 retreat scenario (e.g. Peltier 2009, Whitehouse *et al.* 2012) or with output from a
1320 thermodynamic ice sheet model (Gomez *et al.* 2013, Konrad *et al.* 2015). Values of GIA-
1321 induced apparent mass change for Greenland and Antarctica as listed in the literature should
1322 be applied with caution (Table 9) when applying them to GRACE mass balances. Each of
1323 these estimates may rely on a different GRACE post-processing strategy and may differ in the
1324 approach used for solving the gravimetric inverse problem (*mascon* analysis, forward-
1325 modelling, averaging kernels). Of particular concern is the modelling and filtering of the pole
1326 tide correction caused by the rotational variations related to GIA, affecting coefficients of
1327 harmonic degree $l=2$ and order $m=\pm 1$. As mentioned above, agreement on the modelling of
1328 the rotational feedback has not been reached within the GIA community. Furthermore, the
1329 pole tide correction applied during the determination gravity-field solutions differs between
1330 the GRACE processing centres and may not be consistent with the GIA correction listed. This
1331 inconsistency may introduce a significant bias in the ice-mass balance estimates (e.g. Sasgen



1332 *et al.* 2013, Supplement). Wahr *et al.* 2015 presented recommendations on how to treat the
 1333 pole tides in GRACE analysis; however, a systematic inter-comparison of the GIA predictions
 1334 in terms of their low-degree coefficients and their consistency with the GRACE processing
 1335 standards is required.

1336

1337 Table 9. *Estimated contributions of GIA to the rate of absolute sea level change observed by*
 1338 *altimetry (a), and to the rate of mass change observed by GRACE over the global oceans (b)*
 1339 *the Greenland and Antarctic ice sheets (c), and the rate of mass change observed by GRACE*
 1340 *over land (d) during the altimetry era. The GIA corrections are expressed in mm/yr SLE*
 1341 *except over Greenland and Antarctica where values are given in Gt/yr (ice mass equivalent).*
 1342 *Most of the GIA contributions are expressed as a value \pm one standard deviation; a few*
 1343 *others are given in terms of a plausible range, for some the uncertainties are not specified.*

1344

(a) GIA correction to absolute sea level measured by altimetry

Reference	GIA (mm/yr)	Notes
Peltier (2009) (Table 3)	-0.30 \pm 0.02 -0.29 \pm 0.03 -0.28 \pm 0.02	Average of 3 groups of 4 values obtained by variants of the analysis procedure, using ICE-5G(VM2), over a global ocean, in the range of latitudes 66°S to 66°N and 60°S to 60°N, respectively.
Tamisiea (2011) (Figure 2)	-0.15 to -0.45 -0.20 to -0.50	Simple average over the oceans for a range of estimates obtained varying the Earth model parameters, over a global ocean and between latitudes 66°S and 66°N.
Huang (2013) (Table 3.6)	-0.26 \pm 0.07 -0.27 \pm 0.08	Average from an ensemble of 14 GIA models over a global ocean and between latitude from 66°S to 66°N.
Spada (2017) (Table 1)	-0.32 \pm 0.08	Based on four runs of the Sea Level Equation solver SELEN (Spada and Stocchi, 2007) using model ICE-5G(VM2), with different assumptions in solving the SLE.

(b) GIA contribution to GRACE mass-rate of change over the oceans



Reference	GIA (mm/yr)	Notes
Peltier (2009) (Table 3)	-1.60 ± 0.30	Average of values from 12 corrections for variants of the analysis procedure, using ICE-5G (VM2).
Chambers (2010) (Table 1)	-1.45 ± 0.35	Average over the oceans for a range of estimates produced by varying the Earth models.
Tamisiea (2011) (Figures 3 and 4)	-0.5 to -1.9 -0.9 to -1.5	Ocean average of a range of estimates varying the Earth model, and based on a restricted set, respectively.
Huang (2013) (Table 3.7)	-1.31 ± 0.40 -1.26 ± 0.43	Average from an ensemble of 14 GIA models over a global ocean and between latitude from 66°S to 66°N , respectively.

(c) GIA contribution to GRACE mass-rate of the ice sheets

Reference	Greenland	
	GIA (Gt/yr)	Notes
Simpson et al. (2009) ^r	$-3 \pm 12^{\text{m}}$	Thermodynamic sheet / solid Earth model, 1D (uncoupled); constrained by geomorphology; inversion results in Sutterley <i>et al.</i> (2014).
Peltier (2009) (ICE-5G) ^g	-4^{f}	Ice load reconstruction / solid Earth model, 1D (ICE-5G / similar to VM2); Greenland component of ICE-5G (13 Gt/yr) + Laurentide component of ICE-5G (-17 Gt/yr); inversion results in Khan <i>et al.</i> 2016, Discussion.
Khan <i>et al.</i> (2016) (GGG-1D) ^r	$15 \pm 10^{\text{f}}$	Ice load reconstruction / solid Earth model, 1D (uncoupled); constrained with geomorphology & GPS; Greenland component (+32 Gt/yr) + Laurentide component of ICE-5G (-17 Gt/yr); inversion results in Khan <i>et al.</i> (2016), Discussion.



Fleming *et al.* (2004)^f 3^f
(Green1) Ice load reconstruction / solid Earth model, 1D (uncoupled); constrained with geomorphology; Greenland component (+ 20 Gt/yr) + Laurentide component of ICE-5G (-17 Gt/yr); inversion in Sasgen *et al.* (2012, supplement).

Wu *et al.* (2010)^g -69 ± 19^m Joint inversion estimate based on GPS, satellite laser ranging, and very long baseline interferometry, and bottom pressure from ocean model output; inversion results in Sutterley *et al.* (2014).

Antarctica

Reference	GIA (Gt/yr)	Notes
Whitehouse <i>et al.</i> (2012) (W12a) ^f	60 ⁿ	Thermodynamic sheet / solid Earth model, 1D (uncoupled); constrained by geomorphology; inversion results in Shepherd <i>et al.</i> 2012, supplement (Fig. S8).
Ivins <i>et al.</i> (2013) (IJ05_R2) ^f	40-65 ⁿ	Ice load reconstruction / solid Earth model, 1D; constrained by geomorphology and GPS uplift rates; Ivins <i>et al.</i> 2013; inversion results in Shepherd <i>et al.</i> 2012, Supplement (Fig. S8).
Peltier (2009) (ICE-5G) ^g	140-180 ⁿ	Ice load reconstruction / solid Earth model ICE-5G(VM2); constrained by geomorphology; inversion results in Shepherd <i>et al.</i> 2012, supplement (Fig. S8).
Argus <i>et al.</i> (2014) (ICE-6G) ^g	107 ⁿ	Ice load reconstruction / solid Earth model ICE-6G(VM5a); constrained by geomorphology and GPS; theory recently corrected by Purcell <i>et al.</i> 2016; inversion results in Argus <i>et al.</i> (2014), conclusion 7.8.
Sasgen <i>et al.</i> (2017) (REGINA) ^f	55 ± 22 ^f	Joint inversion estimate based on GRACE, altimetry, GPS and viscoelastic response functions; lateral heterogeneous Earth model parameters; inversion results in Sasgen <i>et al.</i> (2017), Table 1.



Gunter *et al.* (2014) ca. 64 ± 40 ^a Joint inversion estimate based on GRACE, altimetry, (G14)^f (multimodel GPS and regional climate model output; conversion of uncert.) uplift to mass using average rock density; inversion results in, Gunter *et al.* (2014) Table 1.

Martin-Español *et al.* (2016) (RATES)^f 55 ± 8 $45 \pm 7^*$ Joint inversion estimate based on GRACE, altimetry, GPS and regional climate model output; inversion results in Sasgen *et al.* (2017), * is improved for GIA of smaller spatial scales; inversion results in Martin-Español *et al.* (2016), Fig. 6.

1345

1346 ^f regional model; ^g global model; ^m mascon inversion; ^f forward modelling inversion; ^a
1347 averaging kernel inversion; ⁿ inversion method not specified.

1348

1349 (d) GIA correction to GRACE-based terrestrial water storage estimates

1350

1351

GIA MODEL	Mean GIA correction over land excluding Greenland, Antarctica, Iceland, Svalbard, Hudson Bay and Black Sea (mm/yr sea level equivalent/SLE)
A. et al., 2013	0.63
Peltier ICE5G	0.68
Peltier ICE6G_rc	0.71
ANU_ICE6G	0.53

1352

1353 The GRACE-based ocean mass, Antarctica mass and terrestrial water storage changes are
1354 much model dependent. As these GIA corrections cannot be assessed from independent
1355 information, they represent a large source of uncertainties to the sea level budget components
1356 based on GRACE.

1357

1358 2.9 Ocean mass change from GRACE

1359



1360 Since 2002, GRACE satellite gravimetry has provided a revolutionary means for
1361 measuring global mass change and redistribution at monthly intervals with unprecedented
1362 accuracy, and offered the opportunity to directly estimate ocean mass change due to water
1363 exchange between the ocean and other components of the Earth (e.g., ice sheets, mountain
1364 glaciers, terrestrial water). GRACE time-variable gravity data have been successfully applied
1365 in a series of studies of ice mass balance of polar ice sheets (e.g., Velicogna and Wahr, 2006;
1366 Luthcke et al., 2006) and mountain glaciers (e.g., Tamisiea et al., 2005; Chen et al., 2007) and
1367 their contributions to global sea level change. GRACE data can also be used to directly study
1368 long-term oceanic mass change or non-steric sea level change (e.g., Willis et al., 2008;
1369 Leuliette et al., 2009; Cazenave et al., 2009), and provide a unique opportunity to study
1370 interannual or long-term terrestrial water storage (TWS) change and its potential impacts on
1371 sea level change (Richey et al., 2015; Reager et al., 2016).

1372 GRACE time-variable gravity data can be used to quantify ocean mass change from three
1373 different main approaches. One is through measuring ice mass balance of polar ice sheets and
1374 mountain glaciers and variations of TWS, and their contributions to the GMSL (e.g.,
1375 Velicogna and Wahr, 2005; Schrama et al., 2014). The second approach is to directly quantify
1376 ocean mass change using ocean basin mask (kernel) (e.g., Chambers et al., 2004; Llovel et al.,
1377 2010; Johnson and Chambers, 2013). In the ocean basin kernel approach, coastal ocean areas
1378 within certain distance (e.g., 300 or 500 km) from the coast are excluded, in order to minimize
1379 contaminations from mass change signal over the land (e.g., glacial mass loss and TWS
1380 change). The third approach solves mass changes on land and over ocean at the same time via
1381 forward modeling (e.g., Chen et al., 2013; Yi et al., 2015). The forward modeling is a global
1382 inversion to reconstruct the “true” mass change magnitudes over land and ocean with
1383 geographical constraint of locations of the mass change signals, and can help effectively
1384 reduce leakage between land and ocean (Chen et al., 2015).

1385

1386 Estimates of ocean mass changes from GRACE are subject to a number of major error
1387 sources, which include leakage errors from the larger signals over ice sheets and land
1388 hydrology due to GRACE’s low spatial resolution (of at least a few to several hundred km)
1389 and the need of coastal masking, spatial filtering of GRACE data to reduce spatial noise,
1390 errors and biases in geophysical model corrections (e.g., GIA, atmospheric mass) that need to
1391 be removed from GRACE observations first to isolate oceanic mass change and/or polar ice
1392 sheets and mountain glaciers mass balance, and residual measurement errors in GRACE
1393 gravity measurements, especially those associated with GRACE low-degree gravity changes.



1394 In addition, how to deal with the absent degree-1 terms, i.e., geocenter motion in GRACE
 1395 gravity fields is expected to affect on GRACE estimated oceanic mass rates and ice mass
 1396 balances.
 1397

Ocean mass trends (mm/yr)	Time Period	Mass
Chen et al. (2013) (A13 GIA)	2005.01- 2011.12	1.80 ± 0.47
Johnson and Chambers (2013) (A13 GIA)	2003.01- 2012.12	1.80 ± 0.15
Purkey et al. (2014) (A13 GIA)	2003.01- 2013.01	1.53 ± 0.36
Dieng et al. (2015a) (Paulson07 GIA)	2005.01- 2012.12	1.87 ± 0.11
Dieng et al. (2015b) (Paulson07 GIA)	2005.01- 2013.12	2.04 ± 0.08
Yi et al. (2015) (A13 GIA)	2005.01- 2014.07	2.03 ± 0.25
Rietbroek et al. (2016)	2002.04- 2014.06	1.08 ± 0.30
Chambers et al. (2017)	2005.0 – 2015.0	2.11 ± 0.36

1398 *Table 10. Recently published (since 2013) estimates of GRACE ocean rate with GIA*
 1399 *corrections (Mass). Most of the listed studies use either the A13 (A et al., 2013) or*
 1400 *Paulson07 (Paulson et al., 2007) GIA model.*

1401

1402 The uncertainty estimates of the listed studies (Table 10) are computed from different
 1403 methods, with different considerations of error sources into the error budget, and represent
 1404 different confidence levels.

1405

1406 With a different treatment of the GRACE land-ocean signal leakage effect through global
 1407 forward modeling, Chen et al. (2013) estimates ocean mass rates using GRACE RL05 time-



1408 variable gravity solutions over the period 2005-2011, and shows that the ocean mass change
1409 contributes to 1.80 ± 0.47 mm/yr (over the same period), which is significantly larger than
1410 previous estimates over about the same period. Yi et al. (2015) further confirms that correct
1411 calibration of GRACE data and appropriate treatment of GRACE leakage bias are critical to
1412 improve the accuracy of GRACE estimated ocean mass rates. Table 10 summarizes different
1413 estimates of GRACE ocean mass rates.

1414 As demonstrated in Chen et al. (2013), different treatments of just the degree-2 spherical
1415 harmonics of GRACE gravity solution alone can lead to substantial differences in GRACE
1416 estimated ocean mass rates (ranging from 1.71 to 2.17 mm/yr). Similar estimates from
1417 GRACE gravity solutions from different data processing centers can also be different. In the
1418 meantime, long-term degree-1 spherical harmonics variation, representing long-term
1419 geocenter motion and neglected in some of the previous studies (due to the lack of accurate
1420 observations) are also expected to have non-negligible effect on GRACE derived ocean mass
1421 rates (Chen et al., 2013). Different methods for computing ocean mass change using GRACE
1422 data may also lead to different estimates (Chen et al., 2013; Johnson and Chambers, 2013,
1423 Jensen et al., 2013).

1424 To help better understand the potential and uncertainty of GRACE satellite gravimetry in
1425 quantification of the ocean mass rate, Table 11 provides a comparison of GRACE-estimated
1426 ocean mass rates over the period January 2005 to December 2016 based on different GRACE
1427 data products and different data processing methods, including the CSR, GFZ and JPL
1428 GRACE RL05 spherical harmonic solutions (i.e., the so-called GSM solutions), and CSR,
1429 JPL, and GSFC mascon solutions (the available GSFC mascons only cover the period up to
1430 July 2016). The three GRACE GSM results (CSR, GFZ, and JPL) are updates from Johnson
1431 and Chambers (2013), with ΔC_{20} terms replaced by satellite laser ranging results (Cheng and
1432 Ries, 2012), geocenter motion from Swenson et al. (2008), GIA model from A et al. (2013),
1433 an averaging kernel with a land mask that extends out 300 km, and no destriping or
1434 smoothing, as described in Johnson and Chambers (2013). An update of GRACE ocean mass
1435 rate from Chen et al. (2013) is also included for comparisons, which is based on the CSR
1436 GSM solutions using forward modeling (a global inversion approach), with similar treatments
1437 of ΔC_{20} , geocenter motion, and GIA effects.

1438 The JPL mascon ocean mass rate is computed from all mascon grids over the ocean, and
1439 the GSFC mascon ocean mass rate is computed from all ocean mascons, with the
1440 Mediterranean, Black and Red Seas excluded. A coastline resolution improvement (CRI)



1441 filter is already applied in the JPL mascons to reduce leakage (Wiese et al., 2016), and in both
 1442 the GSFC and JPL mascon solutions, the ocean and land are separately defined (Luthcke et
 1443 al., 2013; Watkins et al., 2015). For the CSR mascon results, an averaging kernel with a land
 1444 mask that extends out 200 km is applied to reduced leakage (Chen et al., 2017). Similar
 1445 treatments or corrections of ΔC_{20} , geocenter motion, and GIA effects are also applied in the
 1446 three mascon solutions. When solving GRACE mascon solutions, the GRACE GAD fields
 1447 (representing ocean bottom pressure changes, or combined atmospheric and oceanic mass
 1448 changes) have been added back to the mascon solutions. To correctly quantify ocean mass
 1449 change using GRACE mascon solutions, the means of the GAD fields over the oceans, which
 1450 represents mean atmospheric mass changes over the ocean (as ocean mass is conserved in the
 1451 GAD fields) need to be removed from GRACE mascon solutions. The removal of GAD
 1452 average over the ocean in GRACE mascon solutions has very minor or negligible effect (of ~
 1453 0.02 mm/yr) on ocean mass rate estimates, but is important for studying GMSL change at
 1454 seasonal time scales.

1455 Over the 12-year period (2005-2016), the three GRACE GSM solutions show pretty
 1456 consistent estimates of ocean mass rate, in the range of 2.3 to 2.5 mm/yr. Greater differences
 1457 are noticed for the mascon solutions. The GSFC mascons show the largest rate of 2.61mm/yr.
 1458 The CSR and JPL mascon solutions show relatively smaller ocean mass rates of 1.76 and 2.02
 1459 mm/yr, respectively, over the studied period. Based on the same CSR GSM solutions, the
 1460 forward modeling and basin kernel estimates agree reasonably well (2.52 vs. 2.44 mm/yr). In
 1461 addition to the ΔC_{20} terms, geocenter motion, and GIA correction, the degree-2 non-zonal
 1462 spherical harmonics ΔC_{21} and ΔS_{21} of the current GRACE RL05 solutions are affected by the
 1463 definition of the reference mean pole in GRACE pole tide correction (Wahr et al., 2015). This
 1464 mean pole correction, excluded in all estimates listed in Table 11 (for fair comparison), is
 1465 estimated to contribute ~ - 0.11 mm/yr to GMSL. How to reduce errors from the different
 1466 sources play a critical role in estimating ocean mass change from GRACE time-variable
 1467 gravity data.

1468

1469

Ocean mass change (in mm/yr equivalent sea level)	Linear trend 2005-2016
GSM CSR Forward Modeling (update from Chen et al., 2013)	2.52±0.17
GSM CSR (update from Johnson and Chambers, 2013)	2.44±0.15



GSM GFZ (update from Johnson and Chambers, 2013)	2.30±0.15
GSM JPL (update from Johnson and Chambers, 2013)	2.48±0.16
Mascon CSR (200 km)	1.76±0.16
Mascon JPL	2.02±0.16
Mascon GSFC (update from Luthcke et al., 2013)	2.61±0.16
Ensemble mean	2.3 ± 0.19

1470 *Table 11. Ocean mass rates estimated from GRACE for the period January 2005 – December*
 1471 *2016 (the GSFC mascon solutions cover up to July 2016). The uncertainty is based on 2 times*
 1472 *the sigma of least squares fitting.*
 1473

1474 GRACE satellite gravimetry has brought a completely new era for studying global ocean
 1475 mass change. Owing to the extended record of GRACE gravity measurements (now over 15
 1476 years), improved understanding of GRACE gravity data and methods for addressing GRACE
 1477 limitations (e.g., leakage and low-degree spherical harmonics), and improved knowledge of
 1478 background geophysical signals (e.g., GIA), GRACE-derived ocean mass rates from different
 1479 studies in recent years show clearly increased consistency (Table 11). Most of the results
 1480 agree well with independent observations from satellite altimeter and Argo floats, although
 1481 the uncertainty ranges are still large. The GRACE Follow-On (FO) mission is scheduled to be
 1482 launched in March 2018. The GRACE and GRACE-FO together are expected to provide at
 1483 least over two (or even three) decades of time-variable gravity measurements. Continuous
 1484 improvements of GRACE data quality (in future releases) and background geophysical
 1485 models are also expected, which will help improve the accuracy GRACE observed ocean
 1486 mass change.

1487 For the sea level budget assessment over the GRACE period, we will use the ensemble mean.
 1488

1489 **3. Sea Level Budget results**

1490 In section 2, we have presented the different terms of the sea level budget equation, mostly
 1491 based on published estimates (and in some cases, from their updates). We now use them to
 1492 examine the closure of the sea level budget. For all terms, we only consider ensemble mean
 1493 values.
 1494

1495 **3.1 Entire altimetry era (1993-Present)**

1496

1497 **3.1.1 Trend estimates over 1993-Present**



1498 Because it is now clear that the GMSL and some components are accelerating (e.g., Nerem et
 1499 al., 2018), we propose to characterize the long term variations of the time series by both a
 1500 trend and an acceleration. We start looking at trends. Table 12 gathers the trends estimated in
 1501 section 2. The end year is not always the same for all components (see section 2). Thus the
 1502 word ‘present’ means either 2015 or 2016 depending on the component. As no trend estimate
 1503 is available for the entire altimetry era for the terrestrial water storage contribution, we do not
 1504 consider this component. The residual trend (GMSL minus sum of components trend) may
 1505 then provide some constraint on the TWS contribution.

1506

1507

Component	Trends (mm/yr) 1993-Present
1. GMSL (TOPEX-A drift corrected)	3.07 +/- 0.37
2. Thermosteric sea level (full depth)	1.3 +/- 0.4
3. Glaciers	0.65 +/- 0.15
4. Greenland	0.48 +/- 0.10
5. Antarctica	0.25 +/- 0.10
6. TWS	/
7. Sum of components (without TWS → 2.+3.+4.+5.)	2.7 +/- 0.23
8. GMSL minus sum of components (without TWS)	0.37 +/- 0.3

1508

1509 *Table 12: Trend estimates for individual components of the sea level budget, sum of*
 1510 *components and GMSL minus sum of components over 1993-present. Uncertainties of the*
 1511 *sum of components and residuals represent rooted mean squares of components errors,*
 1512 *assuming that errors are independent.*

1513

1514 Results presented in Table 12 are discussed in section 4.

1515

1516 **3.1.2 Acceleration**

1517 The GMSL acceleration estimated in section 2.2 using Ablain et al. (2017b)’s TOPEX-A drift
 1518 correction amounts to 0.10 mm/yr² for the 1993-2017 time span. This value is in good
 1519 agreement with Nerem et al. (2018) estimate (of 0.084 +/- 0.025 mm/yr²) over nearly the
 1520 same period, after removal of the interannual variability of the GMSL. In Nerem et al.



1521 (2018), acceleration of individual components are also estimated as well as acceleration of the
 1522 sum of components. The latter agrees well with the GMSL acceleration. Here we do not
 1523 estimate the acceleration of the component ensemble means because time series are not
 1524 always available. We leave this for a future assessment.

1525

1526 **3.2 GRACE and Argo period (2005- Present)**

1527

1528 **3.2.1 Sea level budget using GRACE-based ocean mass**

1529 If we consider the ensemble mean trends for the GMSL, thermosteric and ocean mass
 1530 compents given in sections 2.2, 2.3 and 2.9 over 2005-present, we find agreement (within
 1531 error bars) between the observed GMSL (3.5 +/- 0.2 mm/yr) and the sum of Argo-based
 1532 thermosteric plus GRACE-based ocean mass (3.6 +/- 0.4 mm/yr) (see Table 12). The residual
 1533 (GMSL minus sum of components) trend amounts to -0.1 mm/yr. Thus in terms of trends, the
 1534 sea level budget appears closed over this time span within quoted uncertainties.

1535

1536 **3.2.2 Trend estimates over 2005-Present from estimates of individual contributions**

1537

1538 Table 13 gathers trends of individual components of the sea level budget over 2005-present,
 1539 as well sum of components and residuals (GMSL minus sum of components) trend. As for the
 1540 longer period, ensemble mean values are considered for each component.

1541

Component	Trend (mm/yr) 2005-Present
1. GMSL	3.5 +/- 0.2
2. Thermosteric sea level (full depth)	1.3 +/- 0.4
3. Glaciers	0.74 +/- 0.1
4. Greenland	0.76 +/- 0.1
5. Antarctica	0.42 +/- 0.1
6. TWS from GRACE (mean of Reager et al. and Scanlon et al.)	-0.27 +/- 0.15
7. Sum of components (2.+3.+4.+5.+6.)	2.95 +/- 0.21
8. Sum of components (thermosteric full depth + GRACE-based ocean mass)	3.6 +/- 0.4



9. GMSL minus sum of components (including GRACE-based TWS→2.+3.+4.+5.+6.)	0.55 +/- 0.3
10. GMSL minus sum of components (without GRACE-based TWS→ 2.+3.+4.+5.)	0.28 +/- 0.2
11. GMSL minus sum of components (thermosteric full depth + GRACE-based ocean mass)	-0.1 +/- 0.3

1542

1543 *Table 13: Trend estimates for individual components of the sea level budget, sum of*
 1544 *components and GMSL minus sum of components over 2005-present.*

1545

1546

1547 **3.2.3 Year-to-year budget over 2005-Present using GRACE-based ocean mass**

1548

1549 We now examine the year-to-year sea level and mass budgets. Table 14 provides annual mean
 1550 values for the ensemble mean GMSL, GRACE-based ocean mass and Argo-based
 1551 thermosteric component. The components are expressed as anomalies and their reference is
 1552 arbitrary. So to compare with the GMSL, a constant offset for all years was applied to the
 1553 thermosteric and ocean mass annual means. The reference year (where all values are set to
 1554 zero) is 2003.

1555

1556

1557

Year	Ensemble mean GMSL mm	Sum of components mm	GMSL minus sum of components mm
2005	7.00	8.78	-0.78
2006	10.25	10.78	-0.53
2007	10.51	11.35	-0.85
2008	15.33	15.07	0.25
2009	18.78	18.88	-0.10
2010	20.64	20.53	0.11
2011	20.91	21.38	-0.48



2012	31.10	29.33	1.77
2013	33.40	33.87	-0.47
2014	36.65	36.22	0.43
2015	46.34	45.69	0.65

1558

1559 *Table 14. Annual mean values for the ensemble means GMSL and sum of components*
1560 *(GRACE-based ocean mass and Argo-based thermosteric, full depth). Constant offset applied*
1561 *to the sum of components. The reference year (where all values are set to zero) is 2003.*

1562

1563 Figure 15 shows the sea level budget over 2005-2015 in terms of annual bar chart using
1564 values given in Table 14. It compares for years 2005 to 2016 the annual mean GMSL (blue
1565 bars) and annual mean sum of thermosteric and GRACE-based ocean mass (red bars). Annual
1566 residuals are also shown (green bars). These are either positive or negative depending on
1567 years. The trend of these annual residuals is estimated to 0.135 mm/yr.

1568 In Figure 16 is also shown the annual sea level budget over 2005-2015 but now using the
1569 individual components for the mass terms. As we have no annual estimates for TWS, we
1570 ignore it, so that the total mass includes only glaciers, Greenland and Antarctica. The annual
1571 residuals thus include the TWS component in addition to the missing contributions (e.g., deep
1572 ocean warming). For years 2006 to 2011, the residuals are negative, an indication of a
1573 negative TWS to sea level as suggested by GRACE results (Reager et al., 2016, Scanlon et al.,
1574 2018). But as of 2012, the residuals become positive and on average over 2005-2015, the
1575 residual trend amounts +0.28 mm/yr, a value larger than when using GRACE ocean mass.

1576 Finally, Figure 17 presents the mass budget. It compares annual GRACE-based ocean mass to
1577 the sum of the mass components, without TWS as in Figure 16. The residual trends over
1578 2005-2015 time span is 0.14 mm/yr. It may dominantly represent the TWS contribution. From
1579 one year to another residuals can be either positive or negative, suggesting important
1580 interannual variability in the TWS or even in the deep ocean.

1581

1582

1583

1584

1585

1586



1587

1588

1589

1590

1591

1592

1593

1594

1595

1596

1597

1598

1599

1600

1601

1602

1603

1604

1605

1606

1607

1608

1609

1610

1611

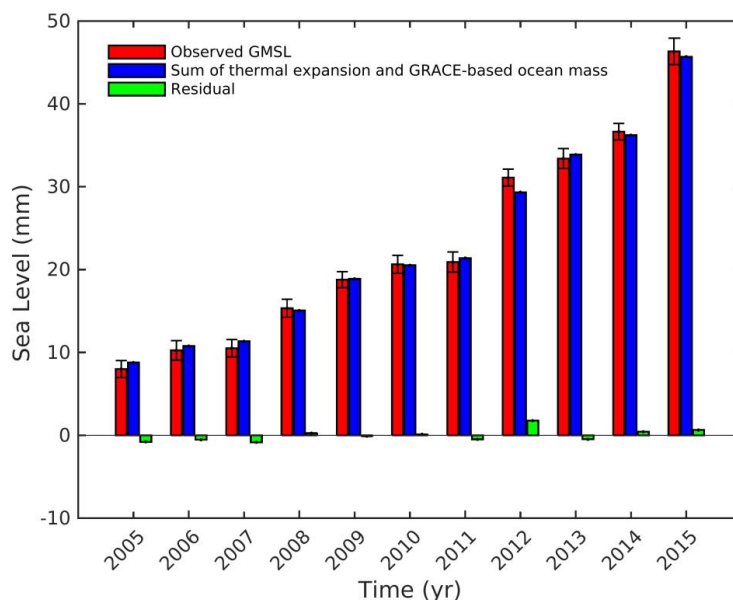


Figure 15: Annual sea level (blue bars) and sum of thermal expansion (full depth) and GRACE ocean mass component (red bars). Black vertical bars are associated uncertainties. Annual residuals (green bars) are also shown.

1611

1612

1613

1614

1615

1616

1617

1618

1619

1620

1621

1622

1623

1624

1625

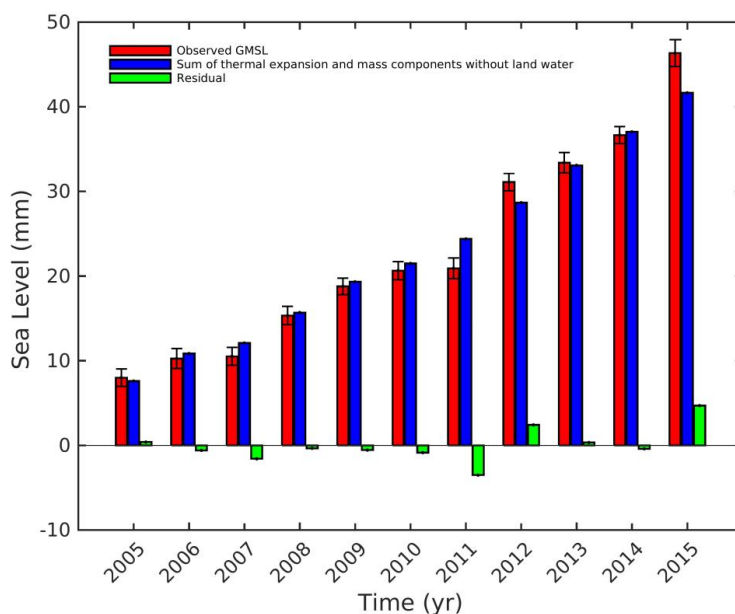
1626

1627

1628

1629

1630





1631

1632

1633 *Figure 16: Annual global mean sea level (blue bars) and sum components without TWS (full*

1634 *depth thermal expansion+ glaciers + Greenland + Antarctica) (red bars). Black vertical bars*

1635 *are associated uncertainties. Annual residuals (green bars) are also shown.*

1636

1637

1638

1639

1640

1641

1642

1643

1644

1645

1646

1647

1648

1649

1650

1651

1652

1653 *Figure 17: Annual GRACE-based ocean mass (red bars) and sum components without TWS*

1654 *(full depth thermal expansion+ glaciers + Greenland + Antarctica) (blue bars). Annual*

1655 *residuals (green bars) are also shown.*

1656

1657 **4. Discussion**

1658 The results presented in section 2 for the components of the sea level budget are based on

1659 syntheses of the recently published literature. When needed, the time series have been

1660 updated. In section 3, we considered ensemble means for each component to average out

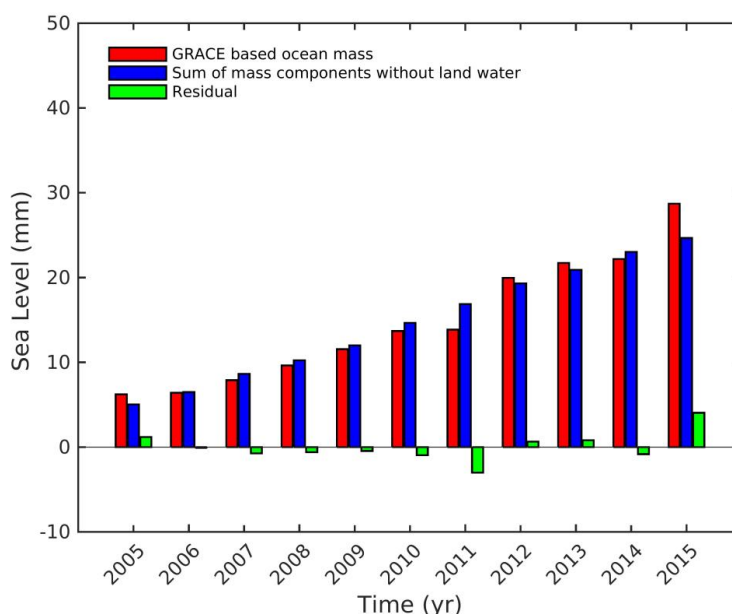
1661 random errors of individual estimates. We examined the closure/non closure of the sea level

1662 budget using these ensemble mean values, for 2 periods: 1993-present and 2005-present

1663 (Argo and GRACE period). Because of the lack of observation-based TWS estimate for the

1664 1993-present time span, we compared the observed GMSL trend to the sum of components

1665 excluding TWS. We found a positive residual trend of 0.37 ± 0.3 mm/yr, supposed to





1666 include the TWS contribution, plus other imperfectly known contributions (deep ocean
1667 warming) and data errors.

1668 For the 2005-present time span, we considered both GRACE-based ocean mass and sum of
1669 individual mass components, allowing us to also look at the mass budget. For TWS, as
1670 discussed in section 2.7, GRACE provides a negative trend contribution to sea level over the
1671 last decade (i.e., increase on water storage on land) attributed to internal natural variability
1672 (Reager et al., 2016), unlike hydrological models that lead to a small (possible not
1673 significantly different from 0) positive contribution to sea level over the same period.
1674 Assuming that GRACE observations are perfect, such discrepancies could be attributed to the
1675 inability of models to correctly account for uncertainties in meteorological forcing and
1676 inadequate modeling of soil storage capacity (see discussion in section 2.7). However, when
1677 looking at the sea level budget over the GRACE time span and using the GRACE-based
1678 TWS, we find a rather large positive residual trend (> 0.5 mm/yr) that needs to be explained.
1679 Since GRACE-based ocean mass is supposed to represent all mass terms, one may want to
1680 attribute this residual trend to an additional contribution of the deep ocean to the abyssal
1681 contribution already taken into account here, but possibly underestimated because of
1682 incomplete monitoring by current observing systems. If such a large positive contribution
1683 from the deep ocean (meaning ocean warming) is real (which is unlikely, given the high
1684 implied heat storage), this has to be confirmed by independent approaches e.g., using ocean
1685 reanalyses, and eventually model-based and top-of-the-atmosphere estimates of the Earth
1686 Energy Imbalance.

1687 In addition to mean trends over the period, we also looked at the annual budget for all years
1688 starting in 2005. For most components, annual mean values are provided during the Argo-
1689 GRACE era, except for the terrestrial water storage component. However, the sea level
1690 budget based on GRACE ocean mass (plus ocean thermal expansion; Figure 15) includes the
1691 TWS contribution. As shown in Figure 15, yearly residuals are small, suggesting near closure
1692 of the sea level budget. The residual trend amounts to 0.13 mm/yr. It could be interpreted as
1693 an additional deep ocean contribution not accounted by the SIO estimate (see section 2.3).
1694 However, when looking at Figure 15, we note that yearly residuals are either positive or
1695 negative, an indication of interannual variability that can hardly be explained by a deep ocean
1696 contribution. The residual trend derived from the difference (GMSL minus sum of
1697 components) (Table 13) amounts -0.1 ± 0.3 mm/yr, suggesting a sea level budget closed
1698 within 0.3 mm/yr over 2005-present, with no substantial deep ocean contribution.



1699 Figure 17 compares GRACE ocean mass to the sum of mass components (excluding TWS,
1700 for the reasons mentioned above). In principle, this mass budget may provide a constraint on
1701 the TWS contribution. The corresponding residual trend amounts to 0.14 mm/yr over the
1702 GRACE period, a value that agrees in sign with hydrological models estimates but disagrees
1703 with GRACE-based TWS estimates. However, given the remaining data uncertainties, any
1704 robust conclusion can hardly be reached. That being said, more work is needed to clarify the
1705 sign discrepancy between GRACE-based and model-based TWS estimates.

1706

1707 **5. Concluding Remarks**

1708 As mentioned in the introduction, the global mean sea level budget has been the object of
1709 numerous previous studies, including successive IPCC assessments of the published literature.
1710 What is new in the effort presented here, is that it involves the international community
1711 currently studying present-day sea level and its components. Moreover, it relies on a large
1712 variety of datasets derived from different space-based and in situ observing systems. Near
1713 closure of the sea level budget as reported here over the GRACE and Argo era suggests that
1714 no large systematic errors affect these independent observing systems, including the satellite
1715 altimetry system. Study of the sea level budget allows improved understanding of the
1716 different processes causing sea level rise, such as ocean warming and land ice melt. When
1717 accuracy increases, it will offer an integrative view of the response of the Earth system to
1718 natural & anthropogenic forcing and internal variability, and provide an independent
1719 constraint on the current Earth Energy Imbalance. Validation of climate models against
1720 observations is another important application of this kind of assessment (e.g., Slangen et al.,
1721 2017).

1722 However, important uncertainties still remain, that affect several terms of the budget; for
1723 example the GIA correction applied to GRACE data over Antarctica or the net land water
1724 storage contribution to sea level. The latter results from a variety of factors but is dominated
1725 by ground water pumping and natural climate variability. Both terms are still uncertain and
1726 accurately quantifying them remains a challenge.

1727 Several ongoing international projects related to sea level should provide in the near future
1728 improved estimates of the components of the sea level budget. This is the case, for example,
1729 of the ice sheet mass balance inter-comparison exercise (IMBIE, 2nd assessment), a
1730 community effort supported by NASA (National Aeronautics and Space Administration) and
1731 ESA, dedicated to reconcile satellite measurements of ice sheet mass balance (Shepherd et al.,



1732 2012). This is also the case for the ongoing ESA Sea level Budget Closure project (Horwath
1733 et al., 2018) that uses a number of space-based Essential Climate Variables (ECVs)
1734 reprocessed during the last 7 years in the context of the ESA Climate Change Initiative
1735 project. The GRACE follow-on mission, scheduled for launch mid-2018, will lengthen the
1736 current mass component time series, with hopefully increased precision and resolution.
1737 Finally, the deep Argo project, still in an experimental phase, will provide important
1738 information on the deep ocean heat content in the coming years. Availability of this new data
1739 set will be open new insight on the total thermosteric component of the sea level budget,
1740 allowing constraining other missing or poorly known contributions, from the evaluation of the
1741 budget.

1742 The sea level budget assessment discussed here essentially relies on trend estimates. But
1743 annual budget estimates have been proposed for the first time over the GRACE-Argo era. It is
1744 planned to provide updates of the global sea level budget every year, as done for more than a
1745 decade for the global carbon budget (Le Queré et al., 2018). In the next assessments, updates
1746 of all components will be considered, accounting for improved evaluation of the raw data,
1747 improved processing and corrections, use of ocean reanalyses, etc. Need for additional
1748 information where gaps exist should also be considered. As a closing remark, study of the sea
1749 level budget in terms of time series, not just trends as done here, will be required.

1750 **List of authors and affiliations:**

1751 Anny Cazenave (LEGOS, France), Benoit Meyssignac (LEGOS, France);
1752 Michael Ablain (CLS, France), Jonathan Bamber (U. Bristol, UK), Valentina Barletta (DTU-
1753 SPACE, Denmark), Brian Beckley (SGT Inc./NASA GSFC, USA), Jérôme Benveniste
1754 (ESA/ESRIN, Italy), Etienne Berthier (LEGOS, France), Alejandro Blazquez (LEGOS,
1755 France), Tim Boyer (NOAA, USA), Denise Caceres (Goethe U., Germany), Don Chambers
1756 (U. South Florida, USA), Nicolas Champollion (U. Bremen, Germany), Ben Chao (IES-AS,
1757 Taiwan), Jianli Chen (U. Texas, USA), Lijing Cheng (IAP-CAS, China), John A. Church (U.
1758 New South Wales, Australia), Stephen Chuter (U. Bristol, UK), J. Graham Cogley (Trent U.,
1759 Canada), Soenke Dangendorf (U. Siegen, Germany), Damien Desbruyères (IFREMER,
1760 France), Petra Döll (Goethe U., Germany), Catia Domingues (CSIRO, Australia), Ulrike Falk
1761 (U. Bremen, Germany), James Famiglietti (JPL/Caltech, USA), Luciana Fenoglio-Marc (U.
1762 Bonn, Germany), Rene Forsberg (DTU-SPACE, Denmark), Gaia Galassi (U. Urbino, Italy),
1763 Alex Gardner (JPL/Caltech, USA), Andreas Groh (TU-Dresden, Germany), Benjamin
1764 Hamlington (Old Dominion U., USA), Anna Hogg (U. Leeds, UK), Martin Horwath (TU-
1765 Dresden, Germany), Vincent Humphrey (ETHZ, Switzerland), Laurent Husson (U. Grenoble,
1766 France), Masayoshi Ishii (MRI-JMA, Japan), Adrian Jaeggi (U. Bern, Switzerland), Svetlana
1767 Jevrejeva (NOC, UK), Gregory Johnson (NOAA/PMEL, USA), Jürgen Kusche (U. Bonn,
1768 Germany), Kurt Lambeck (ANU, Australia), Felix Landerer (JPL/Caltech, USA), Paul
1769 Leclercq (UIO, Norway), Benoit Legresy (CSIRO, Australia), Eric Leuliette (NOAA, USA),
1770 William Llovel (LEGOS, France), Laurent Longuevergne (U. Rennes, France), Bryant D.
1771 Loomis (NASA GSFC, USA), Scott B. Luthcke (NASA GSFC, USA), Marta Marcos (UIB,
1772 Spain), Ben Marzeion (U. Bremen, Germany), Chris Merchant (U. Reading, UK), Mark
1773 Merrifield (UCSD, USA), Glenn Milne (U. Ottawa, Canada), Gary Mitchum (U. South
1774 Florida, USA), Yara Mohajerani (UCI, USA), Maeva Monier (Mercator-Ocean, France),
1775 Steve Nerem (U. Colorado, USA), Hindumathi Palanisamy (LEGOS, France), Frank Paul
1776 (UZH, Switzerland), Begonia Perez (Puertos del Estados, Spain), Christopher G. Piecuch
1777 (WHOI, USA), Rui M. Ponte (AER inc., USA), Sarah G. Purkey (SIO/UCSD, USA), John T.
1778 Reager (JPL/Caltech, USA), Roelof Rietbroek (U. Bonn, Germany), Eric Rignot (UCI and
1779 JPL, USA), Riccardo Riva (TUDELFT, The Netherlands), Dean H. Roemmich (SIO/UCSD
1780 USA), Louise Sandberg Sørensen (DTU-SPACE, Denmark), Ingo Sasgen (AWI, Germany),
1781 E.J.O. Schrama (TUDELFT, The Netherlands), Sonia I. Seneviratne (ETHZ, Switzerland),
1782 C.K. Shum (Ohio State U., USA), Giorgio Spada (U. Urbino, Italy), Detlef Stammer (U.
1783 Hamburg, Germany), Roderic van de Wal (U. Utrecht, The Netherlands), Isabella Velicogna



1784 (UCI and JPL, USA), Karina von Schuckmann (Mercator-Océan, France), Yoshihide Wada
1785 (U. Utrecht, The Netherlands), Yiguo Wang (NERSC/BCCR, Norway), Christopher Watson
1786 (U. Tasmania, Australia), David Wiese (JPL/Caltech, USA), Susan Wijffels (CSIRO,
1787 Australia), Richard Westaway (U. Bristol, UK), Guy Woppelmann (U. La Rochelle, France),
1788 Bert Wouters (U. Utrecht, The Netherlands)

1789

1790 **Acknowledgements and author contributions:**

1791 This community assessment was initiated by A. Cazenave and B. Meyssignac as a
1792 contribution to the Grand Challenge ‘Regional Sea Level and Coastal Impacts’ of the World
1793 Climate Research Programme (WCRP). The results presented in this paper were prepared by
1794 9 different teams dedicated to the various terms of the sea level budget (i.e., altimetry-based
1795 sea level, tide gauges, thermal expansion, glaciers, Greenland, Antarctica, terrestrial water
1796 storage, glacial isostatic adjustment, ocean mass from GRACE). Thanks to the team leaders
1797 (in alphabetic order), M. Ablain, J. Bamber, N. Champollion, J. Chen, C. Domingues, S.
1798 Jevrejeva, J.T. Reager, K. von Schuckmann, G. Spada, I. Velicogna and R. van de Wal, who
1799 interacted with their team members, collected all needed information, provided a synthesized
1800 assessment of the literature and when needed, updated the published results. The coordinators
1801 A.C. and B.M. collected those materials and prepared a first draft of the manuscript, but all
1802 authors contributed to its refinement and to the discussion of the results. Special thanks are
1803 addressed to J. Benveniste, E. Berthier, G. Cogley, J. Church, G. Johnson (PMEL
1804 Contribution Number 4776), B. Marzeion, F. Paul, R. Ponte, and E. Schrama for improving
1805 the successive versions of the manuscript, and to H. Palanisamy for providing all figures
1806 presented in section 3.

1807 The views, opinions, and findings contained in this paper are those of the authors and should
1808 not be construed as an official NOAA, U.S. Government or other institutions position, policy,
1809 or decision.

1810

1811

1812 **References**

- 1813 1. A G., Chambers, D. P., Calculating trends from GRACE in the presence of large
1814 changes in continental ice storage and ocean mass. *Geophys. J. Int.*, pp. 272,
1815 doi:10.1111/j.1365-246X.2008.04012.x, 2008.
- 1816 2. A G., Wahr J. and Zhong S., Computations of the viscoelastic response of a 3-D
1817 compressible Earth to surface loading: an application to Glacial Isostatic Adjustment
1818 in Antarctica and Canada, *Geophysical Journal International* 192.2, 557-572, 2013.
- 1819 3. Ablain M., A. Cazenave, G. Valladeau, and S. Guinehut, “A New Assessment of the
1820 Error Budget of Global Mean Sea Level Rate Estimated by Satellite Altimetry over
1821 1993–2008.” *Ocean Science* 5 (2):193–201. <https://doi.org/10.5194/os-5-193-2009>,
1822 2009.
- 1823 4. Ablain, M., S. Philipps, M. Urvoy, N. Tran, and N. Picot, “Detection of Long-Term
1824 Instabilities on Altimeter Backscatter Coefficient Thanks to Wind Speed Data
1825 Comparisons from Altimeters and Models.” *Marine Geodesy* 35 (sup1):258–75.
1826 <https://doi.org/10.1080/01490419.2012.718675>, 2012.
- 1827 5. Ablain M., A. Cazenave, G. Larnicol, M. Balmaseda, P. Cipollini, Y. Faugère, M. J.
1828 Fernandes, et al., “Improved Sea Level Record over the Satellite Altimetry Era (1993–
1829 2010) from the Climate Change Initiative Project.” *Ocean Science* 11 (1). Copernicus
1830 GmbH:67–82. <https://doi.org/10.5194/os-11-67-2015>, 2015.
- 1831 6. Ablain M., J. F. Legeais, P. Prandi, M. Marcos, L. Fenoglio-Marc, H. B. Dieng, J.
1832 Benveniste, and A. Cazenave, “Satellite Altimetry-Based Sea Level at Global and
1833 Regional Scales.” *Surveys in Geophysics* 38 (1):7–31. [https://doi.org/10.1007/s10712-
1834 016-9389-8](https://doi.org/10.1007/s10712-016-9389-8), 2017a.
- 1835 7. Ablain M., R. Jugier, L. Zawadki, and N. Taburet, “The TOPEX-A Drift and Impacts
1836 on GMSL Time Series.” AVISO Website. October 2017.
1837 [https://meetings.aviso.altimetry.fr/fileadmin/user_upload/tx_ausycslseminar/files/Post
1838 er_OSTST17_GMSL_Drift_TOPEX-A.pdf](https://meetings.aviso.altimetry.fr/fileadmin/user_upload/tx_ausycslseminar/files/Poster_OSTST17_GMSL_Drift_TOPEX-A.pdf), 2017b.
- 1839 8. Abraham J. P., et al., A review of global ocean temperature observations: Implications
1840 for ocean heat content estimates and climate change, *Rev. Geophys.*, 51(3), 450-483,
1841 doi:10.1002/rog.20022, 2013.
- 1842 9. Adrian R et al., Lakes as sentinels of climate change *Limnology and Oceanography*
1843 54:2283-2297 doi:10.4319/lo.2009.54.6_part_2.2283, 2009.
- 1844 10. Ahmed M, Sultan M, Wahr J, Yan E, The use of GRACE data to monitor natural and
1845 anthropogenic induced variations in water availability across Africa *Earth-Science*
1846 *Reviews* 136:289-300/, 2014.
- 1847 11. Argus D.F. Peltier, W. R., Drummond, R., & Moore, The Antarctica component of
1848 postglacial rebound model ICE-6G_C (VM5a) based on GPS positioning, exposure
1849 age dating of ice thicknesses, and relative sea level histories. *Geophysical Journal*
1850 *International* 198, 1, 537-563, 2014.
- 1851 12. Armentano TV, Menges ES, Patterns of Change in the Carbon Balance of Organic
1852 Soil-Wetlands of the Temperate Zone *J Ecol* 74:755-774 doi:Doi 10.2307/2260396,
1853 1986.
- 1854 13. Awange JL, Sharifi MA, Ogonda G, Wickert J, Grafarend EW, Omulo M1, The
1855 falling Lake Victoria water level: GRACE, TRIMM and CHAMP satellite analysis of
1856 the lake basin, *Water Resources Management* 22:775-796, 2008.
- 1857 14. Bahr, D. and Radic, V., Significant contribution to total mass from very small glaciers,
1858 *The Cryosphere*, 6, 763-770, 2012.
- 1859 15. Bahr, D., Pfeffer, W., Sassolas, C. and Meier, M., Response time of glaciers as a
1860 function of size and mass balance: 1. theory, *Journal of Geophysical Research: Solid*
1861 *Earth*, 103, 9777-9782, 1998.



- 1862 16. Balmaseda M.A., K. Mogensen, A. Weaver (2013b). Evaluation of the ECMWF
1863 Ocean Reanalysis ORAS4. *Q. J. R. Meteorol. Soc.* DOI:10.1002/qj.2063, 2013.
- 1864 17. Barletta, V. R., Sørensen, L. S. & Forsberg, R. Scatter of mass changes estimates at
1865 basin scale for Greenland and Antarctica. *The Cryosphere*, 7, 1411-1432, 2013.
- 1866 18. Barnett, T.P.. The estimation of “global” sea level change: A problem of uniqueness.
1867 *J. Geophys. Res.*, 89 (C5), 7980-7988, 1984.
- 1868 19. Beck, H. E., van Dijk, A. I., de Roo, A., Dutra, E., Fink, G., Orth, R., & Schellekens,
1869 J., Global evaluation of runoff from 10 state-of-the-art hydrological
1870 models. *Hydrology and Earth System Sciences*, 21(6), 2881, 2017.
- 1871 20. Becker M, L Lovel W, Cazenave A, Güntner A, Crétaux J-F, Recent hydrological
1872 behavior of the East African great lakes region inferred from GRACE, satellite
1873 altimetry and rainfall observations *C. R. Geosci* 342:223-233, 2010.
- 1874 21. Beckley, B. D., P. S. Callahan, D. W. Hancock, G. T. Mitchum, and R. D. Ray. “On
1875 the ‘Cal-Mode’ Correction to TOPEX Satellite Altimetry and Its Effect on the Global
1876 Mean Sea Level Time Series.” *Journal of Geophysical Research, C: Oceans* 122
1877 (11):8371–84. <https://doi.org/10.1002/2017jc013090>, 2017.
- 1878 22. Belward AS, Estes JE, Kline KD, The IGBP-DIS global 1-km land-cover data set
1879 DISCover: A project overview *Photogrammetric Engineering and Remote Sensing*
1880 65:1013-1020, 1999.
- 1881 23. Bindoff, N., J. Willebrand, V. Artale, et al., Observations: Oceanic climate and sea
1882 level. In *Climate Change 2007: The Physical Science Basis; Contribution of Working*
1883 *Group I to the Fourth Assessment Report of the Intergovernmental Panel on Climate*
1884 *Change*. Edited by S. Solomon, D. Qin, M. Manning, et al., 386–432. Cambridge, UK,
1885 and New York: Cambridge Univ. Press, 2007.
- 1886 24. Boening, C., J. K. Willis, F. W. Landerer, R. S. Nerem, and J. Fasullo, The 2011 La
1887 Niña: So strong, the oceans fell, *Geophys. Res. Lett.*, 39(19), n/a-n/a,
1888 doi:10.1029/2012GL053055, 2012.
- 1889 25. Bosmans, J. H. C., van Beek, L. P. H., Sutanudjaja, E. H., and Bierkens, M. F. P.:
1890 Hydrological impacts of global land cover change and human water use, *Hydrol.*
1891 *Earth Syst. Sci. Discuss.*, <https://doi.org/10.5194/hess-2016-621>, in review, 2016.
- 1892 26. Boyer, T., C. Domingues, S. Good, G. C. Johnson, J. M. Lyman, M. Ishii, V.
1893 Gouretski, J., Antonov, N. Bindoff, J. Church, R. Cowley, J. Willis, and S. Wijffels.
1894 2015. Sensitivity of global ocean heat content estimates to mapping methods, XBT
1895 bias corrections, and baseline climatology, *Journal of Climate*, in press, 2016.
- 1896 27. Bredehoeft, J. D., The water budget myth revisited: why hydrogeologists model?,
1897 *Ground Water*, 40, 340–345, doi:10.1111/j.1745-6584.2002.tb02511.x, 2002.
- 1898 28. Butt N, de Oliveira PA, Costa MH, Evidence that deforestation affects the onset of the
1899 rainy season in Rondonia, Brazil *Journal of Geophysical Research-Atmospheres* 116:
1900 D11120 doi:10.1029/2010jd015174, 2011.
- 1901 29. Bolch, T., Sandberg Sørensen, L., Simonsen, S. B., Mölg, N., Machguth, H., Rastner,
1902 P. & Paul, F. Mass loss of Greenland’s glaciers and ice caps 2003–2008 revealed from
1903 ICESat laser altimetry data. *Geophysical Research Letters*, 40, 875-881, 2013.
- 1904 30. Box, J. E. & Colgan, W. T., Sea level rise contribution from Arctic land ice: 1850-
1905 2100. Snow, Water, Ice and Permafrost in the Arctic (SWIPA) 2017. Oslo, Norway:
1906 Arctic Monitoring and Assessment Programme (AMAP), 2017.
- 1907 31. Brun, F., Berthier, E., Wagnon, P., Kääh, A. and Treichler, D., A spatially resolved
1908 estimate of High Mountain Asia mass balances from 2000 to 2016, *Nature*
1909 *Geoscience*, 2017.



- 1910 32. Cao, G., C. Zheng, B. R. Scanlon, J. Liu, and W. Li, Use of flow modeling to assess
1911 sustainability of groundwater resources in the North China Plain, *Water Resour. Res.*,
1912 49, doi:10.1029/2012WR011899, 2013.
- 1913 33. Calafat, F.M., Chambers, D.P., and M.N. Tsimplis. On the ability of global sea level
1914 reconstructions to determine trends and variability. *J. Geophys. Res.*, 119, 1572-1592,
1915 2014.
- 1916 34. Cazenave, A., Dominh, K., Guinehut, S., Berthier, E., Llovel, W., Ramillien, G.,
1917 Ablain, M., and Larnicol, G., 2009. Sea level budget over 2003–2008: A reevaluation
1918 from GRACE space gravimetry, satellite altimetry and Argo, *Glob. Planet. Change*
1919 **65**:83–88, doi:10.1016/j.gloplacha.2008.10.004, 2009.
- 1920 35. Cazenave, A., Llovel, W., Contemporary Sea Level Rise, *Annu. Rev. Mar. Sci.* 2:145–
1921 73, 10.1146/annurev-marine-120308-081105, 2010.
- 1922 36. Cazenave, A., Champollion, N., Paul, F. and Benveniste, J. Integrative Study of the
1923 Mean Sea Level and Its Components, *Space Science Series of ISSI - Springer*, 416 pp,
1924 vol 58., 2017.
- 1925 37. Cazenave, A, H.B. Dieng, B. Meyssignac, K. von Schuckmann, B. Decharme, and E.
1926 Berthier. “The Rate of Sea-Level Rise.” *Nature Climate Change* 4 (5):358–61.
1927 <https://doi.org/10.1038/nclimate2159>, 2014.
- 1928 38. Chagnon FJF, Bras RL (2005) Contemporary climate change in the Amazon
1929 *Geophysical Research Letters* 32:L13703 doi:10.1029/2005gl022722, 2005.
- 1930 39. Chao, B. F., Y. H. Wu, and Y. S. Li, Impact of artificial reservoir water impoundment
1931 on global sea level, *Science*, 320, 212-214, doi:10.1126/science.1154580, 2008.
- 1932 40. Cheema, M. J., W. W. Immerzeel, and W. G. Bastiaanssen, Spatial quantification of
1933 groundwater abstraction in the irrigated Indus basin, *Ground Water*, 52, 25-36,
1934 doi:10.1111/gwat.12027, 2014.
- 1935 41. Chambers, D. P., J. Wahr, M. E. Tamisiea, and R. Steven Nerem, Reply to Comments
1936 by Peltier et al., 2012 (“Concerning the Interpretation of GRACE Time Dependent
1937 Gravity Observations and the Influence Upon them of Rotational Feedback in Glacial
1938 Isostatic Adjustment.”) *J. Geophys. Res.*, 117, DOI: 10.1029/2012JB009441, 2012.
- 1939 42. Chambers, D. P., Wahr, J., Tamisiea, M. E., and Nerem, R. S., Ocean mass from
1940 GRACE and glacial isostatic adjustment. *Journal of Geophysical Research (Solid*
1941 *Earth)*, 115(B14): L11415, doi:10.1029/2010JB007530, 2010.
- 1942 43. Chambers, D. P., A. Cazenave, N. Champollion, H. Dieng, W. Llovel, R. Forsberg, K.
1943 von Schuckmann, and Y. Wada, Evaluation of the Global Mean Sea Level Budget
1944 between 1993 and 2014, *Surv. Geophys.* 38, 309-327, doi: 10.1007/s10712-016-9381-
1945 3, 2017.
- 1946 44. Chen, Xianyao, Xuebin Zhang, John A. Church, Christopher S. Watson, Matt A. King,
1947 Didier Monselesan, Benoit Legresy, and Christopher Harig. “The Increasing Rate of
1948 Global Mean Sea-Level Rise during 1993–2014.” *Nature Climate Change* 7 (7):492–
1949 95. <https://doi.org/10.1038/nclimate3325>, 2017.
- 1950 45. Chen, J. L., Wilson, C. R., and Tapley, B. D., Contribution of ice sheet and mountain
1951 glacier melt to recent sea level rise, *Nature Geoscience*, DOI: 10.1038/NCEO1829,
1952 2013.
- 1953 46. Chen, J. L., Wilson, C. R., Tapley, B. D., Blankenship, D. D., and Ivins, E. R.,
1954 Patagonia Icefield Melting Observed by GRACE, *Geophys. Res. Lett.*, Vol. 34, No.
1955 22, L22501, 10.1029/2007GL031871, 2007.
- 1956 47. Chen, J. L., Wilson, C. R., Tapley, B. D., Save, H., and Cretaux, J.-F., Long-term and
1957 seasonal Caspian Sea level change from satellite gravity and altimeter
1958 measurements. *Journal of Geophysical Research (Solid Earth)*, 122:2274–2290,
1959 doi:10.1002/2016JB013595, 2017.



- 1960 48. Chen, J. L., C. R. Wilson, and B. D. Tapley (2010), The 2009 exceptional Amazon
1961 flood and interannual terrestrial water storage change observed by GRACE, *Water*
1962 *Resour. Res.*, 46, W12526, doi:10.1029/2010WR009383.
- 1963 49. Chen, J., J. S. Famiglietti, B. R. Scanlon, and M. Rodell, Groundwater Storage
1964 Changes: Present Status from GRACE Observations, *Surv. Geophys.*, 37, 397–417,
1965 doi:10.1007/s10712-015-9332-4, Special Issue: ISSI Workshop on Remote Sensing
1966 and Water Resources, 2017.
- 1967 50. Cheng, M.K., and Ries, J.R., Monthly estimates of C20 from 5 SLR satellites based on
1968 GRACE RL05 models, GRACE Technical Note 07, The GRACE Project, Center for
1969 Space Research, University of Texas at Austin, 2012.
- 1970 51. Cheng L., Trenberth K., Fasullo J., Boyer T., Abraham J. and Zhu J., Improved
1971 estimates of ocean heat content from 1960-2015, *Science Advances*, 3, e1601545,
1972 2017.
- 1973 52. Choblet, G., Husson, L., Bodin, T., Probabilistic surface re- construction of coastal sea
1974 level rise during the twentieth century *J. Geophys. Res.*, 119, 9206-9236, 2014.
- 1975 53. Church, J. et al., Sea level change, in Stocker, T. et al. (eds.) *Climate Change 2013:*
1976 *The Physical Science Basis. Contribution of Working Group I to the Fifth Assessment*
1977 *Report of the Intergovernmental Panel on Climate Change* (Cambridge University
1978 Press, Cambridge, United Kingdom and New York, NY, USA), 2013.
- 1979 54. Church, John, Jonathan Gregory, Neil White, Skye Platten, and Jerry Mitrovica.
1980 “Understanding and Projecting Sea Level Change.” *Oceanography* 24 (2):130–43.
1981 <https://doi.org/10.5670/oceanog.2011.33>, 2011.
- 1982 55. Church, J. A., and N. J. White. A 20th century acceleration in global sea-level rise,
1983 *Geophys. Res. Lett.*, 33, L01602, doi:10.1029/2005GL024826, 2006.
- 1984 56. Church, J. A., and N. J. White, Sea-Level Rise from the Late 19th to the Early 21st
1985 Century, *Surveys in Geophysics*, 32(4-5), 585-602, doi:10.1007/s10712-011-9119-1.,
1986 2011.
- 1987 57. Ciais P et al., Carbon and other biogeochemical cycles. In: Stocker TF et al. (eds)
1988 *Climate change 2013: the physical science basis. Contribution of working group I to*
1989 *the fifth assessment report of the Intergovernmental Panel on Climate Change.*
1990 Cambridge University Press, Cambridge, United Kingdom and New York, NY, USA,
1991 pp 465-570, 2013.
- 1992 58. Cretaux JF et al., SOLS: A lake database to monitor in the Near Real Time water level
1993 and storage variations from remote sensing data *Adv Space Res* 47:1497-1507
1994 doi:10.1016/j.asr.2011.01.004, 2011.
- 1995 59. Cogley, J., Geodetic and direct mass-balance measurements: comparison and joint
1996 analysis, *Annals of Glaciology*, 50, 96-100, 2009.
- 1997 60. Couhert, Alexandre, Luca Cerri, Jean-François Legeais, Michael Ablain, Nikita P.
1998 Zelensky, Bruce J. Haines, Frank G. Lemoine, William I. Bertiger, Shailen D. Desai,
1999 and Michiel Otten. “Towards the 1mm/y Stability of the Radial Orbit Error at
2000 Regional Scales.” *Advances in Space Research: The Official Journal of the Committee*
2001 *on Space Research* 55 (1):2–23. <https://doi.org/10.1016/j.asr.2014.06.041>, 2015.
- 2002 61. Dangendorf, S., M. Marcos, A. Müller, E. Zorita, R. Riva, K. Berk, and J. Jensen,
2003 Detecting anthropogenic footprints in sea level rise. *Nature Communications*, 6, 7849,
2004 2015.
- 2005 62. Dangendorf, Sönke, Marta Marcos, Guy Wöppelmann, Clinton P. Conrad, Thomas
2006 Frederikse, and Riccardo Riva. “Reassessment of 20th Century Global Mean Sea
2007 Level Rise.” *Proceedings of the National Academy of Sciences* 114 (23):5946–51.
2008 <https://doi.org/10.1073/pnas.1616007114>, 2017.



- 2009 63. Davaze, L., Rabatel, A., Arnaud, Y., Sirguey, P., Six, D., Letreguilly, A. and Dumont,
2010 M., Monitoring glacier albedo as a proxy to derive summer and annual mass balances
2011 from optical remote-sensing data, *The Cryosphere*, 12, 271-286, 2018.
- 2012 64. Darras S, IGBP-DIS wetlands data initiative, a first step towards identifying a global
2013 delineation of wetlands. IGBP-DIS Office, Toulouse, France, 1999.
- 2014 65. Davidson NC, How much wetland has the world lost? Long-term and recent trends in
2015 global wetland area *Marine and Freshwater Research* 65:934-941
2016 doi:10.1071/Mf14173, 2014.
- 2017 66. DeAngelis, A., F. Dominguez, Y. Fan, A. Robock, M. D. Kustu, and D. Robinson,
2018 Evidence of enhanced precipitation due to irrigation over the Great Plains of the
2019 United States, *J. Geophys. Res.*, 115, D15115, doi:10.1029/2010JD013892, 2010.
- 2020 67. Decharme B., R. Alkama, F. Papa, S. Faroux, H. Douville and C. Prigent, Global
2021 off-line evaluation of the ISBA-TRIP flood model, *Climate Dynamics*, 38, 1389-
2022 1412, doi:10.1007/s00382-011-1054-9, 2012.
- 2023 68. Decharme, B., Brun, E., Boone, A., Delire, C., Le Moigne, P., and Morin, S. (2016),
2024 Impacts of snow and organic soils parameterization on northern Eurasian soil
2025 temperature profiles simulated by the ISBA land surface model, *The Cryosphere*, 10,
2026 853-877, doi:10.5194/tc-10-853-2016.
- 2027 69. Dieng, H. B., N. Champollion, A. Cazenave, Y. Wada, E. Schrama, and B.
2028 Meyssignac, Total land water storage change over 2003-2013 estimated from a global
2029 mass budget approach, *Environ. Res. Lett.*, 10, 124010, doi:10.1088/1748-
2030 9326/10/12/124010, 2015a.
- 2031 70. Dieng, H. B., Cazenave, A., von Schuckmann, K., Ablain, M., and Meyssignac, B.,
2032 2015b. Sea level budget over 2005-2013: missing contributions and data errors. *Ocean
2033 Science*, 11:789-802, doi:10.5194/os-11-789-2015, 2015b.
- 2034 71. Dieng, H. B., Palanisamy, H., Cazenave, A., Meyssignac, B., and von Schuckmann,
2035 K., The Sea Level Budget Since 2003: Inference on the Deep Ocean Heat Content.
2036 *Surveys in Geophysics*, 36:209-229, doi:10.1007/s10712-015-9314-6, 2015c.
- 2037 72. Dieng, H.B, A.Cazenave, B.Meyssignac, M.Ablain, New estimate of the current rate
2038 of sea level rise from a sea level budget approach, *Geophysical Research Letters*, 44,
2039 doi:10.1002/2017GL073308, 2017.
- 2040 73. Döll, P., H. Hoffmann-Dobrev, F. T. Portmann, S. Siebert, A. Eicker, M. Rodell, and
2041 G. Strassberg, Impact of water withdrawals from groundwater and surface water on
2042 continental water storage variations, *J. Geodyn.*, 59-60, 143-156,
2043 doi:10.1016/j.jog.2011.05.001, 2012.
- 2044 74. Döll, P., M. Fritsche, A. Eicker, and S. H. Mueller, Seasonal water storage variations
2045 as impacted by water abstractions: Comparing the output of a global hydrological
2046 model with GRACE and GPS observations, *Surv. Geophys.*, doi:10.1093/gji/ggt485,
2047 2014a.
- 2048 75. Döll, P., H. Müller Schmied, C. Schuh, F. T. Portmann, and A. Eicker, Global-scale
2049 assessment of groundwater depletion and related groundwater abstractions:
2050 Combining hydrological modeling with information from well observations and
2051 GRACE satellites, *Water Resour. Res.*, 50, 5698-5720, doi:10.1002/2014WR015595,
2052 2014b.
- 2053 76. Döll, P., H. Douville, A. Güntner, H. Müller Schmied, and Y. Wada, Modelling
2054 freshwater resources at the global scale: Challenges and prospects, *Surv. Geophys.*, 37,
2055 195-221, Special Issue: ISSI Workshop on Remote Sensing and Water Resources,
2056 2017.



- 2057 77. Domingues C, Church J, White N, Gleckler PJ, Wijffels SE, et al. 2008. Improved
2058 estimates of upper ocean warming and multidecadal sea level rise. *Nature* 453:1090–
2059 93, doi:10.1038/nature07080, 2008.
- 2060 78. Douglas B., Global sea level rise, *Journal of Geophysical Research: Oceans*
2061 96(C4):6981-6992, 1991.
- 2062 79. Douglas B., Global sea rise: a redetermination, *Surveys in Geophysics* 18(2-3):279-
2063 292, 1997.
- 2064 80. Douglas, B.C., Sea level change in the era of recording tide gauges, in *Sea Level Rise,*
2065 *History and Consequences*, pp. 37–64, eds Douglas, B.C., Kearney, M.S. &
2066 Leatherman, S.P., Academic Press, San Diego, CA, 2001.
- 2067 81. Durack P., Gleckler, P., Landerer, F., and Taylor, K., Quantifying underestimates of
2068 long-term upper-ocean warming, *Nature Climate Change* 4, 999–1005, doi:10.1038/
2069 nclimate2389, 2014.
- 2070 82. Dutriex P et al., Strong sensitivity of Pine Island ice shelf melting to climatic
2071 variability, *Science* 343(6167), 2014.
- 2072 83. Escudier et al., Satellite radar altimetry: principle, accuracy and precision, in ‘Satellite
2073 altimetry over oceans and land surfaces, D.L Stammer and A. Cazenave eds., 617
2074 pages, CRC Press, Taylor and Francis Group, Boca Raton, New York, London, ISBN:
2075 13: 978-1-4987-4345-7, 2018.
- 2076 84. Famiglietti, J. S., The global groundwater crisis, *Nature Clim. Change*, 4, 945-948,
2077 doi:10.1038/nclimate2425, 2014.
- 2078 85. FAO, Global forest resources assessment 2015: how have the world's forests changed?
2079 Rome, 2015.
- 2080 86. Farinotti, D. et al. (2017). How accurate are estimates of glacier ice thickness ?, *The*
2081 *Cryosphere*, 11, 949-970, 2004.
- 2082 87. Farrell W., Clark J., On postglacial sea level, *Geophysical Journal International*
2083 46.3:647-667, 1976.
- 2084 88. Fasullo, J. T., C. Boening, F. W. Landerer, and R. S. Nerem, Australia's unique
2085 influence on global sea level in 2010–2011, *Geophys. Res. Lett.*, 40, 4368–4373,
2086 doi:10.1002/grl.50834, 2013.
- 2087 89. Felfelani, F., Wada, Y., Longuevergne, L., & Pokhrel, Y. N., Natural and human-
2088 induced terrestrial water storage change: A global analysis using hydrological models
2089 and GRACE. *Journal of Hydrology*, 553, 105-118, 2017.
- 2090 90. Feng, W., M. Zhong, J.-M. Lemoine, R. Biancale, H.-T. Hsu, and J. Xia, Evaluation of
2091 groundwater depletion in North China using the Gravity Recovery and Climate
2092 Experiment (GRACE) data and ground-based measurements, *Water Resour. Res.*, 49,
2093 2110–2118, doi:10.1002/wrcr.20192, 2013.
- 2094 91. Fleming K., Lambeck K., Constraints on the Greenland Ice Sheet since the Last
2095 Glacial Maximum from sea-level observations and glacial-rebound models,
2096 *Quaternary Science Reviews*23(9), 1053-1077, 2004.
- 2097 92. Forsberg, R., Sørensen, L. & Simonsen, S: Greenland and Antarctica Ice Sheet Mass
2098 Changes and Effects on Global Sea Level. *Surveys in Geophysics*, 38: 89.
2099 doi:10.1007/s10712-016-9398-7, 2017.
- 2100 93. Foster, S. and D. P. Loucks (eds.), *Non-Renewable Groundwater Resources: A*
2101 *guidebook on socially-sustainable management for water-policy makers*, IHP-VI,
2102 Series on Groundwater No. 10, UNESCO, Paris, France, 2006.
- 2103 94. Frederikse et al, A consistent sea-level reconstruction and its budget on basin and
2104 global scales over 1958-2014, *Journal of Climate*, [https://doi.org/10.1175/JCLI-D-17-](https://doi.org/10.1175/JCLI-D-17-0502.1)
2105 [0502.1](https://doi.org/10.1175/JCLI-D-17-0502.1), 2017.



- 2106 95. Frey, H., Machguth, H., Huss, M., Huggel, C., Bajracharaya, S., Bolch, T., Kulkarni,
2107 A., Linsbauer, A., Salzmann, N. and Stoffel, M., Estimating the volume of glaciers in
2108 the Himalayan-Karakoram region using different methods, *The Cryosphere*, 2014.
- 2109 96. Gardner, A.S., G. Moholdt, J.G. Cogley, B. Wouters, A.A. Arendt, J. Wahr, E.
2110 Berthier, R. Hock, W.T. Pfeffer, G. Kaser, S.R.M. Ligtenberg, T. Bolch, M.J. Sharp,
2111 J.O. Hagen, M.R. van den Broeke, and F. Paul, A reconciled estimate of glacier
2112 contributions to sea level rise: 2003 to 2009. *Science*, 340, 852-857,
2113 doi:10.1126/science.1234532, 2013.
- 2114 97. Gleick, P. H., Global Freshwater Resources: Soft-Path Solutions for the 21st Century,
2115 *Science*, 302, 1524-1528, doi:10.1126/science.1089967, 2003.
- 2116 98. Golytsyn GS, Panin GN, Once more on the water level changes of the Caspian Sea
2117 Vestnik Akademii Nauk SSSR 9:59-63 (in Russian), 1989.
- 2118 99. Gomez N., Pollard D., Mitrovica J.X., A 3-D coupled ice sheet–sea level model
2119 applied to Antarctica through the last 40 ky, *Earth and Planetary Science Letters* 384,
2120 88-99, 2013.
- 2121 100. Gornitz V, Rosenzweig C, Hillel D, Effects of anthropogenic intervention in
2122 the land hydrologic cycle on global sea level rise *Global and Planetary Change*
2123 14:147-161 doi:10.1016/s0921-8181(96)00008-2, 1997.
- 2124 101. Gornitz, V., Sea-level rise: A review of recent past and near-future trends.
2125 *Earth Surf. Process. Landforms*, 20, 7–20. doi: 10.1002/esp.3290200103, 1995.
- 2126 102. Gornitz, V., In Sea Level Rise: History and Consequences, Douglas, B. C., M.
2127 S. Kearney, and S. P. Leatherman (eds.), 97-119, Academic Press, San Diego, CA,
2128 USA, 2001.
- 2129 103. Gornitz, V., Lebedeff, S. and Hansen, J., Global sea level trend in the past
2130 century, *Science*, 215, 1611–1614, 1982.
- 2131 104. Gouretski, V. and K. Peter Koltermann. How much is the ocean really
2132 warming? *Geophysical Research Letters*, 34, L01610, doi:10.1029/2006GL027834,
2133 2007.
- 2134 105. Gregory, J. M., and J. A. Lowe. Predictions of global and regional sea-level
2135 rise using AOGCMs with and without flux adjustment. *Geophys. Res. Lett.*, **27**, 3069–
2136 3072, 2000..
- 2137 106. Gregory, J. M., N. J. White, J. A. Church, M. F. P. Bierkens, J. E. Box, M. R.
2138 van den Broeke, J. G. Cogley, X. Fettweis, E. Hanna, P. Huybrechts, L. F. Konikow,
2139 P. W. Leclercq, B. Marzeion, J. Oerlemans, M. E. Tamisiea, Y. Wada, L. M. Wake, R.
2140 S. W. van de Wal, Twentieth-Century Global-Mean Sea Level Rise: Is the Whole
2141 Greater than the Sum of the Parts?. *J. Climate*, 26, 4476–4499, doi:10.1175/JCLI-D-
2142 12-00319.1, 2013.
- 2143 107. Grinsted, A., An estimate of global glacier volume, *The Cryosphere*, 7, 141–
2144 151, 2013.
- 2145 108. Groh, A., & Horwath, M., The method of tailored sensitivity kernels for
2146 GRACE mass change estimates. *Geophysical Research Abstracts*, 18, EGU2016-
2147 12065, 2016.
- 2148 109. Gunter B.C., Didova O., Riva R.E.M., Ligtenberg S.R.M., Lenaerts J.T.M.,
2149 King M.A., Van den Broeke M.R., Urban T., and others, Empirical estimation of
2150 present-day Antarctic glacial isostatic adjustment and ice mass change, *The*
2151 *Cryosphere* 8(2), 743-760, 2014.
- 2152 110. Haerberli, W. and Linsbauer, A., Brief communication: global glacier volumes
2153 and sea level—small but systematic effects of ice below the surface of the ocean and
2154 of new local lakes on land, *The Cryosphere*, 7, 817-821, 2013.



- 2155 111. Hamlington, B. D., R. R. Leben, R. S. Nerem, W. Han, and K.-Y. Kim,
2156 Reconstructing sea level using cyclostationary empirical orthogonal functions, *J.*
2157 *Geophys. Res.*, 116, C12015, doi:10.1029/2011JC007529, 2011.
- 2158 112. Hamlington, B.D., Thompson, P., Hammond, W.C., Blewitt, G., and R.D.
2159 Ray, Assessing the impact of vertical land motion on twentieth century global mean
2160 sea level estimates, *Journal of Geophysical Research: Oceans*, 121(7), 4980-4993. doi:
2161 10.1002/2016JC011747, 2016.
- 2162 113. Hay, Carling C., Eric Morrow, Robert E. Kopp, and Jerry X. Mitrovica.
2163 “Probabilistic Reanalysis of Twentieth-Century Sea-Level Rise.” *Nature* 517
2164 (7535):481–84. <https://doi.org/10.1038/nature14093>, 2015.
- 2165 114. Henry, O., M.Ablain, B. Meyssignac, A. Cazenave, D. Masters, S. Nerem, and
2166 G. Garric. “Effect of the Processing Methodology on Satellite Altimetry-Based
2167 Global Mean Sea Level Rise over the Jason-1 Operating Period.” *Journal of Geodesy*
2168 88 (4). Springer Berlin Heidelberg:351–61. [https://doi.org/10.1007/s00190-013-0687-](https://doi.org/10.1007/s00190-013-0687-3)
2169 3, 2014.
- 2170 115. Horwath, M., Novotny K, Cazenave, A., Palanisamy, H., Marzeion, B., Paul,
2171 F., Döll, P., Cáceres, D., Hogg, A., Shepherd, A., Forsberg, R., Sørensen, L.,
2172 Barletta, V.R., Andersen, O.B., Rannal, H., Johannessen, J., Nilsen, J.E.,
2173 Gutknecht, B.D., Merchant, Ch.J., MacIntosh, C.R., von Schuckmann, K., *ESA*
2174 *Climate Change Initiative (CCI) Sea Level Budget Closure (SLBC_cci) Sea Level*
2175 *Budget Closure Assessment Report D3.1*. Version 1.0, 2018.
- 2176 116. Hosoda, S., T. Ohira and T. Nakamura. A monthly mean dataset of global
2177 oceanic temperature and salinity derived from Argo float observations. *JAMSTEC*
2178 *Rep. Res. Dev.*, Volume 8, November 2008, 47–59, 2008.
- 2179 117. Khan, S. A., Sasgen, I., Bevis, M., Van Dam, T., Bamber, J. L., Wahr, J.,
2180 Willis, M., Kjær, K. H., Wouters, B., Helm, V., Csatho, B., Fleming, K., Bjørk, A. A.,
2181 Aschwanden, A., Knudsen, P. & Munneke, P. K., Geodetic measurements reveal
2182 similarities between post–Last Glacial Maximum and present-day mass loss from the
2183 Greenland ice sheet. *Science Advances*, 2, 2016.
- 2184 118. Huang, Z., Y. Pan, H. Gong, P. J. Yeh, X. Li, D. Zhou, and W. Zhao,
2185 Subregional-scale groundwater depletion detected by GRACE for both shallow and
2186 deep aquifers in North China Plain, *Geophys. Res. Lett.*, 42, 1791–1799. doi:
2187 10.1002/2014GL062498, 2015.
- 2188 119. Huang Z., The Role of glacial isostatic adjustment (GIA) process on the
2189 determination of present-day sea level rise, Report n° 505, Geodetic Science, The
2190 Ohio State University, 2013.
- 2191 120. Huntington TG, Can we dismiss the effect of changes in land-based water
2192 storage on sea-level rise? *Hydrological Processes* 22:717-723 doi:10.1002/hyp.7001,
2193 2008.
- 2194 121. Hurkmans, R. T. W. L., Bamber, J. L., Davis, C. H., Joughin, I. R.,
2195 Khvorostovsky, K. S., Smith, B. S. & Schoen, N., Time-evolving mass loss of the
2196 Greenland Ice Sheet from satellite altimetry. *The Cryosphere*, 8, 1725-1740, 2014.
- 2197 122. Huss, M. and Hock, R., A new model for global glacier change and sea-level
2198 rise, *Front Earth Science*, 2015.
- 2199 123. Ishii, M., and M. Kimoto, Reevaluation of Historical Ocean Heat Content
2200 Variations with Time-varying XBT and MBT Depth Bias Corrections. *Journal of*
2201 *Oceanography* 65 (3) (June 1): 287–299. doi:10.1007/s10872-009-0027-7., 2009.
- 2202 124. Ivins, E. R., T. S. James, J. Wahr, E. J. O Schrama, F. W. Landerer, and K. M.
2203 Simon, Antarctic contribution to sea level rise observed by GRACE with improved



- 2204 GIA correction, *J. Geophys. Res. Solid Earth*, 118, 3126–3141,
2205 doi:10.1002/jgrb.50208, 2013.
- 2206 125. Jacob, T., J. Wahr, W. T. Pfeffer, and S. Swenson, Recent contributions of
2207 glaciers and ice caps to sea level rise, *Nature* 482, 514–518, doi:10.1038/nature10847,
2208 2012.
- 2209 126. Jensen, L., R. Rietbroek, and J. Kusche, Land water contribution to sea level
2210 from GRACE and Jason-1 measurements, *J. Geophys. Res. Oceans*, 118, 212–226,
2211 doi:10.1002/jgrc.20058, 2013.
- 2212 127. Jevrejeva S et al. Nonlinear trends and multi-year cycle in sea level records,
2213 *Journal of Geophysical Research* 111 2005JC003229, 2006.
- 2214 128. Jevrejeva, S., J. C. Moore, A. Grinsted, A. P. Matthews, and G. Spada,
2215 “Trends and Acceleration in Global and Regional Sea Levels since 1807.” *Global and*
2216 *Planetary Change* 113:11–22. <https://doi.org/10.1016/j.gloplacha.2013.12.004>, 2014.
- 2217 129. Johannesson, T., Raymond, C. and Waddington, E., Time-Scale for
2218 Adjustment of Glaciers to Changes in Mass Balance, *Journal of Glaciology*, 35, 355-
2219 369, 1989.
- 2220 130. Johnson, G. C. and Chambers, D. P., Ocean bottom pressure seasonal cycles
2221 and decadal trends from GRACE Release-05: Ocean circulation implications, *J.*
2222 *Geophys. Res. Oceans*, 118, 4228–4240, doi:10.1002/jgrc.20307, 2013.
- 2223 131. Johnson, G. C., and A. N. Birnbaum. 2017. As El Niño builds, Pacific Warm
2224 Pool expands, ocean gains more heat. *Geophysical Research Letters*, 44, 438-445,
2225 doi:10.1002/2016GL071767, 2017.
- 2226 132. Khan, S. A., Sasgen, I., Bevis, M., Van Dam, T., Bamber, J. L., Wahr, J.,
2227 Willis, M., Kjær, K. H., Wouters, B., Helm, V., Csatho, B., Fleming, K., Bjørk, A. A.,
2228 Aschwanden, A., Knudsen, P. and Munneke, P. K., Geodetic measurements reveal
2229 similarities between post–Last Glacial Maximum and present-day mass loss from the
2230 Greenland ice sheet. *Science Advances*, 2., 2016.
- 2231 133. Kääh, A., Treichler, D., Nuth, C. and Berthier, E., Brief communication:
2232 contending estimates of 2003–2008 glacier mass balance over the Pamir–Karakoram–
2233 Himalaya, *The Cryosphere*, 9, 557–564, 2015.
- 2234 134. Kaser, G., Cogley, J., Dyurgerov, M., Meier, M. and Ohmura, A., Mass
2235 balance of glaciers and ice caps: Consensus estimates for 1961–2004, *Geophysical*
2236 *Research Letters*, 33, L19501, 2006.
- 2237 135. Keenan RJ, Reams GA, Achard F, de Freitas JV, Grainger A, Lindquist E.,
2238 Dynamics of global forest area: Results from the FAO Global Forest Resources
2239 Assessment 2015 *Forest Ecol Manag* 352:9-20 doi:10.1016/j.foreco.2015.06.014,
2240 2015.
- 2241 136. Kemp, A. C., B. Horton, J. P. Donnelly, M. E. Mann, M. Vermeer, and S.
2242 Rahmstorf, Climate related sea level variations over the past two millennia. *PNAS*
2243 108.27: 11017–11022, 2011.
- 2244 137. Khatiwala S, Primeau F, Hall T., Reconstruction of the history of
2245 anthropogenic CO₂ concentrations in the ocean *Nature* 462:346-U110
2246 doi:10.1038/nature08526, 2009.
- 2247 138. King M.A., Altamimi Z., Boehm J., Bos M., Dach R., Elosegui P., and others,
2248 Improved constraints on models of glacial isostatic adjustment: a review of the
2249 contribution of ground-based geodetic observations, *Surveys in geophysics*
2250 31(5):465, 2010.
- 2251 139. Klige RK, Myagkov MS, Changes in the water regime of the Caspian Sea,
2252 *Geol. Journal* 27:299-307, 1992.



- 2253 140. Konikow, L. F., Contribution of global groundwater depletion since 1900 to
2254 sea-level rise, *Geophys. Res. Lett.*, 38, L17401, doi:10.1029/2011GL048604, 2011.
- 2255 141. Konrad H., Sasgen I., Pollard D., Klemann V., Potential of the solid-Earth
2256 response for limiting long-term West Antarctic Ice Sheet retreat in a warming climate,
2257 *Earth and Planetary Science Letters* 432, 254-264, 2015.
- 2258 142. Kopp R.E., Hay C.C., Little C.M., Mitrovica J.X., Geographic variability of
2259 sea-level change, *Current Climate Change Reports* 1(3):192, 2015.
- 2260 143. Kustu, M., Y. Fan, and A. Robock, Large-scale water cycle perturbation due to
2261 irrigation pumping in the US High Plains: A synthesis of observed streamflow
2262 changes, *J. Hydrol.*, 390, 222–244, doi:10.1016/j.jhydrol.2010.06.045, 2010.
- 2263 144. Kustu, M. D., Y. Fan, and M. Rodell, Possible link between irrigation in the
2264 U.S. High Plains and increased summer streamflow in the Midwest, *Water Resour.*
2265 *Res.*, 47, W03522, doi:10.1029/2010WR010046, 2011.
- 2266 145. Lambeck K, Chappell J., *Science* 292(5517):679, 2001.
- 2267 146. Lambeck K., Sea-level change from mid-Holocene to recent time: An
2268 Australian example with global implications, In: Ice Sheets, Sea Level and the
2269 Dynamic Earth, JX Mitrovica and LLA Vermeersen, Eds., Geodynamics Series,
2270 29:33-50, 2002.
- 2271 147. Lambeck K. et al., Paleoenvironmental records, geophysical modelling and
2272 reconstruction of sea level trends and variability on centennial and longer time scales,
2273 *In Understanding sea level rise and variability*, JA Church et al ed., Wiley-Blackwell,
2274 2010.
- 2275 148. Leclercq, P., Oerlemans, J. and Cogley, J., Estimating the glacier contribution
2276 to sea-level rise for the period 1800–2005, *Surveys in Geophysics*, 32, 519–535, 2011.
- 2277 149. Legeais, J-F, Michaël Ablain, Lionel Zawadzki, Hao Zuo, Johnny A.
2278 Johannessen, Martin G. Scharffenberg, Luciana Fenoglio-Marc, et al., “An Accurate
2279 and Homogeneous Altimeter Sea Level Record from the ESA Climate Change
2280 Initiative.” *Earth System Science Data Discussions*, [1–35, doi.org/10.5194/essd-2017-](https://doi.org/10.5194/essd-2017-116)
2281 [116](https://doi.org/10.5194/essd-2017-116), 2018.
- 2282 150. Lehner, B., C. Reidy Liermann, C. Revenga, C. Vörösmarty, B. Fekete, P.
2283 Crouzet, P. Döll, M. Endejan, K. Frenken, J. Magome, C. Nilsson, J. C. Robertson, R.
2284 Rödel, N. Sindorf, and D. Wisser, High-resolution mapping of the world's reservoirs
2285 and dams for sustainable river-flow management, *Fron. Ecol. Environ.*, 9, 494-502,
2286 doi:10.1890/100125, 2011.
- 2287 151. Le Queré et al., Global Carbon Budget 2017, *Earth Syst. Sci. Data*, 10, 405-
2288 448, 2018, doi.org/10.5194/essd-10-405-2018, 2018.
- 2289 152. Lettenmaier, D. P., and P. C. D. Milly, Land waters and sea level, *Nat. Geosci.*,
2290 2, 452-454, doi:10.1038/ngeo567, 2009.
- 2291 153. Leuliette, E. W., and Miller, L., Closing the sea level rise budget with altimetry,
2292 Argo, and GRACE, *Geophys. Res. Lett.*, 36, L04608, doi:10.1029/2008GL036010,
2293 2009.
- 2294 154. Leuliette, E.W., and Willis, J.K., Balancing the sea level budget,
2295 *Oceanography* 24 (2): 122–129, doi:10.5670/oceanog.2011.32, 2011.
- 2296 155. Leuschen, C.: IceBridge Geolocated Radar Echo Strength Profiles, Boulder,
2297 Colorado, NASA DAAC at the National Snow and Ice Data Center,
2298 <http://dx.doi.org/10.5067/FAZTWP500V70>, last access: 15 June 2014
- 2299 156. Levitus S., J.I. Antonov, T.P. Boyer, O.K. Baranova, H.E. Garcia, R.A.
2300 Locarnini, A.V. Mishonov, J.R. Reagan, D. Seidov, E.S. Yarosh and M.M. Zweng,
2301 World ocean heat content and thermosteric sea level change (0-2000 m), 1955-2010,
2302 *Geophys. Res. Lett.*, 39, L10603, doi:10.1019/2012GL051106, 2012.



- 2303 157. Llovel, W., J. K. Willis, F. W. Landerer, and I. Fukumori, Deep-ocean
2304 contribution to sea level and energy budget not detectable over the past decade, *Nature*
2305 *Clim. Change* 4, 1031–1035, doi:10.1038/nclimate2387, 2014.
- 2306 158. Llovel, W., M. Becker, A. Cazenave, J.-F. Crétaux, and G. Ramillien, *C. R.*
2307 *Geosci.* 342, 179–188, doi :10.1016/j.crte.2009.12.004, 2010.
- 2308 159. Lo, M.-H., and J. S. Famiglietti, Irrigation in California’s Central Valley
2309 strengthens the southwestern U.S. water cycle, *Geophys. Res. Lett.*, 40,
2310 doi:10.1002/grl.50108, 2013.
- 2311 160. Loriaux, T. and Casassa, G., Evolution of glacial lakes from the Northern
2312 Patagonia Icefield and terrestrial water storage in a sea-level rise context, *Global and*
2313 *Planetary Change*, 102, 33-40, 2013.
- 2314 161. Lovel TR, Belward AS, The IGBP-DIS global 1 km land cover data set,
2315 DISCover: first results *International Journal of Remote Sensing* 18:3291-3295, 1997.
- 2316 162. Luthcke, S. B., Sabaka, T. J., Loomis, B. D., Arendt, A. A., McCarthy, J. J.,
2317 and Camp, J., Antarctica, Greenland and Gulf of Alaska land-ice evolution from an
2318 iterated GRACE global mascon solution. *Journal of Glaciology*, 59:613–631,
2319 doi:10.3189/2013JoG12J147, 2013.
- 2320 163. Luthcke, S. B., Zwally, H. J., Abdalati, W., Rowlands, D. D., Ray, R. D.,
2321 Nerem, R. S., Lemoine, F. G., McCarthy, J. J., and Chinn, D. S., Recent Greenland Ice
2322 Mass Loss by Drainage System from Satellite Gravity Observations. *Science*,
2323 314:1286–1289, doi:10.1126/science.1130776, 2006.
- 2324 164. Luthcke, S. B., Sabaka, T., Loomis, B., Arendt, A., Mccarthy, J. & Camp, J.,
2325 Antarctica, Greenland and Gulf of Alaska land-ice evolution from an iterated GRACE
2326 global mascon solution. *Journal of Glaciology*, 59, 613-631, 2013.
- 2327 165. Lyman, J. M., S. A. Godd, V. V. Gouretski, et al., Robust warming of the
2328 global upper ocean. *Nature* 465:334–337, 2010.
- 2329 166. MacDicken KG, Global Forest Resources Assessment, What, why and how?
2330 *Forest Ecol Manag* 352:3-8 doi:10.1016/j.foreco.2015.02.006, 2015.
- 2331 167. Martín-Español, A., Zammit-Mangion, A., Clarke, P. J., Flament, T., Helm, V.,
2332 King, M. A., and Wouters, B., Spatial and temporal Antarctic Ice Sheet mass trends,
2333 glacio-isostatic adjustment, and surface processes from a joint inversion of satellite
2334 altimeter, gravity, and GPS data. *Journal of Geophysical Research: Earth*
2335 *Surface*, 121(2), 182-200, 2016.
- 2336 168. Martinec Z., Hagedoorn J., The rotational feedback on linear-momentum
2337 balance in glacial isostatic adjustment, *Geophysical Journal International*
2338 199.3:1823-1846, 2014.
- 2339 169. Merrifield MA et al., An anomalous recent acceleration of global sea level rise.
2340 *J. Clim.* 22: 5772–5781. doi:10.1175/2009JCLI2985.1., 2009.
- 2341 170. Meyssignac B., M. Becker, W. Llovel, and A. Cazenave, An Assessment of
2342 Two-Dimensional Past Sea Level Reconstructions Over 1950–2009 Based on Tide-
2343 Gauge Data and Different Input Sea Level Grids, *Surv Geophys* DOI
2344 10.1007/s10712-011-9171-x, 2011.
- 2345 171. Milne G.A., Gehrels W.R., Hughes C.W., Tamisiea M.E., Identifying the
2346 causes of sea-level change, *Nature Geoscience* 2.7:471, 2009.
- 2347 172. Mitrovica J.X., Milne G.A., On the origin of late Holocene sea-level
2348 highstands within equatorial ocean basins, *Quaternary Science Reviews* 21(20-
2349 22):2179-2190, 2002.
- 2350 173. Mitrovica J.X., Milne G.A., On post-glacial sea level: I. General theory,
2351 *Geophysical Journal International* 154(2):253, 2003.



- 2352 174. Mitrovica J.X., Wahr J., Matsuyama I., Paulson A., The rotational stability of
2353 an ice-age earth, *Geophysical Journal International* 161.2, 491-506, 2005.
- 2354 175. Mitrovica J.X., Wahr J., Ice age Earth rotation, *Annual Review of Earth and*
2355 *Planetary Sciences* 39:577-616, 2011.
- 2356 176. Marzeion, B., Jarosch, A., Hofer, M., Past and future sea-level change from
2357 the surface mass balance of glaciers, *The Cryosphere*, 6, 1295–1322, 2012.
- 2358 177. Marzeion, B., Cogley, J., Richter, K. and Parkes, D., Attribution of global
2359 glacier mass loss to anthropogenic and natural causes, *Science*, 345, 919–92, 2014.
- 2360 178. Marzeion, B., Champollion, N., Haeberli, W., Langley, K., Leclercq, P. and
2361 Paul, F., Observation-Based Estimates of Global Glacier Mass Change and Its
2362 Contribution to Sea-Level Change, *Surveys in Geophysics*, 28, 105-130, 2017.
- 2363 179. Marzeion, B., Kaser, G., Maussion, F. and Champollion, N., Limited influence
2364 of climate change mitigation on short-term glacier mass loss, *Nature Climate Change*,
2365 doi:[10.1038/s41558-018-0093-1](https://doi.org/10.1038/s41558-018-0093-1), 2018.
- 2366 180. Masters, D., R. S. Nerem, C. Choe, E. Leuliette, B. Beckley, N. White, and M.
2367 Ablain., “Comparison of Global Mean Sea Level Time Series from TOPEX/Poseidon,
2368 Jason-1, and Jason-2.” *Marine Geodesy* 35 (sup1):20–41.
2369 <https://doi.org/10.1080/01490419.2012.717862>, 2012.
- 2370 181. Matthews E, Fung I, Methane emission from natural wetlands: Global
2371 distribution, area, and environmental characteristics of sources *Global Biogeochemical*
2372 *Cycles* 1:61-86, 1987.
- 2373 182. Matthews GVT, The Ramsar Convention on wetlands: its history and
2374 development. Ramsar Convention Bureau, Gland, Switzerland, 1993.
- 2375 183. Maussion, F, Butenko, A., Eis, J., Fourteau, K., Jarosch, A., Landmann, J.,
2376 Oesterle, J., Recinos, B., Rothenpieler, T., Vlug, A., Wild, C. and Marzeion; B., The
2377 Open Global Glacier Model (OGGM) v1.0, *subm. to The Cryosphere*, 2018.
- 2378 184. McMillan M. et al. Increased ice losses from Antarctica detected by Cryosat-2,
2379 *Geophys. Res. Lett.*, 41(11), 3899-3905, 2014.
- 2380 185. Meherhomji VM, Probable Impact of Deforestation on Hydrological Processes
2381 *Climatic Change* 19:163-173 doi:10.1007/Bf00142223, 1991.
- 2382 186. Micklin PP, The Aral Crisis - Introduction to the Special Issue Post-Sov Geogr
2383 33:269-282, 1992.
- 2384 187. Milly P. C. D. et al., Terrestrial water-storage contributions to sea-level rise
2385 and variability, in *Understanding Sea-Level Rise and Variability*:226-255, 2010.
- 2386 188. Milly, P. C. D., A. Cazenave, and M. C. Gennero, Contribution of climate-
2387 driven change in continental water storage to recent sea-level rise. *Proc. Natl. Acad.*
2388 *Sci.*, 100, 13158–13161, 2003.
- 2389 189. Mitra S, Wassmann R, Vlek PLG, An appraisal of global wetland area and its
2390 organic carbon stock *Curr Sci India* 88:25-35, 2005.
- 2391 190. Mitsch WJ, Gosselink JG, Wetlands, 2nd ed. Van Nostrand Reinhold, New
2392 York, 1993.
- 2393 191. Mougnot J., E. Rignot, B. Scheuchl, Sustained increase in ice discharge from
2394 the Amundsen Sea Embayment, West Antarctica, from 1973 to 2013, *Geophys. Res.*
2395 *Lett.* 41, 1576-1584, 2014.
- 2396 192. Natarov, S. I., M. A. Merrifield, J. M. Becker, and P. R. Thompson, Regional
2397 influences on reconstructed global mean sea level, *Geophys. Res. Lett.*, 44, 3274-
2398 3282, 2017.
- 2399 193. Nerem, R. S., D. P. Chambers, C. Choe, and G. T. Mitchum. “Estimating Mean
2400 Sea Level Change from the TOPEX and Jason Altimeter Missions.” *Marine Geodesy*
2401 33 (sup1):435–46. <https://doi.org/10.1080/01490419.2010.491031>, 2010.



- 2402 194. Nerem R.S., Beckley B.D., Fasullo J., Hamlington B.D., Masters D. and
2403 Mitchum G.T., Climate Change Driven Accelerated Sea Level Rise Detected In The
2404 Altimeter Era, *PNAS*, 2018.
- 2405 195. Nghiem, S., Hall, D., Mote, T., Tedesco, M., Albert, M., Keegan, K., Shuman,
2406 C., Digirolamo, N. & Neumann, G., The extreme melt across the Greenland ice sheet
2407 in 2012. *Geophysical Research Letters*, 39, 2012.
- 2408 196. Nobre P, Malagutti M, Urbano DF, de Almeida RAF, Giarolla E, Amazon
2409 Deforestation and Climate Change in a Coupled Model Simulation *J Climate* 22:5686-
2410 5697 doi:10.1175/2009jcli2757.1, 2009.
- 2411 197. Oki, T. and S. Kanae, Global hydrological cycles and world water resources,
2412 *Science*, 313, 1068-1072, doi:10.1126/science.1128845, 2006.
- 2413 198. Ozyavas A, Khan SD, Casey JF, A possible connection of Caspian Sea level
2414 fluctuations with meteorological factors and seismicity *Earth Planet Sc Lett* 299:150-
2415 158 doi:10.1016/j.epsl.2010.08.030, 2010.
- 2416 199. Pala, C., Once a Terminal Case, the North Aral Sea Shows New Signs of Life,
2417 *Science*, 312, 183, doi:10.1126/science.312.5771.183, 2006.
- 2418 200. Pala, C., In Northern Aral Sea, Rebound Comes With a Big Catch, *Science*,
2419 334, 303, doi:10.1126/science.334.6054.303, 2011.
- 2420 201. Palmer M. et al., 2016.
- 2421 202. Paul, F., Huggel, C. and Käab, Combining satellite multispectral image data
2422 and a digital elevation model for mapping of debris-covered glaciers, *Remote Sensing*
2423 *of Environment*, 89, 510–518, 2004.
- 2424 203. Paulson, A., Zhong, S., and Wahr, J., Inference of mantle viscosity from
2425 GRACE and relative sea level data. *Geophysical Journal International*, 171:497–508,
2426 doi:10.1111/j.1365-246X.2007.03556.x, 2007.
- 2427 204. Peltier W.R., Global glacial isostatic adjustment and modern instrumental
2428 records of relative sea level history, in: B.C. Douglas, M.S. Kearney, S.P. Leatherman
2429 (Eds.), *Sea-Level Rise: History and Consequences*, vol. 75, Academic Press, San
2430 Diego, 2001, pp. 65–95.
- 2431 205. Peltier W.R., Luthcke S.B., On the origins of Earth rotation anomalies: New
2432 insights on the basis of both “paleogeodetic” data and Gravity Recovery and Climate
2433 Experiment (GRACE) data , *Journal of Geophysical Research: Solid Earth* 114,
2434 B11405, 2009.
- 2435 206. Peltier W.R., Global glacial isostasy and the surface of the ice-age Earth: the
2436 ICE-5G (VM2) model and GRACE, *Annual Review of Earth and Planetary Sciences*
2437 32:111, 2004.
- 2438 207. Peltier W.R., Argus D.F., Drummond R., Space geodesy constrains ice age
2439 terminal deglaciation: The global ICE-6G_C (VM5a) model, *Journal of Geophysical*
2440 *Research: Solid Earth* 120(1):450-487, 2015.
- 2441 208. Peltier W.R., Closure of the budget of global sea level rise over the GRACE
2442 era: the importance and magnitudes of the required corrections for global glacial
2443 isostatic adjustment. *Quaternary Science Reviews*, 28, 1658-1674, 2009.
- 2444 209. Peltier, W. R., R. Drummond, and K. Roy, Comment on "Ocean mass from
2445 GRACE and glacial isostatic adjustment" by D. P. Chambers et al. *Journal of*
2446 *Geophysical Research-Solid Earth*, 117, B11403, 2012.
- 2447 210. Perera J, A Sea Turns to Dust *New Sci* 140:24-27, 1993.
- 2448 211. Pfeffer, W., Arendt, A., Bliss, A., Bolch, T., Cogley, J., Gardner, A., Hagen, J.-
2449 O., Hock, R., Kaser, G., Kienholz, C., Miles, E., Moholdt, G., Mölg, N., Paul, F.,
2450 Radić, V., Rastner, P., Raup, B., Rich, J. and Sharp, M., The Randolph Glacier



- 2451 Inventory: a globally complete inventory of glaciers., *Journal of Glaciology*, 60, 537–
2452 552, 2014.
- 2453 212. Plag H.P., Juettner H.U., Inversion of global tide gauge data for present-day ice
2454 load changes, *Memoirs of National Institute of Polar Research* 54:301, 2001.
- 2455 213. Pokhrel, Y. N., N. Hanasaki, P. J.-F. Yeh, T. Yamada, S. Kanae, and T. Oki,
2456 Model estimates of sea level change due to anthropogenic impacts on terrestrial water
2457 storage, *Nat. Geosci.*, 5, 389–392, doi:10.1038/ngeo1476, 2012.
- 2458 214. Pokhrel, Y. N., S. Koirala, P. J.-F. Yeh, N. Hanasaki, L. Longuevergne, S.
2459 Kanae, and T. Oki, Incorporation of groundwater pumping in a global Land Surface
2460 Model with the representation of human impacts, *Water Resour. Res.*, 51, 78–96,
2461 doi:10.1002/2014WR015602, 2015.
- 2462 215. Postel, S. L., Pillar of Sand: Can the Irrigation Miracle Last? W.W. Norton,
2463 New York USA, ISBN 0-393-31937-7, 1999.
- 2464 216. Purcell A.P., Tregoning P., Dehecq A., An assessment of the ICE6G_C
2465 (VM5a) glacial isostatic adjustment model, *Journal of Geophysical Research: Solid
2466 Earth* 121(5), 3939-3950, 2016.
- 2467 217. Purkey, S. G., Johnson, G. C., and Chambers, D. P., Relative contributions of
2468 ocean mass and deep steric changes to sea level rise between 1993 and 2013, *J.
2469 Geophys. Res. Oceans*, 119, 7509–7522, doi:10.1002/2014JC010180, 2014.
- 2470 218. Purkey, S., and G. C. Johnson, Warming of global abyssal and deep southern
2471 ocean waters between the 1990s and 2000s: Contributions to global heat and sea level
2472 rise budget, *J. Clim.*, 23, 6336–6351, doi:10.1175/2010JCLI3682.1, 2010.
- 2473 219. Radic, V. and Hock, R., Regional and global volumes of glaciers derived from
2474 statistical upscaling of glacier inventory data, *Journal of Geophysical Research Earth
2475 Surface*, 115, F01010, 2010.
- 2476 220. Radic, V. and Hock, R., Regionally differentiated contribution of mountain
2477 glaciers and ice caps to future sea-level rise, *Nature Geoscience*, 4, 91-94, 2011.
- 2478 221. Ramillien G, Frappart F, Seoane L, Application of the regional water mass
2479 variations from GRACE Satellite Gravimetry to large-scale water management in
2480 Africa *Remote Sensing* 6:7379-7405, 2014.
- 2481 222. Ray, R.D., and B.C. Douglas, Experiments in reconstructing twentieth-
2482 century sea levels, *Prog. Oceanogr.* 91, 495–515, 2011.
- 2483 223. Reager, J. T., Gardner, A. S., Famiglietti, J. S., Wiese, D. N., Eicker, A., & Lo,
2484 M. H., A decade of sea level rise slowed by climate-driven hydrology. *Science*,
2485 351(6274), 699-703, doi:10.1126/science.aad8386, 2016.
- 2486 224. Reager, J. T., Thomas, B. F., and Famiglietti, J. S., River basin flood potential
2487 inferred using GRACE gravity observations at several months lead time. *Nature
2488 Geoscience*, 7:588–592, doi:10.1038/ngeo2203, 2014.
- 2489 225. Rhein, M., S.R. Rintoul, S. Aoki, E. Campos, D. Chambers, R.A. Feely, S.
2490 Gulev, G.C. Johnson, S.A. Josey, A. Kostianoy, C. Mauritzen, D. Roemmich, L.D.
2491 Talley and F. Wang: Observations: Ocean. In: Climate Change 2013: The Physical
2492 Science Basis. Contribution of Working Group I to the Fifth Assessment Report of the
2493 Intergovernmental Panel on Climate Change [Stocker, T.F., D. Qin, G.-K. Plattner, M.
2494 Tignor, S.K. Allen, J. Boschung, A. Nauels, Y. Xia, V. Bex and P.M. Midgley (eds.)].
2495 Cambridge University Press, Cambridge, United Kingdom and New York, NY, USA.,
2496 2013.
- 2497 226. Richey, A. S., B. F. Thomas, M.-H. Lo, J. T. Reager, J. S. Famiglietti, K. Voss,
2498 S. Swenson, and M. Rodell, Quantifying renewable groundwater stress with GRACE,
2499 *Water Resour. Res.*, 51, 5217–5238, doi:10.1002/2015WR017349, 2015.



- 2500 227. Rietbroek, R., Brunnabend, S.-E., Kusche, J. and Schröter, J., Resolving sea
2501 level contributions by identifying fingerprints in time-variable gravity and altimetry, *J.*
2502 *Geodyn.*, 59-60, 72-81, 2012.
- 2503 228. Rietbroek, R., Brunnabend, S.-E., Kusche, J., Schröter, J., and Dahle, C.,
2504 Revisiting the contemporary sea-level budget on global and regional scales.
2505 *Proceedings of the National Academy of Sciences*, 113(6):1504–1509,
2506 doi:10.1073/pnas.1519132113, 2016.
- 2507 229. Rignot, E. J., I. Velicogna, M. R. van den Broeke, A. J. Monaghan, and J. T.
2508 M. Lenaerts, Acceleration of the contribution of the Greenland and Antarctic ice
2509 sheets to sea level rise, *Geophys. Res. Lett.*, 38, L05503, doi:10.1029/2011GL046583,
2510 2011.
- 2511 230. Rignot, E., J. Mouginot, and B. Scheuchl, Ice flow of the Antarctic Ice
2512 Sheet, *Science*, **333**(6048), 1427–1430, doi:10.1126/science.1208336, 2011.
- 2513 231. Riva R.E., Gunter B.C., Urban T.J., Vermeersen B.L., Lindenbergh R.C.,
2514 Helsen M.M., and others, Glacial isostatic adjustment over Antarctica from combined
2515 ICESat and GRACE satellite data, *Earth and Planetary Science Letters* 288(3), 516-
2516 523, 2009.
- 2517 232. Riva, R. E. M., J. L. Bamber, D. A. Lavallée, and B. Wouters, Sea-level
2518 fingerprint of continental water and ice mass change from GRACE, *Geophys. Res.*
2519 *Lett.*, 37, L19605, doi:10.1029/2010GL044770, 2010.
- 2520 233. Rodell, M., I. Velicogna, and J. S. Famiglietti, Satellite-based estimates of
2521 groundwater depletion in India, *Nature*, 460, 999-1002, doi:10.1038/nature08238,
2522 2009.
- 2523 234. Roemmich, D., Owens, W.B., The ARGO project: global ocean observations
2524 for understanding for understanding and prediction of climate variability.
2525 *Oceanography* 13 (2), 45–50, 2000.
- 2526 235. Roemmich, D., W. J. Gould, and J. Gilson, 135 years of global ocean warming
2527 between the Challenger expedition and the Argo Programme, *Nature Climate Change*,
2528 2(6), 425-428, doi:10.1038/nclimate1461, 2012.
- 2529 236. Roemmich, D, Gilson J, Sutton P, Zilberman N. 2016. [Multidecadal change](#)
2530 [of the South Pacific gyre circulation](#). *Journal of Physical Oceanography*. 46:1871-
2531 1883. [10.1175/jpo-d-15-0237.1](#), 2016.
- 2532 237. Roemmich, D. and J. Gilson. The 2004–2008 mean and annual cycle of
2533 temperature, salinity, and steric height in the global ocean from the Argo Program,
2534 *Progress in Oceanography*, Volume 82, Issue 2, August 2009, Pages 81-100, 2009.
- 2535 238. Rohrig E, Biomass and productivity. In: Rohrig E (ed.) *Ecosystems of the*
2536 *world*. Elsevier, New York, pp 165-174, 1991.
- 2537 239. Sabine CL et al., The oceanic sink for anthropogenic CO₂ *Science* 305:367-
2538 371 doi:10.1126/science.1097403, 2004.
- 2539 240. Sahagian D., Global physical effects of anthropogenic hydrological alterations:
2540 sea level and water redistribution *Global and Planetary Change* 25:39-48
2541 doi:10.1016/S0921-8181(00)00020-5, 2000.
- 2542 241. Sahagian, D. L., F. W. Schwartz, and D. K. Jacobs, Direct anthropogenic
2543 contributions to sea level rise in the twentieth century, *Nature*, 367, 54-57,
2544 doi:10.1038/367054a0, 1994.
- 2545 242. Sasgen I., Konrad H., Ivins E.R., Van den Broeke M.R., Bamber J.L., Martinec
2546 Z., Klemann V., Antarctic ice-mass balance 2003 to 2012: regional reanalysis of
2547 GRACE satellite gravimetry measurements with improved estimate of glacial-isostatic
2548 adjustment based on GPS uplift rates, *The Cryosphere*, 7, 1499-1512, 2013.



- 2549 243. Sasgen I., Martín-Español A., Horvath A., Klemann V., Petrie E.J., Wouters
2550 B., and others Joint inversion estimate of regional glacial isostatic adjustment in
2551 Antarctica considering a lateral varying Earth structure (ESA STSE Project REGINA),
2552 *Geophysical Journal International* 211(3), 1534-1553, 2017.
- 2553 244. Sasgen, I., Van Den Broeke, M., Bamber, J. L., Rignot, E., Sørensen, L. S.,
2554 Wouters, B., Martinec, Z., Velicogna, I. & Simonsen, S. B., Timing and origin of
2555 recent regional ice-mass loss in Greenland. *Earth and Planetary Science Letters*, 333,
2556 293-303, 2012.
- 2557 245. Sasgen, I., Konrad, H., Ivins, E. R., Van den Broeke, M. R., Bamber, J. L.,
2558 Martinec, Z., & Klemann, V., Antarctic ice-mass balance 2003 to 2012: regional
2559 reanalysis of GRACE satellite gravimetry measurements with improved estimate of
2560 glacial-isostatic adjustment based on GPS uplift rates. *The Cryosphere*, 7, 1499- 1512,
2561 2013.
- 2562 246. Sasgen, I., Martín-Español, A., Horvath, A., Klemann, V., Petrie, E. J.,
2563 Wouters, B., & Konrad, Joint inversion estimate of regional glacial isostatic
2564 adjustment in Antarctica considering a lateral varying Earth structure (ESA STSE
2565 Project REGINA). *Geophysical Journal International*, 211(3), 1534-1553, 2017.
- 2566 247. Scanlon, B. R., I. Jolly, M. Sophocleous, and L. Zhang, Global impacts of
2567 conversions from natural to agricultural ecosystems on water resources: Quantity
2568 versus quality, *Water Resources Res.*, 43(3), W03437, 2007.
- 2569 248. Scanlon, B. R., C. C. Faunt, L. Longuevergne, R. C. Reedy, W. M. Alley, V. L.
2570 McGuire, and P. B. McMahon, Groundwater depletion and sustainability of irrigation
2571 in the U.S. High Plains and Central Valley, *PNAS*, 109, 9320-9325,
2572 doi:10.1073/pnas.1200311109, 2012a.
- 2573 249. Scanlon, B. R., L. Longuevergne, and D. Long, Ground referencing GRACE
2574 satellite estimates of groundwater storage changes in the California Central Valley,
2575 USA, *Water Resour. Res.*, 48, W04520, doi:10.1029/2011WR011312, 2012b.
- 2576 250. Scanlon, B. R., Zhang, Z., Save, H., Sun, A. Y., Schmied, H. M., van Beek, L.
2577 P., & Longuevergne, L., Global models underestimate large decadal declining and
2578 rising water storage trends relative to GRACE satellite data. *PNAS*, 201704665, 2018.
- 2579 251. Schrama, E. J., Wouters, B. & Rietbroek, R., A mascon approach to assess ice
2580 sheet and glacier mass balances and their uncertainties from GRACE data. *Journal of*
2581 *Geophysical Research: Solid Earth*, 119, 6048-6066, 2014.
- 2582 252. Schellekens, J., Dutra, E., Martínez-de la Torre, A., Balsamo, G., van Dijk, A.,
2583 Weiland, F. S., & Fink, G., A global water resources ensemble of hydrological
2584 models: the earth2Observe Tier-1 dataset. *Earth System Science Data*, 9(2), 389,
2585 2017.
- 2586 253. Schwatke C, Dettmering D, Bosch W, Seitz F, DAHITI – an innovative
2587 approach for estimating water level time series over inland waters using multi-mission
2588 satellite altimetry, *Hydrol. Earth Syst. Sci.*, 19, 4345-4364, 2015.
- 2589 254. Shamsudduha, M., R. G. Taylor, and L. Longuevergne, Monitoring
2590 groundwater storage changes in the highly seasonal humid tropics: Validation of
2591 GRACE measurements in the Bengal Basin, *Water Resour. Res.*, 48, W02508,
2592 doi:10.1029/2011WR010993, 2012.
- 2593 255. Sheng Y, Song C, Wang J, Lyons EA, Knox BR, Cox JS, Gao F.,
2594 Representative lake water extent mapping at continental scales using multi-temporal
2595 Landsat-8 imagery *Remote Sensing of Environment* in
2596 press:doi:10.1016/j.rse.2015.1012.1041, 2016.



- 2597 256. Shepherd, A., Ivins E.R., Geruo A., Barletta V.R., Bentley M.J., Bettadpur S.,
2598 and others, A reconciled estimate of ice-sheet mass balance. *Science*, 338(6111),
2599 1183-1189, doi:10.1126/science.1228102, 2012.
- 2600 257. Shukla J, Nobre C, Sellers P., Amazon Deforestation and Climate Change
2601 *Science* 247:1322-1325 doi:10.1126/science.247.4948.1322, 1990.
- 2602 258. Singh A, Seitz F, Schwatke C., Inter-annual water storage changes in the Aral
2603 Sea from multi-mission satellite altimetry, optical remote sensing, and GRACE
2604 satellite gravimetry *Remote Sens Environ* 123:187-195, 2012.
- 2605 259. Slangen, A.B.A., Meyssignac, B., Agosta, C., Champollion, N., Church, J.A.,
2606 Fettweis, X., Ligtenberg, S.R.M., Marzeion, B., Melet, A., Palmer, M.D., Richter, K.,
2607 Roberts, C.D., Spada, G., Evaluating model simulations of 20th century sea-level rise.
2608 Part 1: global mean sea-level change. *J. Clim.* 30(21): 8539–
2609 8563. <https://dx.doi.org/10.1175/jcli-d-17-0110.1>, 2017.
- 2610 260. Sloan S, Sayer JA., Forest Resources Assessment of 2015 shows positive
2611 global trends but forest loss and degradation persist in poor tropical countries, *Forest*
2612 *Ecol Manag*, 352:134-145 doi:10.1016/j.foreco.2015.06.013, 2015.
- 2613 261. Smith LC, Sheng Y, MacDonald GM, Hinzman LD, Disappearing Arctic lakes
2614 *Science* 308:1429-1429 doi:10.1126/science.1108142, 2005.
- 2615 262. Solomon, S. et al. (eds.), *Climate Change 2007: The Physical Science Basis.*
2616 *Contribution of Working Group I to the Fourth Assessment Report of the*
2617 *Intergovernmental Panel on Climate Change*, Cambridge Univ. Press, Cambridge,
2618 UK., 2007.
- 2619 263. Song C, Huang B, Ke L., Modeling and analysis of lake water storage changes
2620 on the Tibetan Plateau using multi-mission satellite data *Remote Sens Environ* 135:25-
2621 35 doi:10.1016/j.rse.2013.03.013, 2013.
- 2622 264. Spada G., Stocchi P., SELEN: A Fortran 90 program for solving the “sea-level
2623 equation”, *Computers & Geosciences* 33.4, 538-562, 2007.
- 2624 265. Spada G., Galassi G., New estimates of secular sea level rise from tide gauge
2625 data and GIA modelling, *Geophysical Journal International* 191(3): 1067-1094, 2012.
- 2626 266. Spada G., Galassi G., Spectral analysis of sea level during the altimetry era,
2627 and evidence for GIA and glacial melting fingerprints, *Global and Planetary Change*
2628 143:34-49, 2016.
- 2629 267. Spada G., Glacial isostatic adjustment and contemporary sea level rise: An
2630 overview. *Surveys in Geophysics* 38(1), 153-185, 2017.
- 2631 268. Spracklen DV, Arnold SR, Taylor CM., Observations of increased tropical
2632 rainfall preceded by air passage over forests *Nature* 489:282-U127
2633 doi:10.1038/nature11390, 2012.
- 2634 269. Sutterley T.C., Velicogna I., Csatho B., van den Broeke M., Rezvan-Behbahani
2635 S., Babonis G., Evaluating Greenland glacial isostatic adjustment corrections using
2636 GRACE, altimetry and surface mass balance data *Environmental Research Letters*
2637 9(1), 014004, 2014.
- 2638 270. Strassberg, G., B. R. Scanlon, and M. Rodell, Comparison of seasonal
2639 terrestrial water storage variations from GRACE with groundwater-level
2640 measurements from the High Plains Aquifer (USA), *Geophys. Res. Lett.*, 34, L14402,
2641 doi:10.1029/2007GL030139, 2007.
- 2642 271. Swenson S, Wahr J., Monitoring the water balance of Lake Victoria, East
2643 Africa, from space *J Hydro* 370:163-176, 2009.
- 2644 272. Syed, T. H., J. S. Famiglietti, D. P. Chambers, J. K. Willis, and K. Hilburn,
2645 Satellite-based global ocean mass balance reveals water cycle acceleration and



- 2646 increasing continental freshwater discharge, 1994–2006, *Proc. Natl. Acad. Sci. U. S. A.*, 107, 17,916–17,921, doi:10.1073/pnas.1003292107, 2010.
- 2647
- 2648 273. Stammer, D., and Cazenave A.. *Satellite Altimetry Over Oceans and Land*
- 2649 *Surfaces*, 617 pp., CRC Press, Taylor and Francis Group, Boca Raton, New York,
- 2650 London, ISBN: 13: 978-1-4987-4345-7, 2018.
- 2651 274. Tamisiea, M. E., Leuliette, E. W., Davis, J. L., and Mitrovica, J. X.,
- 2652 Constraining hydrological and cryospheric mass flux in southeastern Alaska using
- 2653 space-based gravity measurements. *Geophysical Research Letters*, 32:L20501,
- 2654 doi:10.1029/2005GL023961, 2005.
- 2655 275. Tamisiea M.E., Ongoing glacial isostatic contributions to observations of sea
- 2656 level change, *Geophysical Journal International* 186(3):1036, 2011.
- 2657 276. Tapley, B. D., S. Bettadpur, J. C. Ries, P. F. Thompson, and M. M. Watkins,
- 2658 GRACE measurements of mass variability in the Earth system. *Science* 305, 503–505,
- 2659 doi: 10.1126/science.1099192, 2004.
- 2660 277. Tapley, B. D., Bettadpur, S., Ries, J. C., Thompson, P. F., and Watkins, M. M.,
- 2661 The Gravity Recovery and Climate Experiment; Mission Overview and Early Results,
- 2662 *Geophys. Res. Lett.*, Vol. 31, No. 9, L09607, 10.1029/2004GL019920, 2004.
- 2663 278. Taylor, R. G., B. Scanlon, P. Döll, M. Rodell, R. van Beek, Y. Wada, L.
- 2664 Longuevergne, M. LeBlanc, J. S. Famiglietti, M. Edmunds, L. Konikow, T. R. Green,
- 2665 J. Chen, M. Taniguchi, M. F. P. Bierkens, A. MacDonald, Y. Fan, R. M. Maxwell, Y.
- 2666 Yechieli, J. J. Gurdak, D. M. Allen, M. Shamsudduha, K. Hiscock, P. J.-F. Yeh, I.
- 2667 Holman and H. Treidel, Groundwater and climate change, *Nature Clim. Change*, 3,
- 2668 322-329, doi:10.1038/nclimate1744, 2013.
- 2669 279. Thompson, P.R., and M.A. Merrifield, A unique asymmetry in the pattern of
- 2670 recent sea level change, *Geophys. Res. Lett.*, 41, 7675-7683, 2014.
- 2671 280. Tiwari, V. M., J. Wahr, and S. Swenson, Dwindling groundwater resources in
- 2672 northern India, from satellite gravity observations, *Geophys. Res. Lett.*, 36, L18401,
- 2673 doi:10.1029/2009GL039401, 2009.
- 2674 281. Tourian M, Elmi O, Chen Q, Devaraju B, Roohi S, Sneeuw N, A spaceborne
- 2675 multisensor approach to monitor the desiccation of Lake Urmia in Iran *Remote Sens*
- 2676 *Environ* 156:349-360, 2015.
- 2677 282. Turcotte DL, Schubert G, Geodynamics. Cambridge University Press,
- 2678 Cambridge, 2014.
- 2679 283. Valladeau, G., J. F. Legeais, M. Ablain, S. Guinehut, and N. Picot, “Comparing
- 2680 Altimetry with Tide Gauges and Argo Profiling Floats for Data Quality Assessment
- 2681 and Mean Sea Level Studies.” *Marine Geodesy* 35 (sup1):42–60.
- 2682 <https://doi.org/10.1080/01490419.2012.718226>, 2012.
- 2683 284. Van Den Broeke, M. R., Enderlin, E. M., Howat, I. M., Kuipers Munneke, P.,
- 2684 Noël, B. P. Y., Van De Berg, W. J., Van Meijgaard, E. & Wouters, B., On the recent
- 2685 contribution of the Greenland ice sheet to sea level change. *The Cryosphere*, 10, 1933-
- 2686 1946, 2016.
- 2687 285. Velicogna, I., Increasing rates of ice mass loss from the Greenland and
- 2688 Antarctic ice sheets revealed by GRACE. *Geophysical Research Letters*, 36, 2009.
- 2689 286. van der Werf GR et al., Global fire emissions and the contribution of
- 2690 deforestation, savanna, forest, agricultural, and peat fires (1997-2009) *Atmos Chem*
- 2691 *Phys* 10:11707-11735 doi:10.5194/acp-10-11707-2010, 2010.
- 2692 287. Van Dijk, A. I. J. M., L. J. Renzullo, Y. Wada, and P. Tregoning, A global
- 2693 water cycle reanalysis (2003–2012) merging satellite gravimetry and altimetry
- 2694 observations with a hydrological multi-model ensemble, *Hydrol. Earth Syst. Sci.*, 18,
- 2695 2955-2973, doi:10.5194/hess-18-2955-2014, 2014.



- 2696 288. Velicogna, I., Sutterley, T. C., & Van Den Broeke, M. R., Regional
2697 acceleration in ice mass loss from Greenland and Antarctica using GRACE time-
2698 variable gravity data. *Geophysical Research Letters*, 41(22), 8130-8137, 2014.
- 2699 289. Velicogna, I., Wahr, J., Measurements of Time-Variable Gravity Show Mass
2700 Loss in Antarctica, *Science*, DOI: 10.1126/science.1123785, 2006.
- 2701 290. von Schuckmann, K., J.-B. Sallée, D. Chambers, P.-Y. Le Traon, C. Cabanes,
2702 F. Gaillard, S. Speich, and M. Hamon, Monitoring ocean heat content from the current
2703 generation of global ocean observing systems, *Ocean Science*, 10, 547-557,
2704 DOI:10.5194/os-10-547-2012, 2014.
- 2705 291. von Schuckmann K., Palmer M.D., Trenberth K.E., Cazenave A., D. Chambers,
2706 Champollion N. et al., Earth's energy imbalance: an imperative for monitoring, *Nature*
2707 *Climate Change*, 26, 138-144, 2016.
- 2708 292. Vörösmarty CJ, Sahagian D, Anthropogenic disturbance of the terrestrial water
2709 cycle *Bioscience* 50:753-765 doi:10.1641/0006-
2710 3568(2000)050[0753:Adottw]2.0.Co;2, 2000.
- 2711 293. Voss, K. A., J. S. Famiglietti, M. Lo, C. de Linage, M. Rodell, and S. C.
2712 Swenson, Groundwater depletion in the Middle East from GRACE with implications
2713 for transboundary water management in the Tigris-Euphrates-Western Iran region,
2714 *Water Resour. Res.*, 49, doi:10.1002/wrcr.20078, 2013.
- 2715 294. Watson, Christopher S., Neil J. White, John A. Church, Matt A. King, Reed J.
2716 Burgette, and Benoit Legresy, "Unabated Global Mean Sea-Level Rise over the
2717 Satellite Altimeter Era." *Nature Climate Change* 5 (6):565–68.
2718 <https://doi.org/10.1038/nclimate2635>, 2015.
- 2719 295. Wada, Y., L. P. H. van Beek, C. M. van Kempen, J. W. T. M. Reckman, S.
2720 Vasak, and M. F. P. Bierkens, Global depletion of groundwater resources, *Geophys.*
2721 *Res. Lett.*, 37, L20402, doi:10.1029/2010GL044571, 2010.
- 2722 296. Wada, Y., Modelling groundwater depletion at regional and global scales:
2723 Present state and future prospects, *Surv. Geophys.*, 37, 419-451, doi:10.1007/s10712-
2724 015-9347-x, Special Issue: ISSI Workshop on Remote Sensing and Water Resources,
2725 2017.
- 2726 297. Wada, Y., L. P. H. van Beek, and M. F. P. Bierkens, Nonsustainable
2727 groundwater sustaining irrigation: A global assessment, *Water Resour. Res.*, 48,
2728 W00L06, doi:10.1029/2011WR010562, Special Issue: Toward Sustainable
2729 Groundwater in Agriculture, 2012a.
- 2730 298. Wada, Y., L. P. H. van Beek, F. C. Sperna Weiland, B. F. Chao, Y.-H. Wu, and
2731 M. F. P. Bierkens, Past and future contribution of global groundwater depletion to sea-
2732 level rise, *Geophys. Res. Lett.*, 39, L09402, doi:10.1029/2012GL051230, 2012b.
- 2733 299. Wada, Y., M.-H. Lo, P. J.-F. Yeh, J. T. Reager, J. S. Famiglietti, R.-J. Wu, and
2734 Y.-H. Tseng, Fate of water pumped from underground causing sea level rise, *Nature*
2735 *Clim. Change*, doi:10.1038/nclimate3001, early online, 2016.
- 2736 300. Wada, Y., Reager, J. T., Chao, B. F., Wang, J., Lo, M. H., Song, C. and
2737 Gardner, A. S., Satellite Altimetry-Based Sea Level at Global and Regional Scales. In
2738 *Integrative Study of the Mean Sea Level and Its Components* (pp. 133-154). Springer
2739 International Publishing, 2017.
- 2740 301. Wang J, Sheng Y, Hinkel KM, Lyons EA, Drained thaw lake basin recovery on
2741 the western Arctic Coastal Plain of Alaska using high-resolution digital elevation
2742 models and remote sensing imagery *Remote Sensing of Environment* 119:325-336
2743 doi:10.1016/j.rse.2011.10.027, 2012.



- 2744 302. Wang J, Sheng Y, Tong TSD, Monitoring decadal lake dynamics across the
2745 Yangtze Basin downstream of Three Gorges Dam *Remote Sensing of Environment*
2746 152:251-269 doi:10.1016/j.rse.2014.06.004, 2014.
- 2747 303. Wahr J, Nerem R.S., Bettadpur S.V., The pole tide and its effect on GRACE
2748 time-variable gravity measurements: Implications for estimates of surface mass
2749 variations. *Journal of Geophysical Research: Solid Earth* 120(6), 4597-4615, 2015.
- 2750 304. Watkins, M. M., Wiese, D. N., Yuan, D.-N., Boening, C., and Landerer, F. W.,
2751 Improved methods for observing Earth's time variable mass distribution with GRACE
2752 using spherical cap mascons. *Journal of Geophysical Research (Solid Earth)*,
2753 120:2648–2671, doi:10.1002/2014JB011547, 2015.
- 2754 305. Wenzel M and J Schroter, Reconstruction of regional mean sea level
2755 anomalies from tide gauges using neural networks, *J. Geophys. Res.* 115.
2756 doi:10.1029/2009JC005630, 2010.
- 2757 306. Wessem J. M. et al., Modeling the climate and surface mass balance of polar
2758 ice sheets using RACMO2, part 2: Antarctica, *the Cryosphere*, 2017.
- 2759 307. Whitehouse, P. L., et al., A new glacial isostatic adjustment model for
2760 Antarctica: calibrating the deglacial model using observations of relative sea-level and
2761 present-day uplift rates, *Geophys Journal Int.*, 190, 1464-1482, 2012.
- 2762 308. Wiese, D. N., Landerer, F. W., and Watkins, M. M., Quantifying and reducing
2763 leakage errors in the JPL RL05M GRACE mascon solution. *Water Resources*
2764 *Research*, 52:7490–7502, doi:10.1002/2016WR019344, 2016.
- 2765 309. Willis, J.K., Chambers, D.T., Nerem, R.S., Assessing the globally averaged sea
2766 level budget on seasonal to interannual time scales, *J. Geophys. Res.* 113, C06015.
2767 doi:10.1029/2007JC004517, 2008.
- 2768 310. Wisser, D., S. Frohling, S. Hagen, and M. F. P. Bierkens, Beyond peak
2769 reservoir storage? A global estimate of declining water storage capacity in large
2770 reservoirs, *Water Resour. Res.*, 49, 5732–5739, doi:10.1002/wrcr.20452, 2013.
- 2771 311. Whitehouse, P.L., Bentley M.J., Milne G.A., King M.A., Thomas I.D., A new
2772 glacial isostatic adjustment model for Antarctica: calibrating the deglacial model using
2773 observations of relative sea-level and present-day uplift rates, *Geophysical Journal*
2774 *International* 190, 1464-1482, 2012.
- 2775 312. Wiese, D., Yuan, D., Boening, C., Landerer, F. & Watkins, M., JPL GRACE
2776 Mascon Ocean, Ice, and Hydrology Equivalent Water Height RL05M. 1 CRI Filtered,
2777 Ver. 2, PO. DAAC, CA, USA. Dataset provided by Wiese in Nov/Dec 2017, 2016.
- 2778 313. Wijffels, S. E., D. Roemmich, D. Monselesan, J. Church, J. Gilson, Ocean
2779 temperatures chronicle the ongoing warming of Earth. *Nature Climate Change*,
2780 (6), 116-118, bdoi:10.1038/nclimate2924, 2016.
- 2781 314. Wöppelmann, G., and M. Marcos, Vertical land motion as a key to
2782 understanding sea level change and variability, *Rev. Geophys.*, 54, 64–92,
2783 doi:10.1002/2015RG000502, 2016.
- 2784 315. Wouters, B., Bamber, J. Á., Van den Broeke, M. R., Lenaerts, J. T. M., &
2785 Sasgen, I., Limits in detecting acceleration of ice sheet mass loss due to climate
2786 variability. *Nature Geoscience*, 6(8), 613, 2013.
- 2787 316. Wouters, B., R. E. M. Riva, D. A. Lavallée, and J. L. Bamber, Seasonal
2788 variations in sea level induced by continental water mass: First results from GRACE,
2789 *Geophys. Res. Lett.*, 38(3), doi:10.1029/2010GL046128, 2011.
- 2790 317. Wouters, B., Chambers, D. & Schrama, E., GRACE observes small-scale mass
2791 loss in Greenland. *Geophysical Research Letters*, 35, 2008.



- 2792 318. Wu X., Heflin M.B., Schotman H., Vermeersen B.L., Dong D., Gross R. S.,
2793 and others, Simultaneous estimation of global present-day water transport and glacial
2794 isostatic adjustment. *Nature Geoscience* 3.9: 642-646, 2010.
- 2795 319. Yi, S., Sun, W., Heki, K., and Qian, A., An increase in the rate of global mean
2796 sea level rise since 2010. *Geophysical Research Letters*, 42:3998–4006,
2797 doi:10.1002/2015GL063902, 2015.
- 2798 320. Zawadzki L., M. Ablain, Estimating a drift in TOPEX-A Global Mean Sea
2799 Level using Poseidon-1 measurements, paper presented at the OSTST meeting, La
2800 Rochelle, 2016.
- 2801 321. Zhang G, Yao T, Xie H, Kang S, Lei Y, Increased mass over the Tibetan
2802 Plateau: From lakes or glaciers? *Geophys Res Lett*:1-6, 2013.
- 2803 322. Zemp, M., Frey, H., Gärtner-Roer, I., Nussbaumer, S., Hoelzle, M., Paul, F.,
2804 Haeberli, W., Denzinger, F., Ahlstrøm, A., Anderson, B., Bajracharya, S., Baroni, C.,
2805 Braun, L., Cáceres, B., Casassa, G., Cobos, G., Dávila, L., Delgado Granados, H.,
2806 Demuth, M., Espizua, L., Fischer, A., Fujita, K., Gadek, B., Ghazanfar, A., Hagen, J.,
2807 Holmlund, P., Karimi, N., Li, Z., Pelto, M., Pitte, P., Popovnin, V., Portocarrero, C.,
2808 Prinz, R., Sangewar, C., Severskiy, I., Sigurdsson, O., Soruco, A., Usabaliev, R. and
2809 Vincent, C., Historically unprecedented global glacier decline in the early 21st
2810 century, *Journal of Glaciology*, 61, 745–762, 2015.
- 2811